

# **Proteolytic Processing of *Drosophila melanogaster* FGFs**

Dissertation

For the award of the degree

“Doctor rerum naturalium” (Dr.rer.nat.)

Of the Georg-August-Universität Göttingen

within the doctoral program for biology

of the Georg-August University School of Science

submitted by

Eva-Maria Rieß

from Detmold

Göttingen 2015

### Thesis Committee

Dr. Gerd Vorbrüggen

Department of Molecular Developmental Biology/Group for Molecular Cell Dynamics, MPI for Biophysical Chemistry

Prof. Dr. Ernst Wimmer

Department of Developmental Biology, J.-F.-B.-I. of Zoology and Anthropology

Prof. Dr. Reinhard Schuh

Group for Molecular Organogenesis, MPI for Biophysical Chemistry

### Members of the Examination Board

Reviewer:

Prof Dr. Gerd Vorbrüggen

Department of Molecular Developmental Biology/Group for Molecular Cell Dynamics, MPI for Biophysical Chemistry

Second Reviewer:

Prof. Dr. Ernst Wimmer

Department of Developmental Biology, J.-F.-B.-I. of Zoology and Anthropology

Further members of the Examination Board:

Prof. Dr. Reinhard Schuh

Group for Molecular Organogenesis, MPI for Biophysical Chemistry

Prof. Dr. Gregor Bucher

Department of Developmental Biology, J.-F.-B.-I. of Zoology and Anthropology

Prof. Dr. Ahmed Mansouri

Group for Molecular Cell Differentiation, MPI for Biophysical Chemistry

Dr. Roland Dosch

Dept. of Developmental Biochemistry, University Medical Center Göttingen

Date of the oral examination: 15.07.2015

<b>Abstract</b>	<b>1</b>
<b>Abbreviations</b>	<b>2</b>
<b>1 Introduction</b>	<b>4</b>
1.1 Fibroblastic Growth factors	4
1.1.1 FGFs in vertebrates	4
1.1.2 <i>Drosophila</i> FGFs: Branchless	5
1.1.3 <i>Drosophila</i> FGFs: Pyr and Ths	6
1.2 FGF signalling	7
1.2.1 FGF signalling in vertebrates	7
1.2.2 FGF signalling in <i>Drosophila</i>	8
1.3 Biological function of FGF signalling in <i>Drosophila</i>	10
1.3.1 <i>Drosophila</i> mesoderm formation	10
1.3.2 <i>Drosophila</i> tracheal patterning	12
1.4 Hypoxia	15
1.4.1 Hypoxia in vertebrates	15
1.4.2 Hypoxia in <i>Drosophila</i>	17
1.5 Proteolytic processing	18
1.5.1 Subtilisin proprotein convertases and Furin	18
1.5.2 Proteolytic processing in <i>Drosophila</i>	20
1.6 Analysis of proteolytic processing in <i>Drosophila</i> FGFs	22
<b>2 Material and Methods</b>	<b>23</b>
2.1 Methods	23
2.1.1 Molecular Cloning	23
2.1.1.1 Polymerase chain reaction (PCR)	23
2.1.1.2 DNA Agarose gel electrophoresis	23
2.1.1.3 DNA Gel extraction	23
2.1.1.4 Measurement of DNA concentration	23
2.1.1.5 DNA digestion with restriction endonucleases	23
2.1.1.6 DNA Ligation	24
2.1.1.7 Site-directed mutagenesis	24
2.1.1.8 Introduction of deletions	24
2.1.1.9 Gateway TOPO-cloning	24
2.1.1.10 Gateway LR Recombination	24
2.1.1.11 Preparation of chemically competent cells <i>E. coli</i> cells	25
2.1.1.12 Transformation of chemically competent cells <i>E. coli</i> cells	25
2.1.1.13 Plasmid DNA isolation	25
2.1.1.14 Sequencing	25
2.1.2 Cell Culture	26
2.1.2.1 Maintenance of <i>Drosophila</i> cell lines	26
2.1.2.2 Freezing and thawing of <i>Drosophila</i> cell lines	26
2.1.2.3 Transient Transfection of <i>Drosophila</i> cell lines	26
2.1.2.4 Preparation of cell lysates for Western blot	27
2.1.2.5 Preparation of cell culture supernatant for Western blot	27
2.1.3 Proteomic Methods	27
2.1.3.1 SDS Protein Gel Electrophoresis	27
2.1.3.2 Western Blot and Protein Immunodetection of Western Blot	28

2.1.4	<i>Drosophila</i> Techniques	28
2.1.4.1	Maintenance of <i>Drosophila melanogaster</i> strains	28
2.1.4.2	GAL4/UAS system for ectopic gene expression	28
2.1.4.3	GAL80 system for temporally controlled ectopic gene expression	29
2.1.4.4	Collection and fixation of <i>Drosophila</i> embryos	29
2.1.4.5	Hypoxic and Hyperoxic treatment	29
2.1.4.6	Trachea analysis of <i>Drosophila</i> larvae	30
2.1.4.7	X-Gal staining	30
2.1.4.8	Embryo Immunostaining	30
2.1.4.9	Fixation of <i>Drosophila</i> larva tissues	31
2.1.4.10	Acetone treatment for RNA in situ hybridization	31
2.1.4.11	RNA in situ hybridization of <i>Drosophila</i> larval tissues	31
2.1.4.12	Bright field microscopy	32
2.1.4.13	Confocal microscopy	32
2.1.5	Computing	32
2.1.5.1	Primer Design	32
2.1.5.2	Alignment of DNA sequences	32
2.1.5.3	Alignment of protein sequences	32
2.2	Material	33
2.2.1	Plasmids	33
2.2.2	Oligonucleotides	37
2.2.3	Fly stocks	39
2.2.3.1	Fly stocks generated for this work	39
2.2.3.2	Other fly stocks	39
2.2.4	Antibodies	40
2.2.4.1	Primary antibodies	40
2.2.4.2	Secondary antibodies	41

### **3 Results** **42**

---

3.1	Branchless processing in the larva	42
3.1.1	Bnl processing in the wing disc	43
3.1.2	Furin-mediated processing of Bnl is necessary for the formation of the air sac	46
3.1.3	Bnl processing in the dorsal terminal trachea	48
3.1.3.1	Furin processing is needed for the formation of TTBs at the dorsal connectives	48
3.1.3.2	Furin-mediated processing of Bnl is rate limiting for the formation of dorsal TTBs	51
3.1.4	Fur1-mediated processing during hypoxia	55
3.1.4.1	Tracheal remodelling due to hypoxia	56
3.1.4.2	Fur1 processing is involved in tracheal modelling due to hypoxia	57
3.2	Processing of Pyramus and Thisbe	60
3.2.1	Pyr and Ths are cleaved in cell culture	61
3.2.2	Conservation of Furin cutting sites in Pyr and Ths	63
3.2.2.1	Pyr and Ths contain Furin cutting sites conserved within <i>Drosophila melanogaster</i> FGFs	63
3.2.2.2	Pyr and Ths contain Furin cutting sites partially conserved within other <i>Drosophilids</i>	64
3.2.3	Relevance of Furin cutting sites for the proteolytic processing of Pyr and Ths	65

3.2.3.1	Inhibition of Fur1 is not preventing cleavage of Pyr	66
3.2.3.2	Inhibition of Furin is not explicitly verifying Furin-mediated cleavage of Ths	67
3.2.4	Biological effect of Pyr and Ths processing	68
3.2.4.1	Inhibition of Furin-mediated processing affects the formation of Eve-positive cells	69
3.2.4.2	Mutation of Furin cleavage sites in Pyr and Ths results in minor biological effects	71
3.2.5	Processing of Pyr and Ths is not Fur1-mediated	74
3.2.5.1	Mutation of Furin cleavage sites is not preventing cleavage in cell culture	74
3.2.6	Identification of the Pyr cleavage site	77
3.2.6.1	Mapping of the Pyr cleavage site	77
3.2.6.2	Deletion of presumptive Pyr cutting site is not preventing cleavage	82
3.2.7	Identification of the Ths cleavage site	83
3.2.7.1	Mapping of the Ths cleavage site	83
3.2.7.2	Deletion of the presumptive Ths cutting site is preventing cleavage	85
<b>4</b>	<b>Discussion</b>	<b>87</b>
4.1	Fur-mediated processing is used to regulate Bnl signalling during larval terminal branch formation	88
4.2	Formation of the adult air sac during larval development is dependent on Fur-mediated processing of Bnl	90
4.3	Remodelling of the larval tracheal network during hypoxia is regulated by Furin proteases	90
4.4	Fur1-mediated processing is the rate-limiting step of Bnl signalling	94
4.5	All <i>Drosophila</i> FGFs are processed	96
4.6	Differential functions of Pyr and Ths	97
	<b>Summary and Conclusion</b>	<b>101</b>
	<b>References</b>	<b>103</b>
	<b>Acknowledgements</b>	<b>117</b>
	<b>Curriculum Vitae</b>	<b>118</b>

# Abstract

FGF signalling is of major importance for organisms ranging from invertebrates to mammals where it is involved in a broad range of processes throughout the development and adulthood. FGF signalling in *Drosophila melanogaster* includes three FGF ligands and two FGF receptors. However, *Drosophila* FGFs are approximately three times the size of vertebrate FGFs, containing additional domains that show no homology to other FGF ligands.

Recently it has been discovered that in the case of Bnl these additional C- and N-terminal domains are proteolytically removed releasing a protein of approximate size of a vertebrate FGF. Fur1-mediated cleavage of Bnl is crucial for its activity and therefore essential for tracheal patterning in the embryo.

Following up on former findings, this work investigated the role of Fur1-mediated processing for all Bnl-regulated processes in greater depth. The conducted experiments showed that indeed Fur1-mediated processing is essential for all tested processes including the formation of terminal trachea in the larva and the air sac primordium. Moreover first experiments suggest that Fur1-mediated processing of Bnl is part of the regulatory mechanism for the tracheal remodelling during hypoxia. Further the collected data allowed the conclusion that Fur1 is not only involved in a regulatory process, but is indeed representing the rate-limiting factor for Bnl signalling.

It could be demonstrated that all *Drosophila* FGFs are cleaved thereby removing the large additional domains and releasing proteins of approximately the size of a vertebrate FGF. However, Pyr and Ths are not processed by the Fur1 protease as *in silico* analysis initially suggested.

Taken together, the results of this study suggest that proteolytic processing functions as a novel general regulatory mechanism for FGF signalling in *Drosophila*. Additionally the collected data is offering a possible mechanism for the adaptation of tracheal patterning to the oxygen content of the environment.

# Abbreviations

aa	amino acid
ASP	air sac primordium
Bnl	Branchless
bp	base pair
BSA	Bovine Serum Albumin
Btl	Breathless
C-	Carboxy-
Da	Daughterless
DAPI	4',6-Diamidin-2'-phenylindoldihydrochlorid
DNA	Deoxyribonucleic acid
Dpp	Decapentaplegic
EGF	Epidermal growth factor
EGFP	Enhanced green fluorescent protein
ER	Endoplasmic reticulum
Eve	Even-skipped
FGF	fibroblastic growth factor
FGFR	FGF receptor
FS	Furin site
Fur1	Furin1
GFP	Green fluorescent protein
HRP	Horse radish peroxydase
HSPG	Heparan Sulphate Proteoglycan
Htl	Heartless
kDa	Kilo Dalton
Kr	Krüppel
L	Lysine
MFS	Mutated furin site

N-	Amino-
PAGE	Polyacrylamide Gel Electrophoresis
PBS	Phosphate Buffered Saline
PBT	PBS with 0,01% Tween-20
PC	Prohormone convertase
PCR	Polymerase Chain Reaction
Pyr	Pyramus
R	Arginine
RFP	Red fluorescent protein
RNA	Ribonucleic acid
RNAi	RNA interference
rpm	revolutions per minute
SDS	Sodium Dodecyl Sulphate
SPC	Subtilisin-like proprotein convertases
TGF- $\beta$	Transforming growth factor- $\beta$
TGN	<i>trans</i> -Golgi network
Ths	Thisbe
TTB	thick terminal branches
UAS	Upstream Activating Sequence
UV	ultraviolet
X-Gal	5-Brom-4-chlor-3-indoxyl- $\beta$ -D-galactopyranosid
$\alpha$ 1-PDX	Alpha1-antitrypsin variant Portland
$\mu$ g	microgram
$\mu$ g	microlitre



# 1 Introduction

## 1.1 Fibroblastic Growth factors

Fibroblastic growth factors (FGFs) form a highly conserved family of secreted signalling factors that have been found in a wide range of organisms from invertebrates to vertebrates. FGF signalling is crucial for a broad range of biological processes throughout the whole development. During embryonic development FGFs are involved in the regulation of the cell proliferation, migration and differentiation. Beyond embryonic development FGFs function as homeostatic factors and are involved in wound tissue repair and angiogenesis. Given the important role that FGF signalling plays for regulatory processes it came without a surprise that defects in FGF signalling are increasingly linked to a range of human diseases like skeletal dysplasia, neurodegenerative disease and cancers (Krejci et al. 2009; Turner and Grose 2010).

### 1.1.1 FGFs in vertebrates

For the mammalian family of FGF signalling factors 23 members have been identified until today (Ornitz and Itoh 2001). The first observations that led to the discovery of FGF proteins was that bovine pituitary extracts function as mitogens in fibroblast cell cultures (Armelin 1973). Subsequently the first FGF protein, basic FGF2, was described after purification from bovine brain extracts (Gospodarowicz 1974). All vertebrate FGFs share a homologous core domain of 120-130 amino acids and are relatively small proteins ranging in their molecular weight from 17 to 34 kDa. The core domain is structured into 12 antiparallel  $\beta$ -strands, which are linked to the binding of heparan sulfate proteoglycans (HSPGs) and the FGF receptors (Eriksson et al. 1991; Zhu et al. 1991). HSPGs are a group of glycoproteins found on the cell surface or within the extracellular matrix (ECM) that carry heparin sulfates glycosaminoglycan (HSGAG) chains (Hacker et al. 2005). Alongside this conserved core domain FGFs have additional amino- (N-) and carboxy- (C-) terminal tails of variable length, which largely account for the diverse biological functions of the different FGF family members (Ornitz and Itoh 2001).

Phylogenic analysis grouped FGFs into seven subgroups based on their relatedness. Five of these subfamilies have classical N-terminal signalling peptides and are secreted from the producing cell as soluble signalling molecules (Ornitz and Itoh 2001; Itoh and Ornitz 2004). Of the remaining two FGF subfamilies, the FGFs 11-14 act intracellular, while the last group (FGF19, 21 and 23) have a reduced affinity to HSGAG and function in an endocrine manner (Ornitz and Itoh 2001).

In vertebrates there are four known FGFR (FGFR1- FGFR4) which function as receptor tyrosin kinases (Beenken and Mohammadi 2009). FGFRs are structured into three extracellular immunoglobulin domains (D1-D3), a transmembrane domain and an intracellular tyrosine kinase domain. Through alternative splicing of the Ig3 domain tissue-specific isoforms with different binding specificities can be generated (Mohammadi et al. 2005). Each FGFR can be bound by a set of multiple FGF ligands. Additionally most FGF ligands can bind to more than one FGFR subtype. The promiscuous binding of FGFs to FGFRs results in a large number of receptor-ligand combinations, which is the basis for the observed broad regulatory potential of FGF signalling.

Vertebrate FGFs are known to bind to HSGAG through the HSGAG binding site (HBS), which is located in the FGF core domain. The binding of the FGF ligand to an FGFR is strictly HSGAG-dependent (Lin and Perrimon 2000; Hacker et al. 2005; Dreyfuss et al. 2009). In this manner FGF-HSGAG-FGFR complexes are formed that subsequently allow the formation of receptor dimers (Yayon et al. 1991; Schlessinger et al. 2000). Dimerization of the FGFR leads to the activation of cytoplasmic kinase domains, which in turn leads the autophosphorylation of the receptor. Subsequently the phosphorylation triggers the activation of the downstream signal transduction cascade (Mohammadi et al. 1996).

### **1.1.2 *Drosophila* FGFs: Branchless**

Compared to the 23 mammalian FGFs *Drosophila melanogaster* (in the remaining named *Drosophila*) has only three different FGF proteins: The FGF10 homologue Branchless (Bnl) and the two FGF8 homologues Thisbe (Ths, also known as FGF8-like1) and Pyramus (Pyr, also known as FGF8-like2) (Sutherland et al. 1996; Ornitz and Itoh 2001; Gryzik and Müller 2004; Stathopoulos 2004). Bnl is a 770 amino acid protein with a calculated molecular mass of 84kDa (Sutherland et al. 1996). Thus it is unusually large compared to vertebrate FGFs, which range in size between 17 and 34kDa. It has a conserved FGF core domain that is flanked by large C- and N-terminal regions that are not present in vertebrate FGFs and show no homology to any known protein. Additionally these sequences contain several stretches of repeated amino acid, including glutamines and serines, which have no known purpose. Similar to vertebrate FGFs, Bnl has a HSGAG binding domain that enables binding of HSGAG sugar side chains of HSPGs (Sutherland et al. 1996).

In vertebrates FGF10 is involved in lung formation (Min et al. 1998). Its direct *Drosophila* homologue Bnl has been shown to be crucial for the formation of the

tracheal network during embryonic and larval development. Bnl is directing the tracheal outgrowth by functioning as a chemoattractant to the tracheal cell, which express the FGFR Breathless (Btl) (Klambt et al. 1992; Reichman-Fried et al. 1994; Lee et al. 1996; Sutherland et al. 1996).

The expression of *bnl* during *Drosophila* embryonic development is highly dynamic. It is first detected during embryonic stage 5, where it can be found in the area of the cephalic furrow and at the posterior transversal furrow. At stage 11, just before the onset of tracheal branching, *bnl* appears in small epidermal clusters close to the tracheal sac at the positions where the primary trachea are about to form. These expression domains disappear during ongoing development and new *bnl* expression domains form corresponding to the subsequent outgrowth of the tracheal network (Sutherland et al. 1996).

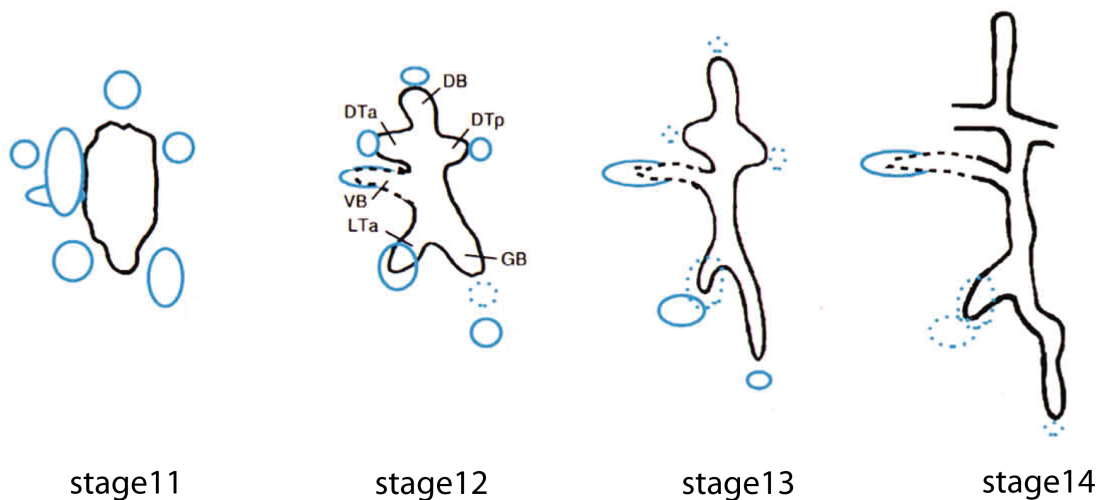


**Figure 1: *bnl* expression in a typical hemisegment (modified from Sutherland, 1996)**

Developing tracheal system and *bnl* expression domains. Solid blue circles indicate *bnl* expression; dotted blue, regions of weaker or variable expression.

### 1.1.3 *Drosophila* FGFs: Pyr and Ths

Pyr and Ths are homologues to vertebrate FGF8, derived from a gene duplication. Pyr contains 766 amino acids and has a predicted molecular weight of 87kDa, while Ths contains 748 amino acids and has a predicted weight of 82 kDa (Gryzik and Müller 2004; Stathopoulos 2004). Both proteins contain a conserved FGF core domain and large additional C-terminal sequences of unknown function. Similar to Bnl both Pyr and Ths carry N-terminal signalling peptides and are secreted from the expressing cells (Gryzik and Müller 2004; Stathopoulos 2004). Interestingly both Fgf8-like proteins do

not carry a HSGAG binding domain, which suggests that Pyr and Ths do not interact with HSPGs (Stathopoulos 2004).

During early embryonic development *pyr* and *ths* show identical expression patterns. During cellularization both are expressed in a broad stripe within the lateral neurogenic ectoderm (Stathopoulos 2004). However during later embryonic development the expression of *pyr* and *ths* diverges. During early embryonic development *ths* is expressed in the ventral region, while *pyr* expression can be found in the dorsal region. When the invagination of the mesoderm is completed mesodermal cells spread along the ectoderm into a monolayer. This process is thought to be mediated by the FGF8-like mediated activation of the FGFR Heartless (Htl) that is expressed in the mesodermal cells (Beiman et al. 1996; Gisselbrecht et al. 1996; Shishido et al. 1997). Thus the dynamic expression of its ligand Pyr and Ths are thought to provide a mechanism to the underlying mesoderm cells causing them to move dorsally (Kadam et al. 2009; Klingseisen et al. 2009; McMahon et al. 2010).

## 1.2 FGF signalling

### 1.2.1 FGF signalling in vertebrates

In FGFRs ligand binding is mediated by the immunoglobulin domains and results in a conformational change of the FGFR, which ultimately results in the dimerization of two neighbouring FGFR molecules. Subsequently both receptor molecules are phosphorylated at conserved tyrosine residues by the other molecules tyrosine kinase domain, thereby activating downstream signal transduction (Mohammadi et al. 2005; Katoh and Nakagama 2014). Following the phosphorylation of the receptor dimer the adaptor protein Fibroblast growth factor receptor substrate 2 (FRS2) is recruited via a phosphotyrosine-binding (PTB) domain (Lin et al. 1998). Interaction of FRS2 and the FGFR is followed by a tyrosine phosphorylation of FRS2 which enables the recruitment of other factors such as Growth factor receptor-bound 2 (Grb2) and the guanine nucleotide exchange factor Son of sevenless (Sos) (Kouhara et al. 1997; Eswarakumar et al. 2005). Recruitment of these factors subsequently enables the activation of the membrane-bound GTPase Ras. The facilitation of GTP-GDP exchange results in the activation of the MAP kinase cascade (MAPKKK/RAF; MAPKK/MEK and MAPK/ERK1/2), which ultimately leads to the activation of nuclear transcription factors such as c-Myc, AP1 or members of the E-twenty-six (ETS) family and the expression of target genes (Bottcher and Niehrs 2005; Turner and Grose 2010).

An alternative pathway of FGF signalling involves Grb2-associated binding protein 1 (Gab1), which recruits the PI3-kinase cascade and activates the cell survival pathway (Kouhara et al. 1997). Additionally the phospholipase C $\gamma$  (Plc $\gamma$ ) can be activated by FGF signalling, which leads to the rearrangement of actin cytoskeleton and cell migration (Bottcher and Niehrs 2005; Turner and Grose 2010). Other possible downstream signalling pathways include P38 kinase, Jun N-terminal kinase and Signal transducer and activator of transcription (Stat) signalling (Boilly et al. 2000; Hart et al. 2000).

### 1.2.2 FGF signalling in *Drosophila*

There are three known FGF ligands (Bnl, Pyr and Ths) and two FGFRs (Btl and Htl) in *Drosophila*. Bnl is the only ligand to the FGFR Btl and Btl signalling is a major factor for the formation of the tracheal network (Klambt et al. 1992; Reichman-Fried et al. 1994; Lee et al. 1996; Sutherland et al. 1996). Pyr and Ths are both signalling through the same FGFR Htl (Gryzik and Müller 2004; Stathopoulos 2004). Htl signalling is involved in the migration of the mesoderm during gastrulation and the differentiation of resulting specialized cell like pericardial cell, somatic muscle founders and fat body cells (Beiman et al. 1996; Gisselbrecht et al. 1996; Shishido et al. 1997).

The two *Drosophila* FGFRs, Btl and Htl, are receptor tyrosine kinases (RTKs). Like other RTKs Btl and Htl are activating the mitogen-activated protein kinase (MAPK) which finally leads to the expression of target genes, such as *even-skipped* (*eve*), *mef2*, *pointed* and *sprouty* (Hacohen et al. 1998; Metzger and Krasnow 1999; Halfon et al. 2000).

Analogue to vertebrate FGF signalling *Drosophila* FGFRs are not directly recruiting the downstream receptor kinase (Drk), the *Drosophila* homologue of the vertebrate homologue Grb2, via intracellular phosphotyrosine domains. Instead an adaptor protein is binding constitutively to the FGFR and provides a scaffold for component binding (Vincent et al. 1998; Imam et al. 1999; Wilson et al. 2004). However, although the FGFRs and its downstream signalling components are conserved between vertebrates and insects, the *Drosophila* homologue of the adaptor protein FSR2 is not involved in FGF signalling in *Drosophila*. Instead the adaptor protein downstream of FGFR (Dof, also known as Stumps and Heartbroken) is binding to the intracellular domain of both *Drosophila* FGFRs (Michelson et al. 1998; Vincent et al. 1998; Imam et al. 1999). Dof has been shown to be essential for all processes mediated by FGF signalling in *Drosophila* embryogenesis, including the formation of the mesoderm and development of the tracheal network (Michelson et al. 1998; Vincent et al. 1998; Imam et al. 1999). The binding of Dof to the activated FGFR results in the phosphorylation of Dof at

several tyrosine residues (Csiszar et al. 2010; Muha and Muller 2013). Subsequently the tyrosine phosphatase Corkscrew (Csw), a homologue of vertebrate SHP2, is recruited and subsequently activates the MAPK pathway (Perkins et al. 1992; Petit et al. 2004). Additionally to Csw two more potential Dof binding partners, Drk and Scr64b, have been proposed to contribute to MAPK pathway activation. Dof contains binding sites for Drk, which recruits the Ras GTP exchange factor Son of sevenless (Sos). Sos in turn propagates the signal to the MAPK cascade via the small GTPase Ras85 (Wassarman et al. 1995). A third route has been proposed through Scr64b which has been shown to be linked to Dof directly (Csiszar et al. 2010).

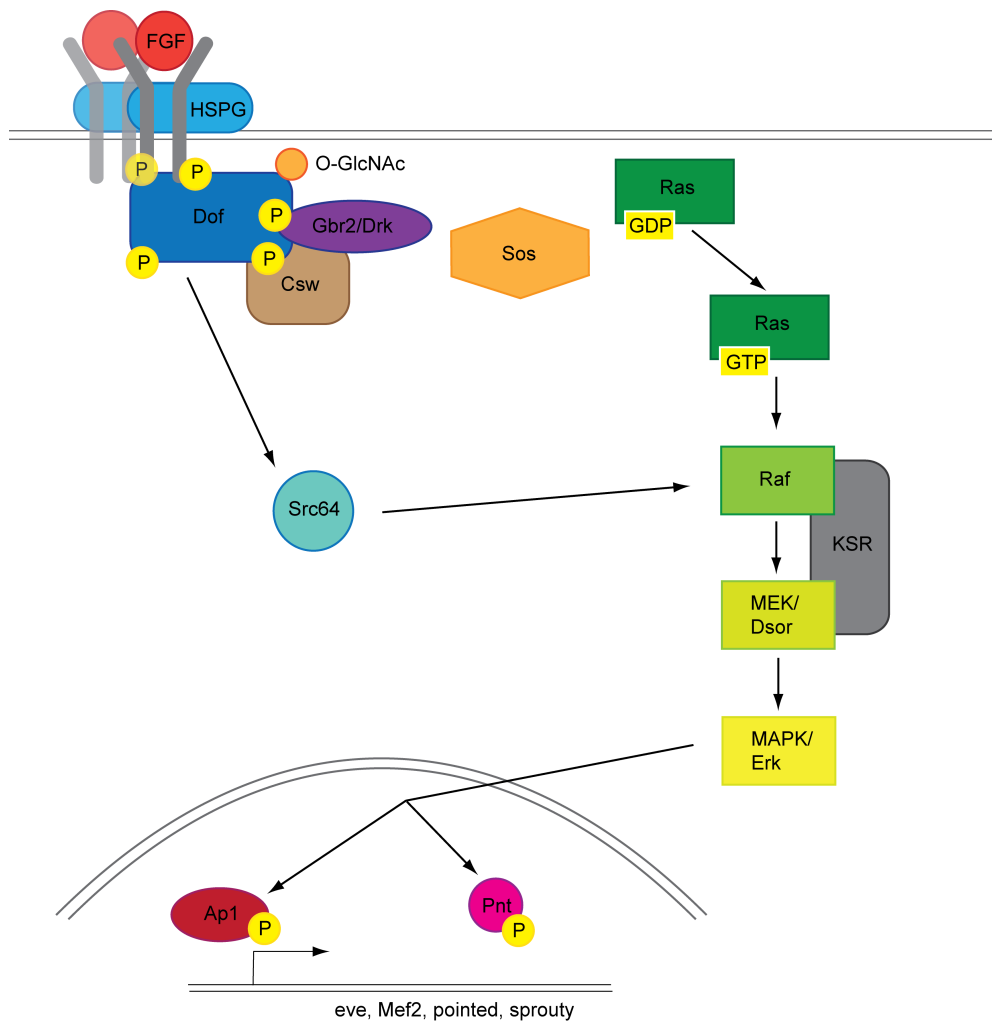


**Figure 2: Schematic model of the FGF signalling cascade in *Drosophila* (modified from Muha and Müller 2013)**

Interaction with HSPGs is stabilizing the binding of the FGFs to their FGFRs. Activation of the FGFR leads to the phosphorylation of their tyrosine kinase domains and subsequently to the phosphorylation of the adaptor protein Dof. Dof can direct the signal towards different signalling cascades, including the Csw/Shp2, Grb2/Drk and Src64B pathways, which have been proposed to contribute to the activation of the MAPK.

## 1.3 Biological function of FGF signalling in *Drosophila*

The limited number of FGFs and FGFRs and the defined regulated developmental processes make *Drosophila* an attractive model for the study of FGF signalling during development. Processes known to be regulated by FGF signalling include the patterning of the tracheal network as well as the migration and differentiation of the mesoderm.

### 1.3.1 *Drosophila* mesoderm formation

Signalling of *Pyr* and *Ths* through the FGFR *Htl* plays a crucial role for the development of the mesoderm during embryonic development (Beiman et al. 1996; Gisselbrecht et al. 1996; Shishido et al. 1997). It is involved in the movement of mesodermal cells (Stathopoulos 2004; Wilson et al. 2005; Kadam et al. 2009; Klingseisen et al. 2009; Clark et al. 2011; Kadam et al. 2012), the differentiation of the pericardial cells (Stathopoulos 2004; McMahon et al. 2008; Kadam et al. 2009; Klingseisen et al. 2009), migration of the caudal visceral mesoderm (CVM) (Mandal et al. 2004; Kadam et al. 2012; Reim et al. 2012) and glial differentiation, migration and axonal wrapping in the eye imaginal disc (Franzdottir et al. 2009).

The earliest influence of *Htl*-signalling can be seen during mesoderm migration where the mesoderm undergoes a dorsolateral migration along the ectoderm to form a monolayer (Stathopoulos 2004; Wilson et al. 2005). Interestingly this is not a single process controlled by a single set of regulatory factors, but instead migration of the mesodermal cells is a multi-step process (McMahon et al. 2010; Clark et al. 2011). This multi-step process can be divided into four temporally distinct migratory events that require the input of different signalling factors: First the mesodermal tube formation followed by the collapse of the mesoderm and dorsal migration and spreading and finally monolayer formation. While the collapse of the mesoderm and the monolayer formation are controlled by FGF signalling the dorsal movement appears to be FGF-independent (McMahon et al. 2010; Clark et al. 2011).

The first step of this complex process is the invagination of the mesoderm. This process is dependent on the factors *Dorsal*, *Snail*, *Twist* and many others (Thisse et al. 1987; Leptin 1991; Reuter and Leptin 1994; Leptin and Affolter 2004). The collapse of the mesodermal tube onto the ectoderm is dependent on *Htl* activation via *Ths*, which additionally might involve *Rap1* (McMahon et al. 2010; Clark et al. 2011). Dorsal spreading of the mesodermal cells along the ectoderm is controlled by a currently unknown mechanism. But since mesodermal spreading is not affected in *pyr* and *ths*

mutants FGF signalling seems not to be directly involved in the process (McMahon et al. 2010; Clark et al. 2011). After dorsal spreading is completed, mesodermal cells that are in no direct contact to the ectoderm intercalate to form a monolayer. This process is controlled by signalling of both Pyr and Ths through Htl (McMahon et al. 2010; Clark et al. 2011). Additionally the GTPase Roughened (Rap1) and the beta-integrin subunit Myospheroid (Mys) are of major importance for the monolayer formation (McMahon et al. 2010).

Additionally Pyr and Ths also play key roles during the pathfinding, survival and migration of the longitudinal visceral muscle (LVM) founder cells. These cells migrate in two distinct groups bilaterally from the caudal visceral mesoderm along the trunk visceral mesoderm towards the anterior in a bilateral fashion (Kadam et al. 2012; Reim et al. 2012). *pyr* and *ths* expression is crucial for the survival of the muscle founder cells during this migration. Independent of this function *pyr* and *ths* are involved in the guidance during migration. Double mutants for *pyr* and *ths* as well as *htl* mutants display almost complete death of the LVM founder cells during mid-migration with no cell reaching their destination resulting in the formation of very few LMVs (Kadam et al. 2012; Reim et al. 2012).

The most striking defect in phenotype for the *htl* mutant is the loss of heart cells and the loss of dorsal muscles that can be detected with an antibody against the marker Even-skipped (*Eve*) (Beiman et al. 1996; Gisselbrecht et al. 1996; Shishido et al. 1997). These defects can be explained by the influence of Htl signalling on the gastrulation movement described above. The *htl* mutant shows defects in monolayer formation and migration of the mesodermal cells (Stathopoulos 2004; Wilson et al. 2005). Therefore the mesodermal cells fail to receive the differentiating Decapentaplagic (*Dpp*) signal that is located at the dorsal ectoderm, which ultimately results in the loss of the most dorsal structures derived from the mesoderm: the pericardial cells and the dorsal somatic musculature (Frasch 1995; Halfon et al. 2000; Gryzik and Müller 2004; Stathopoulos 2004). The detection of these defects has been used to monitor Htl signalling and thus the activity of the two ligands to the Htl receptor, Pyr and Ths (Kadam et al. 2009; Tulin and Stathopoulos 2010).

While both Fgf8-like proteins have similar function not all of the processes regulated by Htl signalling are relying on Pyr and Ths in equal measure. Even though Pyr and Ths are signalling through the same receptor they play differential roles during *Drosophila* development. A possible explanation for these diverged roles of the two FGFs would be the regulation by proteolytic cleavage as suggested by Tulin et al. (2010).



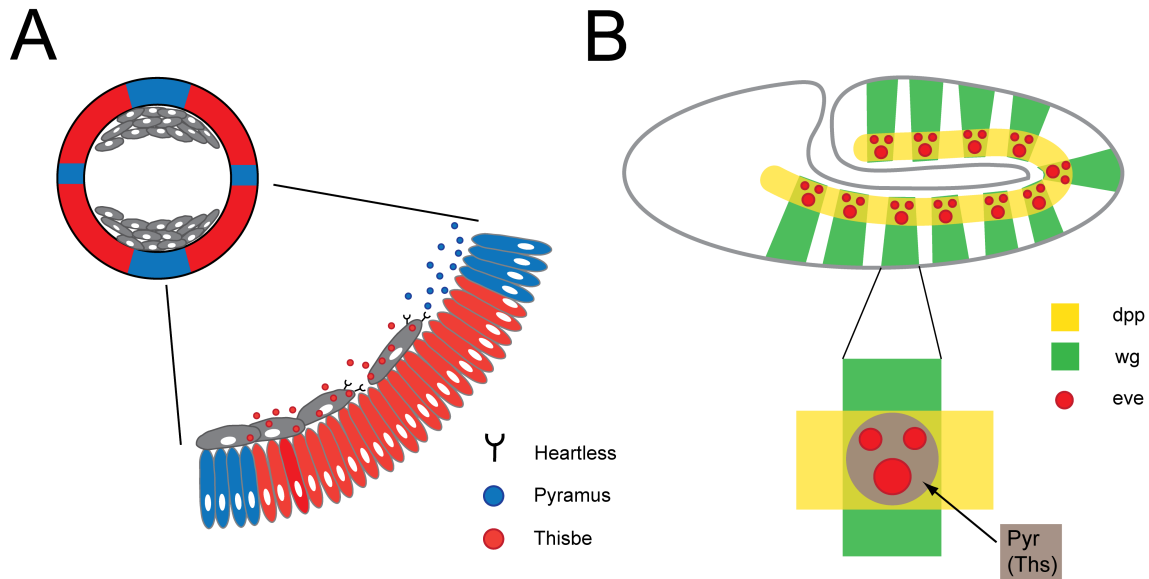


**Figure 3: Model for FGF signalling through Heartless (modified from Kadam et al., 2009)**

(A) Proper regulation of the mesoderm migration is relying on the location of the Pyr and Ths expression domains. Both ligands play differential roles and are required for the patterning of the mesoderm. (B) Specification of the dorsal mesoderm lineages, including the Eve-positive cells (depicted in red), multiple signalling factors are needed for differentiation (including Dpp and Wg). FGFs (depicted in brown) are possibly feeding into this process.

### 1.3.2 *Drosophila* tracheal patterning

The tracheal network is a system of interconnected epithelial tubes used for the transport of oxygen through the body of *Drosophila* throughout its whole life cycle. The tracheal network is organized bilaterally and in a hierarchical pattern. Oxygen is entering through the spiracles, transported through the larger primary and secondary trachea and finally diffuses towards individual cells through the narrow terminal (or tertiary) trachea (Uv 2003; Cabernard and Affolter 2005; Affolter and Caussinus 2008). Primary and secondary trachea emerge in a very specific pattern with a fixed number of trachea in a specified position. This patterning is achieved in a number of complex developmental processes including the generation of epithelial tubes, their subsequent elongation and ramification (Uv 2003; Cabernard and Affolter 2005; Affolter and Caussinus 2008).

The development of the tracheal network starts during embryonic stage 10 with the formation of 10 independent pairs of epithelial clusters, the tracheal placodes. These placodes are formed by an incomplete invagination from the epithelium leaving behind short stalks that connect the placodes to the surface of the embryo forming the spiracular branch. Each placode consist of approximately 20 cells and divide twice,

resulting in approximately 80 tracheal cells each. After these initial cell divisions the tracheal cells undergo no further cell division until metamorphosis (Sato and Kornberg 2002; Cabernard and Affolter 2005). At embryonic stage 11 the cells of the tracheal pits start migrating outwards to form the six primary trachea branches: the dorsal branch (DB), the dorsal trunk anterior and posterior (DTa and DTp), the visceral branch (VB), lateral branches anterior and posterior/ganglionic branch (LBa and LBp/GB). DTa and DTp branches stretch further anterior and posterior until they eventually fuse to form the dorsal trunk (Samakovlis et al. 1996; Uv 2003). Outgrowth of the secondary tracheal branches starts at embryonic stage 14, where the leading cells, which are forming the tips of the multicellular primary branches, form unicellular outgrowths (Samakovlis et al. 1996; Uv 2003). Some of these secondary branches then elongate and finally form the terminal branches, while others fuse to branches of the neighbouring metamere by so called fusion branches. Subsequently the terminal branches form the connection between the tracheal network and the cells of the target tissue and supply them with oxygen (Samakovlis et al. 1996; Uv 2003).

During larval development the terminal branches remain plastic and able to ramify. Similar to angiogenesis, the terminal branches of the larval tracheal network invade oxygen-starved tissues. Hence the tracheal network is able to adjust to environmental oxygen conditions throughout larval development (Wigglesworth 1954; Locke 1958; Wigglesworth 1983; Jarecki et al. 1999; Metzger and Krasnow 1999; Centanin et al. 2008).

During metamorphosis the tracheal network must be adjusted to satisfy the oxygen requirement of the forming adult while at the same time the pupa needs to be supplied with adequate amounts of oxygen. The transformation of the tracheal network to achieve these goals starts during 3<sup>rd</sup> larval instar, when the imaginal tracheoblasts start proliferating (Manning and Krasnow 1993). Structures formed by the imaginal tracheoblasts are the coiled tracheal branches unique to the pupa and the air sac primordium (ASP), which was long thought to be a dilatation of the trachea. The larval ASPs are large reservoirs juxtaposed with major muscles and the brain that later form the air sac of the adult (Sato and Kornberg 2002). One of these air sacs is forming on the wing imaginal disc that later forms most of the adult thorax including most of the dorsal thoracic epidermis, the wing and flight musculature. Induction of the air sac starts at the transverse connective (TC) 2, which is connected to the wing imaginal disc. This air sac is associated with the support of the adult flight musculature (Cohen 1993).

Formation of this air sac is strongly dependent on FGF signalling. Similar to Bnl signalling in the formation of the embryonic tracheal network Bnl is providing a guidance

cue for the developing air sac. In return the air sac precursor cells form *btl* expressing cytonemes that extend into the direction of the *bni* expressing cells (Sato and Kornberg 2002; Roy and Kornberg 2011). Additionally a specific subpopulation of the formed cytonemes expresses *tkv* and is thus able to mediate Dpp signalling of the wing disc tracheal cells (Sato and Kornberg 2002; Roy and Kornberg 2011). The dependency on Bnl signalling has made the wing imaginal disc air sac an interesting model system for Bnl signalling in the larva.

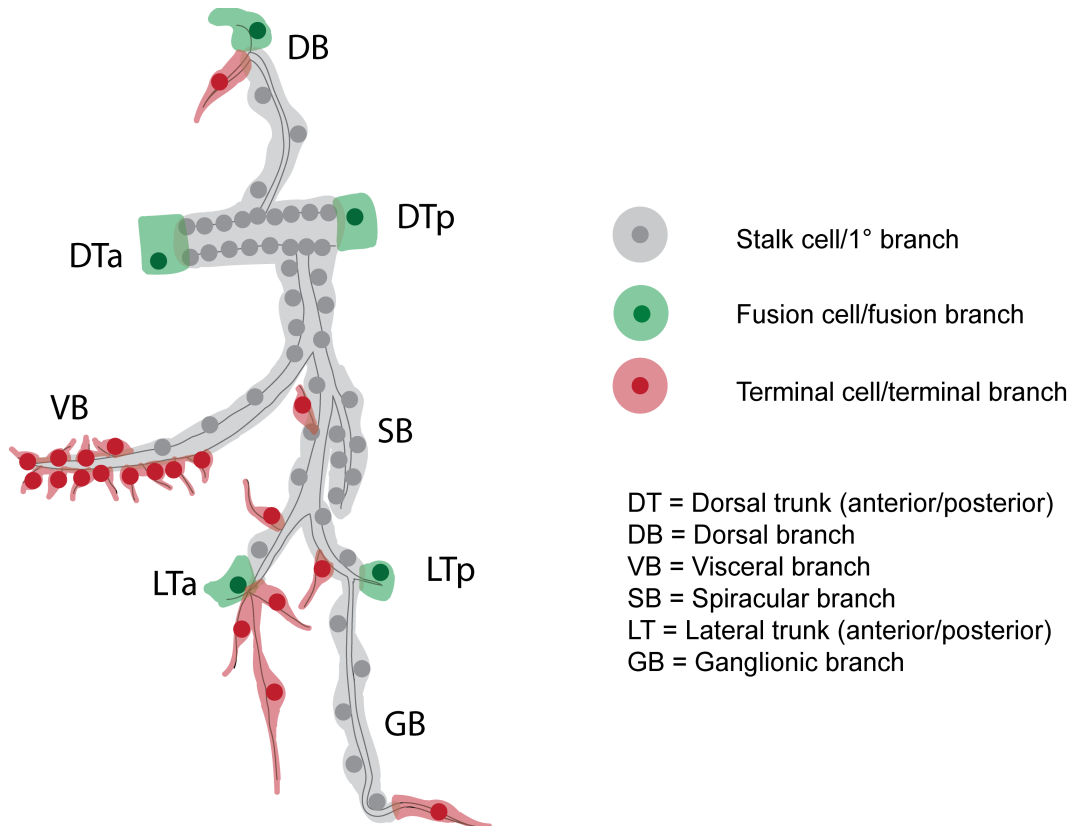


**Figure 4: *Drosophila* tracheal system (modified from Uv et al, 2003)**

Lateral view of a metamere in the embryonic tracheal network. Each metamere is formed by 80 tracheal cells that are arranged in a specific fashion with multicellular primary branches forming the basic framework and unicellular terminal branches reaching into the target tissue. Specialised fusion cells are mediating the connection to the neighbouring metamere.

During pupal development most larval tissues die and pupal and adult tissues form from imaginal cells. These imaginal cells are tissue specific progenitor cells that remain quiescent during earlier development (Kylsten and Saint 1997).

The tracheal network is one of the structures that is histolyzed and build from new during metamorphosis. At metamorphosis most of the posterior trachea are lost (tracheal metameres Tr6 to Tr10) and new branches are supplied from Tr4 and Tr5 to

form the pupal abdominal trachea (PAT). Additionally new branches form from Tr2 to supply the flight muscle (Sato and Kornberg 2002; Cabernard and Affolter 2005; Weaver and Krasnow 2008). Even though most of the anterior trachea are retained, most of the larval tracheal cells are replaced by imaginal cells (Cabernard and Affolter 2005; Guha and Kornberg 2005). As two possible candidates for the formation of the pupal trachea either dedifferentiated tracheal cells or the spiracular branch imaginal cells have been suggested (Weaver and Krasnow 2008; Chen and Krasnow 2014). Recently it has been verified that the PAT are indeed derived from imaginal progenitors using the larval trachea as scaffold before the posterior larval tissue is decaying (Chen and Krasnow 2014). Progenitor outgrowth is directed by Bnl signalling. It has been shown that *bnl* is not expressed in the surrounding tissue, such as previously in the described examples of tracheal outgrowth, but instead within the larval trachea. At the same time larval trachea no longer express *btl* and therefore no longer react to the Bnl signal (Weaver and Krasnow 2008; Chen and Krasnow 2014). Thus the formation of the pupal, which gives rise to the adult tracheal network, is based on Bnl signalling.

## 1.4 Hypoxia

The sufficient supply of oxygen is of major importance for the thriving and survival of most organisms. For unicellular organism this is achieved by the diffusion of oxygen through the cell membrane. The evolution of multicellular organisms brought up the necessity of efficient mechanisms for the supply and transport of oxygen as well as the supply of nutrients and the removal of waste. Local or global hypoxia, the shortage of oxygen, is detrimental for the organism. Therefore a multitude of coping mechanisms have been developed to improve oxygen supply in deprived tissues

### 1.4.1 Hypoxia in vertebrates

In vertebrates oxygen is absorbed through the lungs and transported, carried by the blood and distributed through blood vessels. Both parts of this system are composed of tubes of different sizes: the aveoli of the lung and the blood vessels of the circulatory system. While the larger tubes of these systems are mainly used for the transport of oxygen, the smaller vessels deliver the oxygen into individual cells of the organism where it leaves the vessel by diffusion into the source tissue. In cases of hypoxia the described system needs to adjust in order to ensure proper oxygen supply (Carmeliet 2003). In vertebrates the adaptation to global or local hypoxia is mainly carried out by improving the transport of oxygen from the respiratory surface to the oxygen consuming tissues and increased effectiveness of ATP production by utilizing anaerobe glycolysis instead of oxidative mechanisms (Hochachka et al. 1996). This is achieved, amongst

other things, by the use of Hypoxia-Inducible Factors (HIFs) (Pugh and Ratcliffe 2003), that encode for transcription factors that are involved in the alteration of angiogenesis through Vascular Endothelial Growth factor (VEGF) signalling (Ferrara et al. 2003). HIFs are a master regulator of angiogenesis and therefore regulate a broad number of genes and subsequent alterations of the vascular system in response to oxygen deprivation (Semenza and Wang 1992; Wang and Semenza 1993). They are composed of the oxygen regulated  $\alpha$ -subunits and the constitutive  $\beta$ -subunits. Under sufficient oxygen conditions enzymes from the prolyl hydroxylase family (PHD) complex to oxygen and subsequently hydroxylate the HIF- $\alpha$  subunit on two conserved proline residues located within the HIF- $\alpha$  oxygen-dependent degradation domain (ODDD) (Kaelin and Ratcliffe 2008). Hydroxylation of the proline residues leads to the binding of the von Hippel–Lindau E3 ubiquitin ligase complex and the subsequent ubiquitination of HIF- $\alpha$ , targeting it for proteasomal degradation (Kaelin and Ratcliffe 2008). During oxygen shortage the  $\alpha$ -subunit is stabilized and translocates to the nucleus where it binds to the  $\beta$ -subunit and forms a transcriptional complex with p300 and CBP (Jiang et al. 1997; Mahon et al. 2001). The complex subsequently binds to the hypoxia response element (HRE) where it enhances the expression of target genes (Wenger et al. 2005). Amongst these target genes are a number of pro-angiogenic factors including vascular endothelial growth factor (VEGF), angiopoietin-1, angiopoietin-2, platelet-derived growth factor (PDGF) and the basic fibroblast growth factor (bFGF) (Carmeliet et al. 1998). As a result of the expression of these pro-angiogenic factors the vascular system is altered to respond to the oxygen need of the affected tissues. This is achieved by multiple adjustments within the vascular system like the increase of vascular permeability, endothelial cell proliferation, sprouting, migration, adhesion, and the formation of new tubes (Fong 2008).

The study of angiogenesis during hypoxia is of special interest for understanding the dynamics of tumour growth. During the formation of a tumour the increased proliferation and metabolism of the tissue lead to a greater demand for oxygen and therefore for a localized hypoxia (Krock et al. 2011). The inhibition of angiogenesis during early tumour formation, to cut the tumour from the supply of oxygen and nutrients needed to supply a larger tumour, thus constitutes a rewarding target for the therapy of cancer (Parangi et al. 1996). Additionally a connection between hypoxia during tumour formation and the expression and localization of *furin* has been established. Previous studies have shown that hypoxia during tumour growth is stimulating the expression of *furin* (McMahon et al. 2005). Additionally the relocalization of Furin from the *trans*-Golgi network to the cell surface is enhancing cancer cell invasion (Arsenault et al. 2012). Taken together an interesting connection between hypoxia and Furin can be established.

### 1.4.2 Hypoxia in *Drosophila*

The Insect respiratory system is composed of trachea, an epithelial tubular structure, which form an intricate network to deliver oxygen into all internal tissues throughout the whole life cycle (Manning and Krasnow 1993; Kornberg 2002; Cabernard and Affolter 2005). The dramatic changes in the body plan *Drosophila* is going through during its lifetime go along with changing oxygen needs of the animal. Especially the rapid increase of volume in the larval stages requires a fast sensing of oxygen levels and immediate adaption of the oxygen delivery system in order to respond to the changing oxygen needs of the larva (Wigglesworth 1954; Locke 1958; Wigglesworth 1983; Jarecki et al. 1999; Metzger and Krasnow 1999; Centanin et al. 2008). During this phase the terminal branches of the tracheal network are plastic and able to react to the environmental oxygen condition, which ensures adequate supply of oxygen to all larval tissues (Wigglesworth 1954; Locke 1958; Wigglesworth 1983; Jarecki et al. 1999; Metzger and Krasnow 1999; Centanin et al. 2008).

In *Drosophila* the transcription factor Similar (Sima) is the only known homologue to HIF-1 $\alpha$  and thus the master regulator of the hypoxia response (Bacon et al. 1998). Similar to its vertebrate homologue Sima is carrying an ODDD that is responsible for oxygen sensitivity (Lavista-Llanos et al. 2002) and a hydroxylation site that is hydroxylated in an oxygen dependent manner (Arquier et al. 2006). The *Drosophila* homologue of PHD is Fatiga (Fga). Similar to the vertebrate homologue there are three known isoforms, FgaA (homologues to PHD2), FgaB and FgaC (homologues to PHD3), of which one (FgaB) is hypoxia inducible (Acevedo et al. 2010). After hydroxylation Sima is subsequently targeted by the *Drosophila* von Hippel Lindau E3 ubiquitin ligase (dVHL) and targeted for proteasomal degradation (Aso et al. 2000; Hsouna et al. 2010).

During hypoxia Sima is no longer hydroxylated and degraded. As a consequence Sima accumulates in the cell, translocates to the nucleus and binds to the  $\beta$ -subunit Tango (Tgo). Hif binds to so called hypoxia response elements (HREs), thereby triggering the expression of the genes of interest. *Bnl* and *btl* have been suggested to be regulated by Hif (Centanin et al. 2008). Nevertheless, until now no HREs corresponding to *bnl* and *btl* could be identified.

*Drosophila* larvae raised under hypoxia develop an increased number of terminal trachea, while larvae raised under hyperoxia show a decreased number of terminal trachea. Additionally the morphology of the trachea is affected by the oxygen conditions during larval development. While the terminal trachea grow straight during hyperoxia and normoxia, hyperoxia causes the terminal trachea to take a curly shape (Jarecki et

al. 1999; Centanin et al. 2008). Taken together former data suggest that terminal trachea outgrowth is regulated by oxygen demand, but the exact mechanism remains unclear. The suggested mechanisms for tracheal remodelling during hypoxia include the upregulation of *bnl* and *btl* expression (Jarecki et al. 1999; Centanin et al. 2008). Since *bnl* and *btl* are major factors for the formation of the tracheal network, including the formation of terminal trachea, their upregulation would explain the adjustments of the tracheal network to the oxygen conditions. Nevertheless the involvement of *bnl* and *btl* could not be verified as the regulatory factor for tracheal remodelling during hypoxia yet.

## 1.5 Proteolytic processing

Proteolytic processing can play a key role in the regulation of signal transduction pathways. Proteases can control the amount of critical components by removing regulatory proteins, activation of dormant factors or the release of intermembrane proteins (Turk et al. 2012). Thus proteolytic processing adds another layer of regulation to signal transduction and aid in the fine-tuning of their spatial and temporal control.

Proteases show a high degree of specificity when binding and processing their substrates. Substrate recognition is influenced by a number of different factors like the localization of the protease and the substrate, pH and the substrate specificity of the protease. Substrate specificity is often based on the structural properties of the active site or by so called adaptor proteins that mediate the binding of protease and substrate (Turk et al. 2012).

### 1.5.1 Subtilisin proprotein convertases and Furin

Proteases form a group of enzymes that are able to catalyze the hydrolysis of peptide bounds, resulting in the fragmentation of the substrate peptide. They have evolved multiple times during evolution and can be found in animals, plants, bacteria, archaea and viruses (Turk et al. 2012). Proteases can be divided into serine, threonine, cysteine, aspartic and metallo proteases depending on the residue or ion that carries out the catalysis in the active site (Turk et al. 2012).

Subtilisin proprotease convertases (SPC) are a family of calcium dependent serine proteases. They are known to be involved in the proteolytic activation of many secreted proteins. The first member of the SPC family, Kex2, was discovered to be responsible for the proteolytic maturation of the  $\alpha$ -Mating Factor in *Sacheromyces cerevesia* (Wickner and Leibowitz 1976; Achstetter and Wolf 1985). Since then multiple other members of the SPC family have been identified. These include Furin, the Prohormone

Convertases (PCs, PC 1/3, PC2, PC4, PC5/6, PC7) and Pace4, which are produced as zymogen and need autoproteolysis for activation (Rockwell et al. 2002; Thomas 2002).

Of special interest for this work is the SPC Furin, which can be found in all vertebrate species and many invertebrates. Human Furin is a 794 amino acid transmembrane protein. It carries an N-terminal signal peptide that promotes transport of the inactive proprotein to the ER. Similar to other members of the SPC family Furin prodomain contains, in addition to the signalpeptide, cleavage sites that allow for autoproteolytic processing (Anderson et al. 1997; Thomas 2002).

Unlike the Kexin protease, which cleaves C-terminal of a dibasic residue, Furin has the more distinguished recognition motive of  $-R-X-K/R-R\downarrow-$  (X is an arbitrary amino acid and the arrow indicates cleavage site). Since the P2 basic residue (K/R) is not essential for cleavage,  $-R-X-X-R\downarrow-$  represents the minimal Furin cutting site (Molloy et al. 1992). In exceptional cases additional to this more favourable minimal Furin site a less favourable  $-K/R-X-X-X-K/R-R\downarrow-$  is cleaved by Furin (Molloy et al. 1992; Thomas 2002).

The localization of Furin has been described as very dynamic. It cycles between the *trans*-Golgi network, the endosome and the cell surface (Molloy et al. 1994; Molloy et al. 1999). The dynamic trafficking of Furin offers a partial explanation for its diverse numbers of substrates and thus its involvement in a diverse number of processes. While the mechanism of Furin trafficking is not yet fully understood, it has been considered that both anterograde and retrograde transport are Clathrin-mediated (Teuchert et al. 1999a; Teuchert et al. 1999b; Crump et al. 2001).

Furin is important for several different processes during embryogenesis and homeostasis. Additionally Furin-mediated processing plays an important role in diseases including cancer progression and anthrax (Molloy et al. 1992; Arsenault et al. 2012).

In the central nervous system (CNS) Furin is processing a number of different factors including the neurotrophins proNGF and neural cell adhesion cueing proteins (Bresnahan et al. 1990; Kalus et al. 2003; Seidah 2011). For example the essential cell surface receptor Neuropilin that functions in Semaphorin-dependent axon guidance and (VEGF)-dependent angiogenesis is inhibited due to the Furin-mediated processing of Semaphorin 3F (Sema3F) (Parker et al. 2010; Seidah 2011). Processing of Sema3F inhibits competitively the binding of VEGF to Neuropilin, resulting in an antiangiogenic effect (Parker et al. 2010). Furthermore, Furin-mediated processing plays a role in the regulation of the effectiveness of several retroviruses (Hallenberger et al. 1992) and



influenza viruses, as well as neurotropic viruses, such as the influenza virus serotypes H1N1 and H5N1 (Walker et al. 1994; Pasquato and Seidah 2008; Sun et al. 2010; Seidah 2011). This is carried out by the Furin-mediated processing of surface glycoproteins of infectious viruses and parasites which leads to the formation of the mature and fusogenic envelope glycoprotein (Molloy et al. 1999).

Additionally Furin is playing an important role in cancer progression. It has been recently discovered that hypoxia is enhancing cancer cell invasion through relocalization of Furin from the *trans*-Golgi network to the cell surface (Arsenault et al. 2012). The assessment of the mechanism revealed that both Rab4GTPase-dependent recycling and interaction of Furin with the cytoskeletal anchoring protein, Filamin-A are essential for this hypoxia induced relocalization of Furin (Arsenault et al. 2012).

### 1.5.2 Proteolytic processing in *Drosophila*

In *Drosophila* the three identified members of the SPC family are Amontillado (Amon), DFurin1 (DFur1) and DFurin2 (DFur2). While Amon is related to vertebrate PC2, DFur1 and DFur2 are closely related to vertebrate Furin.

Amon is involved in the development of the embryonic nervous system. *amon* mutants, although showing no morphological defects, are partially embryonic lethal and show an impaired hatching behaviour and stunted larval growth (Siekhaus and Fuller 1999; Rayburn et al. 2002).

Similar to their mammalian homologues both *Drosophila* Furins are serine proteases and transmembrane proteins. They carry N-terminal signal peptides and locate preferentially in the *trans*-Golgi network. Their prodomain is removed by autocatalytic cleavage. Unlike its human homologue Dfur1 exists in three different isoforms (Dfur1, DFur1-CRR and DFur1-X) that differ in their subcellular localization (de Bie et al. 1995; Roebroek et al. 1995).

*Dfur1* and *Dfur2* transcripts are maternally supplied and the proteins expressed ubiquitously in the early embryo. During later development *Dfur1* expression can be detected in multiple organs including the central nervous system (CNS), hindgut and lateral clusters of epithelial cells (Hayflick et al. 1992; Roebroek et al. 1993; de Bie et al. 1995). *Dfur2* expression can be seen in the embryonic nervous system and in the developing trachea during late embryonic development (Roebroek et al. 1995).

Proteolytic processing is a common mechanism in the regulation of multiple processes during *Drosophila* development. It is crucial for the regulation of many signal transduction pathways including TGF- $\beta$ , Delta/Notch and EGF signalling (Molloy et al.

1992; Blaumueller et al. 1997; Logeat et al. 1998; Lee et al. 2001; Urban et al. 2001; Künnapuu et al. 2009).

Bone morphogenic protein (BMP) signalling is of major importance for embryonic development. BMPs owe their name to the ability to ectopically induce bone formation in non-bony tissue. Additionally BMPs are needed for the establishment of the dorsoventral body axis during early development and induction of epidermal fate. All TGF- $\beta$  ligands, including the vertebrate BMPs and the *Drosophila* homologue Decapentaplegic (Dpp) and Glas Bottom Boat (Gbb) are initially produced as inactive precursor proteins. Dpp and Gbb are cleaved by DFur 1 and DFur2, which releases the active protein (Künnapuu et al. 2009; Fritsch et al. 2012).

Analysis of Dpp revealed a total of three different Furin cleavage sites, which are used in a multi-step process by DFur1 and DFur2 in an alternating fashion (Künnapuu et al. 2009). Using only two of the three Furin sites at a time proteolytic processing is producing two different isoforms. Cleavage at Furin site II and Furin site III is resulting in the larger Dpp26 while cleavage at Furin site II and Furin site I is producing Dpp23 (Künnapuu et al. 2009). This processing has shown to be tissue specific and the resulting Dpp isoforms are necessary to differentiate between the development of wings and legs compared to the development of the gut (Künnapuu et al. 2009; Wharton and Derynck 2009).

Notch signalling is a prominent example for juxtacrine signalling in *Drosophila*. Binding of Notch to the proteins Delta, Jagged or Serrate, expressed by neighbouring cells, is known to participate in a process known as lateral inhibition (reviewed in Ehrbauer et al., 2006). Processing of the Notch receptor is essential for its function during development. Notch is initially cleaved in the *trans*-Golgi by a Furin-like protease (Blaumueller et al. 1997; Logeat et al. 1998). While one of the resulting fragments contains most of the extracellular domain, the second fragment is carrying the rest of the extracellular domain as well as the intermembrane domain and the intracellular domain. The two fragments form a heterodimer at the cell surface (Logeat et al. 1998; Rand et al. 2000). Upon ligand binding Notch is cleaved twice by different proteases. While the first cleavage releases the extracellular domain from the receptor, the second cleavage releases the intracellular domain (Brou et al. 2000; Fortini 2002; Lieber et al. 2002). Subsequently the released intracellular domain enters the nucleus where it interacts with members of the CLS family and starts expression of downstream genes (reviewed in Ehrbauer et al., 2006).

The cleavage of the EGF ligand Spitz (Spi) by the serine protease Rhomboid is an especially interesting case of proteolytic processing during *Drosophila* development. Spi is cleaved within its transmembrane domain. Cleavage by Rhomboid is releasing a secreted form of the ligand, which is then binding to its receptor DER (Drosophila EGF Receptor) (Lee et al. 2001; Urban et al. 2001).

## 1.6 Analysis of proteolytic processing in *Drosophila* FGFs

As described above (1.5.2) *Drosophila* SPCs are involved in the regulation of multiple signal transduction pathways including the signalling of the TGF- $\beta$  homologue Dpp and the juxtacrine signalling factor Notch. But recently Bnl has been shown to be a novel ligand for DFur1 (Koledachkina 2010). Processing occurs C- and N-terminally from the FGF core domain, thereby releasing a fragment with the FGF domain, which roughly resembles the size of its vertebrate homologue. Cleavage of Bnl has been shown to be indispensable for the activity and secretion. Inhibition of the Fur1 protease results in the disruption of the tracheal network, thereby duplicating the *bnl* loss-of-function phenotype (Koledachkina 2010). So far the necessity for Furin-mediated cleavage of Bnl was demonstrated for Bnl signalling during larval development only. This work is investigating the role of Bnl processing further. The investigated processes include Bnl signalling during later development and hypoxia. Additionally the hypothesis of Furin-mediated processing of Bnl as a regulatory mechanism or even rate-limiting step of Bnl signalling will be tested.

Finally the two FGF8-like proteins, Pyr and Ths, have recently shown to be cleaved into fragments that roughly correspond to the size of a vertebrate FGF by an unknown protease. Additional experiments with truncated constructs of Pyr and Ths, corresponding to the observed cleaved fragments, show that the cleaved fragments are functional and secreted. Moreover, these truncated constructs seem to induce Htl-signalling more potently than the full-length proteins (Tulin and Stathopoulos 2010).

Taken together proteolytic processing, possibly executed by the protease Fur1, might constitute a regulatory mechanism for all *Drosophila* FGF signalling, possibly executed by the protease Fur1.

## 2 Material and Methods

### 2.1 Methods

#### 2.1.1 Molecular Cloning

##### *2.1.1.1 Polymerase chain reaction (PCR)*

PCR was used to obtain DNA fragments for further cloning or to confirm success of previous cloning steps. Phusion High-Fidelity DNA polymerase (Finnzymes or NEB respectively) was used for PCR products produced for further cloning while Hot Star Master Mix (Quiagen) was used for analytical PCRs. PCR program was adjusted to suit the used polymerase and primer pair. All PCRs were performed in the Biorad T100 Cycler.

##### *2.1.1.2 DNA Agarose gel electrophoresis*

For analysis or purification of DNA probes, they were loaded into agarose gels (0.8 - 1.5% agarose in 1xTAE buffer with added ethidium bromide (Roth). Additional loading of an appropriate DNA Ladder 1kb or 100bp DNA Ladder (NEB) allowed estimation of the DNA probes approximate size. Stained DNA was visualized with transilluminator UV solo TS (Biometra).

##### *2.1.1.3 DNA Gel extraction*

Desired fragments visualized with an UV-lamp on the 366nm setting and cut from the agarose gel with a scalpel and extracted with the QIAquick Gel Extraktion Kit (Quiagen) according to the manufacturer's manual.

##### *2.1.1.4 Measurement of DNA concentration*

DNA concentration was determined by administering a 1µl aliquot of the probe to the NanoDrop 1000 Spectrophotometer (Thermo Scientific) and measured at 260nm according to the manufacturer's manual.

##### *2.1.1.5 DNA digestion with restriction endonucleases*

Digestion reactions were carried out as described by (Sambrook et al. 1989). For analytical reactions 1-2µg of DNA and for preparative reaction 5µg of DNA were incubated with a suitable amount of restriction endonucleases in a volume of 10-20µl of the buffer recommended by the manufacturer. The incubation was done at 37°C if not indicated otherwise by the manufacturer. Analytical reactions were incubated for 1 hour

while preparative reactions were incubated for up to 3 hours and purified by agarose gel electrophoresis followed by gel extraction.

#### *2.1.1.6 DNA Ligation*

For a ligation reaction (Sambrook et al. 1989), 50-100ng of linearized vector DNA was combined with a purified PCR fragment or digested vector fragment in the molar ratio 1:3. 1µl of T4-Ligase (Fermentas) and a suitable amount of T4Ligase buffer (Fermentas) was added. Reactions were performed in a total volume of 10-30µl at room temperature for 1-2 hours.

#### *2.1.1.7 Site-directed mutagenesis*

Point mutations were introduced by oligonucleotides containing the desired mutation additional to complementary flanking regions (Weiner et al. 1994). These oligonucleotides were acquired in both possible orientation and used in combination with oligonucleotides for one of the termini each in PCR. The two resulting fragment were extracted and used as a template for a consecutive PCR using the terminal oligonucleotides as primers. The 2<sup>nd</sup> PCR results in the full size fragment carrying the desired point mutation. These fragments were purified and subsequently introduced into pENTR/D-TOPO. Resulting clones were sequenced and checked for the substituted nucleotides.

#### *2.1.1.8 Introduction of deletions*

The basic approach that was used for the mutating single nucleotides (2.1.1.7) was used in a modified version to introduce deletions via PCR. For this purpose the design of the oligonucleotides has to be carefully adjusted.

#### *2.1.1.9 Gateway TOPO-cloning*

For directional topo-cloning of PCR fragments the pENTR/D-TOPO cloning Kit (Invitrogen) was utilized. The PCR reaction was set up according to the manufacturer's protocol with a forward primer containing a specific overhang at its 5' end to ensure directional cloning. The One Shot TOP10 chemically competent *E. coli* cells supplied with the Kit were used for following transformation of the created construct.

#### *2.1.1.10 Gateway LR Recombination*

For the LR recombination the LR Gateway recombination kit (Invitrogen) was used according to the manufacture's manual. 100-150ng of the destination vector was combined with 50-100ng of the entry vector pENTR/ D-topo containing the desired DNA

fragment inside an rfA-recombination cassette. One Shot TOP10 chemically competent *E. coli* cells were used for following transformation of the created construct.

#### *2.1.1.11 Preparation of chemically competent cells E. coli cells*

LB cultures were inoculated with 1ml of an overnight culture of the desired *E.coli* strain per 100ml of LB medium. Cultures were incubated at 37°C on a shaker until reaching an OD<sub>600</sub> of between 0.2 and 0.4. The cells were then cooled down on ice for two minutes and subsequently spun down in sterile containers using a centrifuge precooled to 4°C for 10 minutes at 7000rpm. The resulting pellet was resuspended in 30ml ice cold TfbI-buffer (100mM RbCl, 50mM MnCl<sub>2</sub>, 10mM CaCl, 30mM potassiumacetat, 15% (w/v) glycerol brought to pH5.8 with acetic acid) and incubated on ice for 30-60minutes. The buffer is removed by centrifugation at 4°C and 7000rpm for 10 minutes and the pellet is resuspended in 3ml ice-cold TfbII- buffer (10mM MOPS, 10mM RbCl, 75mM CaCl<sub>2</sub>, 15% (w/v) glycerol brought to pH7.0 with NaOH) and incubated on ice for 15minutes. The suspension was quickly aliquoted, frozen in liquid nitrogen and stored at -80°C.

#### *2.1.1.12 Transformation of chemically competent cells E. coli cells*

Heat-shock transformation was carried out according to (Inoue et al. 1990). 5-10 µl of a ligation reaction or Gateway cloning reaction was added to an aliquot of chemically competent *E.coli* that was thawed on ice. After 20 minutes of incubation on ice the cells were heat-shocked at 42°C for 60 seconds and transferred back onto the ice. 300µl of LB medium were added to the *E.coli* cells before incubation at 37°C for 1h under constant agitation. The culture was split into two unequal aliquots, which were plated onto LB-agar plates containing the appropriate antibiotic to ensure proper selection for desired clones.

#### *2.1.1.13 Plasmid DNA isolation*

Plasmid DNA was isolated using the Plasmid Plus Midi Kit (Quiagen). A single colony of transformed *E.Coli* cells was cultured overnight in 50ml LB medium containing an appropriate antibiotic under constant agitation and harvested the next day by centrifugation at 4000rpm for 20 minutes. Isolation of the plasmid from cultured cells was carried out according to the manufacture's manual.

#### *2.1.1.14 Sequencing*

For sequencing 1-1.5µg of Plasmid DNA were diluted in a total volume of 15µl pure water. Oligonucleotides were supplied in a 10pmol/µl concentration if necessary. The

probes were sent to the MWG sequencing facility where the sequencing reaction was carried out.

## **2.1.2 Cell Culture**

### *2.1.2.1 Maintenance of Drosophila cell lines*

*Drosophila* cell culture lines Kc167 and S2R+ (DGRC) were maintained in Schneiders medium (Gibco) supplemented with 10% fetal calf serum (FCS) (Thermo Scientific) and 100µg/ml penicillin/streptomycin (Gibco). Cells were cultured in 25cm<sup>2</sup> bottles or 6-well plates (Corning and Greiner Bio One).

### *2.1.2.2 Freezing and thawing of Drosophila cell lines*

For freezing cell lines a healthy culture of approximately 5x10<sup>6</sup> cell/ml was harvested by centrifugation. The cells were resuspended in freezing medium (Schneiders medium + 20% FCS +10% DMSO, sterilized by filtration) to a concentration of 2x10<sup>7</sup> cell/ml. Aliquots of 0.5ml cell suspension are placed into cryogenic vials. The cryogenic vial are incubated for 24h in a freezing container (Nalgene, Mr. Frosty) filled with isopropanol at -80°C to ensure slow freezing of the suspension. On the following day the aliquots are transferred into liquid nitrogen for permanent storage.

For thawing frozen cell lines a 25cm<sup>2</sup> flask is prepared with 5ml of an appropriate medium. The frozen specimen is removed from the liquid nitrogen and thawed by adding medium into the cryogenic vial and pipetting up and down. The thawed specimen is then placed into the prepared flask and incubated for 1-2h at 25°C. The culture is controlled via inverted microscope. If the cells are adhering to the bottom of the flask the supernatant is carefully removed and replaced with fresh medium to remove the remaining DMSO. This procedure was repeated after 24h.

### *2.1.2.3 Transient Transfection of Drosophila cell lines*

Confluent cell cultures were plated into 6-well plates and incubated for about 24h to approximately 70% confluency. The transfection was conducted with the Effectene Transfection Kit (Quiagen). The manufacturer's protocol was modified for *Drosophila* cell culture lines. For each well of a 6-well plate 1 µg of plasmid DNA was combined with 200µl of EC buffer, 20µl of Enhancer reagent, 8µl of Effectene reagent and a suitable amount of cell culture medium. The mix was then added drop-wise into the cell culture. On the next day the cell culture medium was removed, the adherent cells were washed 3 times with sterile PBS and serum-free medium was added to the cells. The cells were

incubated for 2 days at 25°C. Cells and supernatant was harvested as described 2.1.2.4 and 2.1.2.5.

#### *2.1.2.4 Preparation of cell lysates for Western blot*

Cells were washed twice with 1xPBS and harvested. PBS buffer was subsequently removed and replaced with 100µl 1x loading buffer (50 mM Tris-HCl pH 6.8, 1% SDS, ~0,01% bromphenol blue, 50 mM Dithiothreitol (DTT), 5% Glycerol). Lysis was carried out by incubation at 95°C for 5 minutes.

#### *2.1.2.5 Preparation of cell culture supernatant for Western blot*

Drosophila cells were grown and transfected as described above (2.1.2.3). 24h after transfection standard cell culture medium was replaced with a medium containing no FCS and culture maintained for another 48h. Cell culture medium was harvested and remaining cells removed by centrifugation at 1500rpm. Cell-free supernatants were concentrated using trichloroacetic acid (TCA) protein precipitation. For this purpose 100% TCA solution (500g TCA, 227g water) was added to the specimen to a final concentration of 10-15%. Samples were incubated at -20°C over night to induce precipitation. Precipitation was harvested by centrifugation at 15000rpm at 8°C for 20 minutes. Resulting pellets washed with ice cold acetone (Merck) and air dried. Supernatant pellets were dissolved in 50µl 1x loading buffer and incubated for 5 minutes at 95°C.

### **2.1.3 Proteomic Methods**

#### *2.1.3.1 SDS Protein Gel Electrophoresis*

For SDS Gel Electrophoresis a modified approach after Laemmli (1970) was used. Protein polyacrylamide gels (PAGEs) were precast using 8% and 10% concentrations of acrylamide in the resolving gel (375 mM Tris-Cl pH 8.8, 0,1% SDS, 0,1% ammonium persulfate (APS), 0,08% tetramethylethylenediamin (TEMED), appropriate percentage of 30% acrylamide-bisacrylamide solution) and 5% acrylamide in the stacking gel (5% acrylamide, 130 mM Tris-Cl pH 6.8, 0,1% SDS, 0,1% APS, 1µg/ml TEMED). Samples were mixed with an appropriate amount of 4x loading buffer and incubated at 95°C for 5 minutes prior to loading. Samples were loaded along with Spectra Multicolor Broad Range Protein Ladder (Pierce Biotechnologie) or PageRuler Prestained protein ladder (Fermentas) and run Mini Protean II System (Bio Rad) until the dye front reaches the end of the gel. Electrophoresis was performed in running buffer (25 mM Tris, 250 mM Glycine, 0,1% SDS) and at constant amperage of 30mA per used PAGE.



### 2.1.3.2 *Western Blot and Protein Immunodetection of Western Blot*

Western blotting was performed using the Mini Protean II system (BioRad) and nitrocellulose membrane (GE Healthcare). Blotting was performed in 1x transferbuffer (5 mM Tris, 250 mM Glycine, 20% methanol) at a constant voltage of 50 V for 1hour 30 minutes. All subsequent steps were performed rocking on a shaker at room temperature if not mentioned otherwise. The membrane was quickly rinsed 3 times with 1xPBT (1x PBS with 0,01% Tween-20) and subsequently blocked for 2hours in 1x blocking buffer (Sigma Alderich) to avoid strong cross reactions of antibodies used for protein detection. The membrane was incubated overnight at 4°C with an appropriately concentrated primary antibody diluted in in 1x blocking buffer. On the following day the primary antibody is removed by washing the membrane 3 times for 15minutes with 1xPBT and the HRP-coupled secondary antibody is applied in the same fashion and incubated for 2hours. The secondary antibody is removed by washing 3 times for 15minutes with 1xPBT. Finally the detection of the antibody signal is achieved by incubation of the membrane with Super Signal West Dura Extended Duration Substrate (Pierce) according to the manufacturers manual, which will result in a chemiluminescent signal. This signal is detected by using LAS 1000Plus IDX2 Intelligent Dark Box II luminescence detector (Fujifilm). Reprobing is achieved by using Western Blot stripping buffer (Thermo Scientific) according to the manufacturers manual to remove primary and secondary antibodies from the first probing. The stripped membrane is washed 3 times for 15minutes with 1xPBT and the detection is repeated as described above.

### 2.1.4 *Drosophila Techniques*

#### 2.1.4.1 *Maintenance of Drosophila melanogaster strains*

Fruit flies were maintained in plastic vials on a food containing corn flour, soya flour, molasses and yeast. Flies were kept on 25°C or 18°C.

#### 2.1.4.2 *GAL4/UAS system for ectopic gene expression*

To achieve a temporally and spatially specific expression patterning in *Drosophila* embryos and larvae the GAL4/UAS-expression system was utilized (Brand and Perrimon 1993). In this system the yeast factor GAL4 is expressed in a specific spacio-temporal pattern. The GAL4 protein interacts with the upstream activating sequence (UAS) and thereby allows the expression of a downstream target gene. In the experimental setting transgenic flies carrying a *gal4* coding sequence under the control of a specific promotor were mated with transgenic flies carrying the sequence for the gene of interest downstream of the UAS. The resulting progeny is expressing the gene

of interest in a temporal and spatial pattern determined by the promotor upstream of the *gal4* sequence.

#### *2.1.4.3 GAL80 system for temporally controlled ectopic gene expression*

An additional level of spatio-temporal control of expression was added by utilizing the GAL80 system (Lee and Luo 1999; Suster et al. 2004). In this system temperature-sensitive GAL80 construct is expressed under a specific promotor. GAL80 is inhibiting GAL4 expression and thereby prevents the expression of the target gene. Expression of GAL80 can be initiated by placing the flies at 18°C, while storage at 29°C is preventing expression of GAL80 and enabling expression of the target gene.

#### *2.1.4.4 Collection and fixation of Drosophila embryos*

For embryo collections flies were transferred into a cage and provided with apple juice agar plate with added yeast paste. Embryos were harvested from the plate with brush and sieves and thoroughly washed with water to remove residual yeast paste. The chorion was removed by incubation in 50% bleach for 3 minutes followed by another thorough wash with water. For fixation the dechorionated embryos were transferred into a vial containing 1ml fixation solution (4%paraformaldehyde (PFA), 50mM EGTA) and 6ml heptane and incubated on a shaker for 20min at room temperature. For the following devitellinization the aqueous phase was removed, 5ml of methanol were added and the vial was shaken vigorously. The heptan and embryos remaining in the interphase were discarded. Devitellinized embryos were washed with methanol 3-5 times and stored in methanol short term at 4°C or long term at -20°C.

#### *2.1.4.5 Hypoxic and Hyperoxic treatment*

For hypoxic and hyperoxic treatment 50-100 embryos were collected for 6h at 25°C on apple juice agar plates and transferred into vials containing fly food with no living yeast. The vials are closed off with permeable stoppers to enable gas exchange and thereby ensure stable concentrations of oxygen within the vials. The vials were then placed into custom-made air tight chambers that were then flushed with premixes of either 5% oxygen and 95% nitrogen or 60% oxygen and 40% nitrogen (Westphalen). The containers were placed at 25°C and the embryos incubated in hypoxic/hyperoxic conditions until reaching 3<sup>rd</sup> instar wandering stage. During the incubation chambers were flushed with fresh gas daily to ensure stable oxygen concentrations.

#### 2.1.4.6 Trachea analysis of *Drosophila* larvae

Larvae were collected in 3<sup>rd</sup> instar “wandering stage”. After collection larvae were killed by placing them at -20°C for at least 1hour. Larvae were subsequently mounted in 80% glycerol and analyzed by bright field microscopy.

#### 2.1.4.7 X-Gal staining

Larvae were collected from vials in “wandering stage” 3<sup>rd</sup> instar. Larvae were washed with water and stored on ice to induce cold rigor. Desired tissues were then dissected from the larvae in ice-cold PBS buffer and subsequently fixed for 5min in 2% glutaraldehyde in PBS under rotation. For each staining the staining solution was mixed freshly by combining 75µl of 100mM K<sub>3</sub>[Fe<sup>III</sup>(CN)<sub>6</sub>], 75µl of 100mM K<sub>4</sub>[Fe<sup>II</sup>(CN)<sub>6</sub>], 150µl x-Gal solution (20mg/ml in dimethylformamide (DMF)) and 1,2ml PBT. After fixation the sample was rinsed with PBT and staining solution added. The staining is incubated on a shaker was checked frequently. After desired intensity was reached removal of the staining solution and multiple washing steps with PBT stopped the reaction. The stained specimen was placed into 50% glycerol (in water) and incubated until the tissue was equilibrated or overnight. For further analysis the larval tissues were embedded in 100% glycerol and subsequently analyzed by bright field microscope.

#### 2.1.4.8 Embryo Immunostaining

The following steps were performed at room temperature and under constant rotation if not mentioned otherwise. Fixed embryos were rehydrated by washing once in 50% 1xPBT and 50% methanol and 3 times in 1xPBT. The embryos were blocked for 20minutes in blocking buffer (5% sheep serum in 1xPBT) to avoid cross-reactions of the antibodies. The embryos were incubated with a suitable concentration of the primary antibody diluted in blocking buffer for 1 hour at room temperature or overnight at 4°C. The primary antibody was removed by washing the embryos 3 times for 15 minutes with 1xPBT. A suitable secondary antibody was added to the embryos in the same fashion, incubated for 2 hours and removed by washing the embryos 3 times for 15 minutes with 1xPBT. If signal amplification was needed a biotin-coupled secondary antibody was used together with the ABC Elite PK6100 Kit (Vector Laboratories). For the amplification reaction 10µl of solution A was mixed with 10µl solution B in 500µl of PBT and incubated for 30 minutes before use. The embryos were incubated with the premixed solution for 45-60 minutes. After washing 3 times for 15 minutes with 1xPBT the staining was developed by adding a solution derived from adding SIGMAFAST 3,3'-Diaminobenzidine and H<sub>2</sub>O<sub>2</sub> tablets (Sigma Aldrich) into 1ml of water thereby detecting peroxidase activity of the HRP-coupled secondary antibody that is contained in the AB-

solution. The reaction was stopped by washing multiple times with 1xPBT. For mounting in benzyl benzoate or Canada balsam the stained embryos were dehydrated through a graded ethanol series before mounting.

#### *2.1.4.9 Fixation of Drosophila larva tissues*

Larvae from the “wandering stage” 3<sup>rd</sup> instar were picked from the vial and immobilized by storing on ice. Preparation of the larval tissues was performed in ice-cold PBS and precooled preparation dishes. The desired tissues were collected in 12-well plates. The following steps were carried out at room temperature and under mild shaking. PBS was replaced by 4%PFA in PBS and the specimens were fixed for 20 minutes. After fixation the larval tissues were washed 3 times for 15minutes with PBT.

#### *2.1.4.10 Acetone treatment for RNA in situ hybridization*

To improve the quality of the *in situ* hybridization an acetone treatment after (Nagaso et al. 2001) is carried out. Unless indicated otherwise all steps are performed at room temperature and under mild agitation. For improved staining fixed samples were washed twice with ethanol for 5 minutes and subsequently incubated in 50% Xylene in Ethanol for 1 hour. The mixture was removed and the larval tissues washed twice with ethanol for 5 minutes. The samples were then rehydrated by immersion in a graded methanol series before they were incubated in 80% acetone in water for 10 minutes at -20°C. The acetone was removed and the samples washed twice for 5minutes with PTwx (0.1%Tween-20, 0.1% Triton X-100 in PBS). For refixation the tissues were incubated with 4%PFA in PBS for 20 minutes and subsequently washed again with PTwx to remove the fixing solution.

#### *2.1.4.11 RNA in situ hybridization of Drosophila larval tissues*

Unless indicated otherwise all steps are performed at room temperature and under mild agitation. The fixed larval tissues were incubated with 50% Hyb solution (50% Formamide, 5x SSC) and PBT for 20min at RT and 3 times in Hyb solution for 20 minutes at 60°C for prehybridization. For hybridization the Hyb solution was discarded and 2µl of DIG labelled RNA probe in 20 µl of Hyb was added to the specimen. Hybridization was performed overnight at 60°C in water bath. On the following day the labeled RNA probe was discarded and the samples washed 3 times with Hyb solution at 60°C. The samples were briefly rinsed with 50% Hyb solution in PBT before washing 3 times for 20 minutes with PBT. Subsequently an anti-DIG-AP antibody (diluted in PBT) was placed on the larval tissues and incubated for 1 hour. The specimens were then washed 3 times for 20 minutes with PBT and 3 times for 5 minutes with NBT buffer

(100mM NaCl, 50mM  $MdCl_2$ , 100mM Tris-HCl pH9.5, 0.1% Triton X-100). For the staining reaction the larval tissues were incubated in a mixture of 4.5 $\mu$ l NBT and 3.5 $\mu$ l BCIP (50mg/ml 5-Brom-4-Chlor-3-Indolylphosphat in DMF) in 1ml PBT in darkness until the desired intensity of the staining was reached. The staining reaction was interrupted by washing with PBT and the stained tissues placed in 50% glycerol over night for dehydration. The following day the specimens were mounted in 100% glycerol and examined by light microscopy.

#### *2.1.4.12 Bright field microscopy*

Stained embryos and larval tissues were analyzed using Zeiss Axiophot microscope (Carl Zeiss AG) with x10 or x20 magnification objectives.

#### *2.1.4.13 Confocal microscopy*

Embryos and larval tissues stained with fluorescent dyes and fluorophore-coupled secondary antibodies were analyzed with either the Zeiss LSM780 or the Leica TCS SP2 confocal microscope with x10 or x20 magnification objectives.

### **2.1.5 Computing**

#### *2.1.5.1 Primer Design*

Oligonucleotides for molecular cloning, site-directed mutagenesis and deletions were designed using programs from the DNASTAR suite.

#### *2.1.5.2 Alignment of DNA sequences*

Alignments of DNA sequences for the control of sequenced cloning products were conducted using programs from the DNASTAR suite.

#### *2.1.5.3 Alignment of protein sequences*

Alignments of multiple protein sequences for comparison of homologues were conducted using programs from the DNASTAR suite.

## 2.2 Material

### 2.2.1 Plasmids

Plasmid Number	Insert	Vector	Manufacturing
EMRP1	WgSP-EGFP-rfA-Myc	pUbi	cloned by Tatyana Koledashkina
EMRP2	Pyr	pENTR/D-TOPO	cloned by Tatyana Koledashkina
EMRP3	Pyr	pUbi-WgSP-EGFP-rfA-Myc	LR-recombination of EMRP1 and EMRP3
EMRP4	Ths	pENTR/D-TOPO	PCR with EMRP05 and EMRP06 Cloned via NheI and AscI
EMRP5	Ths	pUbi-WgSP-EGFP-rfA-Myc	LR-recombination of EMRP1 and EMRP4
EMRP6	$\alpha$ -Pdx	pUbi	From pCDNA3.1- $\alpha$ 1-PDX (from Tatyana Koledashkina) Cloned via XbaI and SpeI
EMRP7	Pyr MFS1	pENTR/D-TOPO	PCR with EMRP02, EMRP13, EMRP14 and EMRP03 Cloned via NheI and AscI
EMRP8	Pyr MFS1	pUbi-WgSP-EGFP-rfA-Myc	LR-recombination of EMRP1 and EMRP7
EMRP9	Pyr MFS1 R $\rightarrow$ L	pENTR/D-TOPO	PCR with EMRP02, EMRP15, EMRP16 and EMRP03 Cloned via NheI and AscI
EMRP10	Pyr MFS1 R $\rightarrow$ L	pUbi-WgSP-EGFP-rfA-Myc	LR-recombination of EMRP1 and EMRP9
EMRP11	Pyr MFS1+2	pENTR/D-TOPO	PCR with EMRP02, EMRP17, EMRP18 and EMRP03 Cloned via NheI and AscI
EMRP12	Pyr MFS1+2	pUbi-WgSP-EGFP-rfA-Myc	LR-recombination of EMRP1 and EMRP11
EMRP13	Pyr MFS1-3	pENTR/D-TOPO	PCR with EMRP02, EMRP19, EMRP20 and EMRP03 Cloned via NheI and AscI
EMRP14	Pyr MFS1-3	pUbi-WgSP-EGFP-rfA-Myc	LR-recombination of EMRP1 and EMRP13
EMRP15	Pyr MFS1-4	pENTR/D-TOPO	PCR with EMRP02, EMRP13, EMRP21 and EMRP22  Cloned via NheI and AscI
EMRP16	Pyr MFS1-4	pUbi-WgSP-EGFP-rfA-Myc	LR-recombination of EMRP1 and EMRP15

EMRP17	Pyr MFS1-5	pENTR/D-TOPO	PCR with EMRP02, EMRP13, EMRP23 and EMRP24  Cloned via NheI and AscI
EMRP18	Pyr MFS1-5	pUbi-WgSP-EGFP-rfA-Myc	LR-recombination of EMRP1 and EMRP17
EMRP19	Pyr MFS1-6	pENTR/D-TOPO	PCR with EMRP02, EMRP25, EMRP26 and EMRP03  Cloned via NheI and AscI
EMRP20	Pyr MFS1-6	pUbi-WgSP-EGFP-rfA-Myc	LR-recombination of EMRP1 and EMRP19
EMRP21	Ths MFS1	pENTR/D-TOPO	PCR with EMRP05, EMRP27, EMRP28 and EMRP06  Cloned via NheI and AscI
EMRP22	Ths MFS1	pUbi-WgSP-EGFP-rfA-Myc	LR-recombination of EMRP1 and EMRP21
EMRP23	ThsMFS1+2	pENTR/D-TOPO	PCR with PCR with EMRP05, EMRP29, EMRP30 and EMRP06  Cloned via NheI and AscI
EMRP24	ThsMFS1+2	pUbi-WgSP-EGFP-rfA-Myc	LR-recombination of EMRP1 and EMRP23
EMRP25	ThsMFS1-3	pENTR/D-TOPO	PCR with PCR with EMRP05, EMRP31, EMRP32 and EMRP06  Cloned via NheI and AscI
EMRP26	ThsMFS1-3	pUbi-WgSP-EGFP-rfA-Myc	LR-recombination of EMRP1 and EMRP25
EMRP27	Pyr	pUASTattB-rfA	LR-recombination of pUASTattb-rfA and EMRP2
EMRP28	Pyr MFS1	pUASTattB-rfA	LR-recombination of pUASTattb-rfA and EMRP2
EMRP29	Pyr MFS1-3	pUASTattB-rfA	LR-recombination of pUASTattb-rfA and EMRP14
EMRP30	Pyr MFS1-6	pUASTattB-rfA	LR-recombination of pUASTattb-rfA and EMRP19
EMRP31	Ths	pUASTattB-rfA	LR-recombination of pUASTattb-rfA and EMRP4
EMRP32	ThsMFS1	pUASTattB-rfA	LR-recombination of pUASTattb-rfA and EMRP21

EMRP33	ThsMFS1-3	pUASTattB-rfA	LR-recombination of pUASTattb-rfA and EMRP25
EMRP34	Py276	pENTR/D-TOPO	PCR with EMRO1 and EMRO33 TOPO-cloning
EMRP35	Py276	pUbi-WgSP-EGFP-rfA-Myc	LR-recombination of EMR1 and EMRP36
EMRP36	Pyr293	pENTR/D-TOPO	PCR with EMRO1 and EMRO34 TOPO-cloning
EMRP37	Pyr293	pUbi-WgSP-EGFP-rfA-Myc	LR-recombination of EMRP1 and EMRP36
EMRP38	Pyr310	pENTR/D-TOPO	PCR with EMRO1 and EMRO35 TOPO-cloning
EMRP39	Pyr310	pUbi-WgSP-EGFP-rfA-Myc	LR-recombination of EMRP1 and EMRP38
EMRP40	Pyr310MFS1	pENTR/D-TOPO	PCR with EMRO1, EMRO13, EMRO14 and EMRO35 TOPO-cloning
EMRP41	Pyr310MFS1	pUbi-WgSP-EGFP-rfA-Myc	LR-recombination of EMRP1 and EMRP40
EMRP42	Pyr310MFS1 R→L	pENTR/D-TOPO	PCR with EMRO1, EMRO15, EMRO16 and EMRO35 TOPO-cloning
EMRP43	Pyr310MFS1 R→L	pUbi-WgSP-EGFP-rfA-Myc	LR-recombination of EMRP1 and EMRP42
EMRP44	Pyr350	pENTR/D-TOPO	PCR with EMRO1 and EMRO36 TOPO-cloning
EMRP45	Pyr350	pUbi-WgSP-EGFP-rfA-Myc	LR-recombination of EMRP1 and EMRP44
EMRP46	Pyr430	pENTR/D-TOPO	PCR with EMRO1 and EMRO37 TOPO-cloning
EMRP47	Pyr430	pUbi-WgSP-EGFP-rfA-Myc	LR-recombination of EMRP1 and EMRP46
EMRP48	Ths130	pENTR/D-TOPO	PCR with EMRO3 and EMRO38 TOPO-cloning



EMRP49	Ths130	pUbi-WgSP-EGFP-rfA-Myc	LR-recombination of EMRP1 and EMRP48
EMRP50	Ths150	pENTR/D-TOPO	PCR with EMRO3 and EMRO39 TOPO-cloning
EMRP51	Ths150	pUbi-WgSP-EGFP-rfA-Myc	LR-recombination of EMRP1 and EMRP50
EMRP52	Ths199	pENTR/D-TOPO	PCR with EMRO3 and EMRO40 TOPO-cloning
EMRP53	Ths199	pUbi-WgSP-EGFP-rfA-Myc	LR-recombination of EMRP1 and EMRP52
EMRP54	Ths247	pENTR/D-TOPO	PCR with EMRO3 and EMRO41 TOPO-cloning
EMRP55	Ths247	pUbi-WgSP-EGFP-rfA-Myc	LR-recombination of EMRP1 and EMRP54
EMRP56	Ths323	pENTR/D-TOPO	PCR with EMRO3 and EMRO42 TOPO-cloning
EMRP57	Ths323	pUbi-WgSP-EGFP-rfA-Myc	LR-recombination of EMRP1 and EMRP56
EMRP58	Pyr $\Delta$ 293-310	pENTR/D-TOPO	PCR with EMRO1, EMRO43, EMRO44 and EMRO3 TOPO-cloning
EMRP59	Pyr $\Delta$ 293-310	pUbi-WgSP-EGFP-rfA-Myc	LR-recombination of EMRP1 and EMRP58
EMRP60	Pyr $\Delta$ 277-310	pENTR/D-TOPO	PCR with EMRO1, EMRO45, EMRO46 and EMRO3 TOPO-cloning
EMRP61	Pyr $\Delta$ 277-310	pUbi-WgSP-EGFP-rfA-Myc	LR-recombination of EMRP1 and EMRP60
EMRP62	Thsr $\Delta$ 140-150	pENTR/D-TOPO	PCR with EMRO4, EMRO47, EMRO48 and EMRO6 TOPO-cloning
EMRP63	Thsr $\Delta$ 140-150	pUbi-WgSP-EGFP-rfA-Myc	LR-recombination of EMRP1 and EMRP62

## 2.2.2 Oligonucleotides

Oligo Number	Oligo Name	Oligo Sequence (5'→3')
EMRO1	Pyr-topo	CACCGCGAAAAATGTTTTAACATTG
EMRO2	Pyr-for	GCGAAAAATGTTTTAACATTG
EMRO3	Pyr-rev	TAAATCTATATAATACAAGCTAACAAAATACTTACC
EMRO4	Ths-topo	CACCTTATGTACAGTAGAAGATTACG
EMRO5	Ths-for	TTATGTACAGTAGAAGATTACG
EMRO6	Ths-rev	CGCAAATCTCTGATGAGTGAACC
EMRO7	PyrSP-topo	CACCATGTTCCACAAGTTCATGCC
EMRO8	ThsSP-topo	CACCATGTCTGAATCAGTTAGAGAG
EMRO9	Pyr-TAG-rev	CTATAAATCTATATAATACAAGCTAACAAAATACTTACC
EMRO10	Ths-TAG-rev	CTACGCAAATCTCTGATGAGTGAACC
EMRO11	$\alpha$ 1-PDX-for	CATTAAGAAGACAAAGGG
EMRO12	$\alpha$ 1-PDX-rev	CCGGCAATGGCCTGTTCC
EMRO13	PyrMFS1-for	CTCCATGGCCGCCACGGGTTGCAAC
EMRO14	PyrMFS1-rev	GTTGCAACCCGTGGCGGCCATGGAG
EMRO15	PyrMFS1 R→L-for	AAACTCCATAAACGCCACAAGTTGCAACAAA
EMRO16	PyrMFS1R→L-rev	TTTGTGCAACTTGTGGCGTTTATGGAGTTT
EMRO17	PyrMFS2-for	CAACGCGGTCGCCAGGGGCAGTACG
EMRO18	PyrMFS2-rev	CGTACTGCCCTGGCGACCGCGTTG
EMRO19	PyrMFS3-for	CGTCGCGGCTTGAGGGGCAGCAGC
EMRO20	PyrMFS3-rev	GCTGCTGCCCTCCAAGCCGCGACG
EMRO21	PyrMFS4-for	GGAGGGCGAGCAGGGCGAGGC
EMRO22	PyrMFS4-rev	GCCTCGCCCTGCZCGCCCTCC
EMRO23	PyrMFS5-for	CGTCGCAAGGGGGACAGGCGAAAAGGCTCGGCGGGAGCA
EMRO24	PyrMFS5-rev	TGCTCCCGCCGAGCCTTTTCGCTGTCCCCCTTGCGACG
EMRO25	PyrMFS6-for	CTTCTTGGTGGCCTCGGGTTGC
EMRO26	PyrMFS6-rev	GCAACCCGAGGCCACCAAGAAG

EMRO27	ThsMFS1-for	GTTGGCATGGGGGAGCTGGGAGATACCTGC
EMRO28	ThsMFS1-rev	GCAGGTATCTCCCAGCTCCCCATGCCAAC
EMRO29	ThsMFS2-for	CAGCAAGGGCAAGGGCGGGCGAAGAAAG
EMRO30	ThsMFS2-rev	CTTTCTTCGCCCCGCCCTTGCCCTTGCTG
EMRO31	ThsMFS3-for	GAAGGGACCCATAGGGAAGTTC
EMRO32	ThsMFS3-rev	GAACTTCCCTATGGGTCCCTTC
EMRO33	Py276	CAACTCATTATTGTTACTGC
EMRO34	Pyr293	ATGGAGTTTGCGATTTCTGTG
EMRO35	Pyr310	CAGCTGCCGCTTCTTTTGTG
EMRO36	Pyr350	CGGCGACGTCTACGCCGTT
EMRO37	Pyr430	CCGCTTGCGACGACTGGCCG
EMRO38	Ths130	CTTACCTCGGTGCGTGAACCCG
EMRO39	Ths150	GGCCTCGATCTTGTTGAACATG
EMRO40	Ths199	ATTTTGGTTATTCGATTTGTGGCG
EMRO41	Ths247	TTGCTGCTGTTGCTGCCTCTG
EMRO42	Ths323	CATTGCTGCTGTTGTGATCG
EMRO43	Pyr $\Delta$ 293-310-for	CCTGCAGAGAAATCGCAAACCTCCATCAACGCCGTCGCCAGC GGCAGTACG
EMRO44	Pyr $\Delta$ 293-310-rev	CGTACTGCCGCTGGCGACGGCGTTGATGGAGTTTGCGATTT CTCTGCAGG
EMRO45	Pyr $\Delta$ 277-310-for	CAACAGCAGTAACAATAATGAGTTGCAACGCCGTCGCCAGC GGCAGTACG
EMRO46	Pyr $\Delta$ 277-310-rev	CGTACTGCCGCTGGCGACGGCGTTGCAAACCTCATTATTGTTA CTGCTGTTG
EMRO47	Thsr $\Delta$ 140-150-for	CCAAGAAGAGCGTCAACGATGAGCAGTTTTTCCGCCATC
EMRO48	Thsr $\Delta$ 140-150-rev	GATGGCGGAAAAACTGCTCATCGTTGACGCTTTCTTGG

## 2.2.3 Fly stocks

### 2.2.3.1 Fly stocks generated for this work

Stock number	Genotype	Source/ Description
EMRF1	y[1] w[*];;[Pw+mC]UAST- Pyr	Transgene of EMRP27
EMRF2	y[1] w[*];;[Pw+mC]UAST- pyrMFS1	Transgene of EMRP28
EMRF3	y[1] w[*];;[Pw+mC]UAST- PyrMFS1-3	Transgene of EMRP29
EMRF4	y[1] w[*];;[Pw+mC]UAST- PyrMFS1-6	Transgene of EMRP30
EMRF5	y[1] w[*];;[Pw+mC]UAST- Ths	Transgene of EMRP31
EMRF6	y[1] w[*];;[Pw+mC]UAST- Ths1-3	Transgene of EMRP33

### 2.2.3.2 Other fly stocks

Stock number	Genotype	Source/ Description
104696	y[*] w[*]; P{w+mW.hs=GawB}Fur1NP4490 / TM6, P{w=UAS-lacZ.UW23-1}UW23-1	Kyoto DGRC
112825	w[*]; P{w+mW.hs=GawB}NP2211 / TM3, Sb[1] Ser[1]	Kyoto DGRC
8860	w[1118] P{w[+mW.hs]=GawB}Bx[MS1096]	Bloomington
36523	y[1] w[*]; P{w[+mW.hs]=GawB}C-765	Bloomington
26793	y[1] w[*]; wg[Sp-1]/CyO; P{w[+mW.hs]=GawB}29BD	Bloomington
TKF9	y[*] w[*];;Pw+mCUAST- $\alpha$ 1-PDX/TM3,Ser	Tatyana Koledaskina
1747	y[1] w[*]; P{GawB}71B	Bloomington
5460	w[*];; P{da-GAL4}/P{da-GAL4}	Bloomington
10341	ry[506] P{ry[+t7.2]=PZ}Fur1[rL205]/TM3, ry[RK] Sb[1] Ser[1]	Bloomington
109128	y[1] w[67c23]; P{GAL4-btl.S}2	Kyoto DGRC
9488	w[*]; P{w[+mW.hs]=GawB}Mz97 P{w[+mC]=UAS-Stinger}2	Bloomington
8164	w <sup>1118</sup>	Bloomington
8410	P{w[+mC]=DII-UAS-lacZ}1, y[1] w[1118]	Bloomington

6384	ry506 P{PZ}bnl00857/TM3, Sb[1]	Bloomington
41914	y[1] sc[*] v[1]; P{y[+7.7] v[+1.8]=TRIP.HMS02311}attP2	Bloomington
30029	y[1] w[1118]; P{w[+mC]=tubP-GAL4}LL7 P{ry[+7.2]=neoFRT}82B/TM6B, Tb[1]	Bloomington
Gö935	w[*];P{w[+*]=KrGal4-40.0}	Departmental stock
RS249	w[*]UAS-bnl[b4-2]; Sco/CyO	Reinhard Schuh
RS245	w+;UAS-λbt1/TM3	Reinhard Schuh
	w[1118]; P{w[+mW.Scer\FRT.hs]=RS3}CG1516[CB- 0292-3]	Ronald Kühnlein
RKF771	y[1] w[*]; P{w[+mC]=tubP-Gal80[ts]}20; P{w[+mC]=tubPGAL4}/TM6B, Tb P{w[1]	Ronald Kühnlein
	w[*];;P{btl-moe.mRFP1}3, /TM6B, Tb[1]	Markus Affolter
	{w[+mC]=UAS-srcEGFP}M7A, w[1118];; P{btl- moe.mRFP1}3, /TM6B, Tb[1]	Gerd Vorbrüggen
	y[*] w[*];;Pw+mCUAST-α1-PDX, P{btl-moe.mRFP1}3, /TM6B, Tb[1]	Gerd Vorbrüggen

## 2.2.4 Antibodies

### 2.2.4.1 Primary antibodies

Antibody	Source	Producer	Epitope	Dilution
Anti-GFP	rabbit	Synaptic Systems	EGFP	1:2000 (for Western blot)  1:1000 (for Immunohistochemistry)
Anti-MYC	mouse	Iowa-Hybridoma Bank	MCY tag	1:30
Anti-Eve	rabbit	Gift from Manfred Frasch	Eve	1:2000

*2.2.4.2 Secondary antibodies*

<b>Antibody</b>	<b>Source</b>	<b>Producer</b>	<b>Label</b>	<b>Dilution</b>
Mouse IgG	goat	Pierce	HRP	1:10000
Rabbit IgG	goat	Pierce	HRP	1:10000
DIG	sheep	Roche	Alkaline phosphatase	1:2000
Rabbit IgG	goat	Invitrogen	Alexa 568	1:500
Rabbit IgG	goat	Vector Laboratories	biotinylated	1:500

## 3 Results

### 3.1 Branchless processing in the larva

Proteolytic processing is a powerful mechanism commonly used for the control of growth factors and other signalling molecules or the modification of their function. The specific cleavage of signalling molecules can lead both to activation and inactivation of the original protein and is often accompanied by severe changes in size, structure and function of the proteins. Examples of *Drosophila* signalling molecules modified by proteolytic processing include the EGF ligand Spitz (Lee et al. 2001; Urban et al. 2001), the TGF- $\beta$  ligand Decapantaplegic (Künnapu et al. 2009), Spätzle (DeLotto and DeLotto 1998) or Notch (Blaumueller et al. 1997; Lieber et al. 2002). Proteolytic processing can regulate the spatio-temporal patterning of signalling, similar to other posttranslational modifications like phosphorylation and methylation, thereby adding another layer of plasticity.

Bnl processing has shown to be essential for its activation and thus for FGF signalling during *Drosophila* embryonic development (Koledachkina 2010). The cleavage is conducted by the Fur1 proprotein convertase, which cleaves Bnl at four distinct cutting sites N- and C-terminal of its central domain. This cleavage results in the release of the central fragment that contains the FGF-domain and corresponds to the size of a vertebrate FGF.

*fur1* and *bnl* are co expressed during embryogenesis which leads to the complete processing of Bnl during embryonic development. Therefore it is not possible to distinguish between Fur1-mediated cleavage as a novel regulatory mechanism of Bnl activity and processing of Bnl as a general process during Bnl secretion similar to the removal of the signal peptide in the ER.

However, the importance of Bnl for tracheal patterning is not exclusive to embryonic development but continues throughout larval and pupal stages (Jarecki et al. 1999; Sato and Kornberg 2002; Centanin et al. 2008; Roy and Kornberg 2011). The processing of Bnl by Fur1 could be either restricted to Bnl signalling in the embryo, or it could be required also during later developmental stages and could represent a new regulatory mechanism for Bnl signalling in selected tissues and developmental stages in *Drosophila*.

Two different models are commonly used to assess Bnl signalling in the larva: The air sac primordium (ASP) on top of the wing imaginal disc and the formation of thick

terminal branches (TTBs) of the dorsal branches. Both models will be used during this work to study the role of Fur1-mediated processing for Bnl signalling.

### 3.1.1 Bnl processing in the wing disc

During embryonic development Bnl is expressed in a highly dynamic pattern at locations where primary and secondary branches form and expression is shut off close to the end of embryonic development when tracheal patterning is completed (Sutherland et al. 1996). However, it had previously been shown that Bnl expression starts again in the first instar larva and is expressed throughout all larval stages shaping the tracheal network of the larva (Jarecki et al. 1999; Sato and Kornberg 2002; Chen and Krasnow 2014). Bnl signalling therefore plays an important role for the growth and patterning of the larval tracheal network and thus the analysis of tracheal patterning in the larva constitutes a good model of studying Bnl signalling in the larva.

The ASP of the wing imaginal disc gives rise to the air sac in the adult thorax, a reservoir that is thought to oxygenate thoracic structures like the flight musculature (Sato and Kornberg 2002). During the 3<sup>rd</sup> larval instar the ASP is forming from a trachea close to the basal surface of the wing disc from where it grows towards the centre of the wing disc. Both the initiation of APS formation and the following outgrowth and shaping of the air sac are strongly dependent on Bnl signalling (Kornberg 2002; Cabernard and Affolter 2005). The developing air sac of *Drosophila* has shown to be a valuable model and the investigation of this structure has shed some light into multiple processes such as tissue invasion during branching morphogenesis and directed tubule formation (Kornberg 2002; Cabernard and Affolter 2005; Wang et al. 2010).

If Fur1-mediated processing of Bnl plays a role in the formation of the ASP Fur1 should be co-expressed at least partially with Bnl in the wing disc. In order to investigate the expression pattern of these two genes Gal4 lines integrated in the *bnl* or *fur1* promoter regions were utilized. The two Gal4 lines were used to drive the expression of UAS constructs containing the coding sequences for *lacZ* which allows the visualization of the expression pattern of *bnl* and *fur1* in the wing disc.

X-Gal staining of dissected wing imaginal discs reveals that *bnl*-Gal4 is driving expression of *lacZ* diffusely at the posterior side of the disc dorsally from the hinge region, close to the area where the air sac is to be expected (Figure 5) (Cabernard and Affolter 2005). This expression domain is highly related to the expression pattern of *bnl* mRNA shown before (Sato and Kornberg 2002) indicating that the *bnl* GAL4 line drives expression in the *bnl* expression domain in the wing disc. *fur1*-Gal4 is driving expression in a well-defined oval region dorsally of the hinge region, which not only



verifies the presence of both Bnl and Fur1 within the wing disc but also suggests a partially overlapping expression domain of the two genes. To map *bnl* and *fur1* expression into more detail the GAL4 lines were used to drive expression of GFP in the presence of a *btl*-RFPmoesin construct. In this construct an RFPmoesin fusion protein is expressed under the control of the *btl* promoter thereby visualizing the forming air sac (Ribeiro et al. 2004; Cabernard and Affolter 2005). Testing for the expression of the driver lines and visualizing the air sac at the same time revealed that *fur1* Gal4 line is not expressed in the exact area underneath the forming the air sac, but rather distal of it.

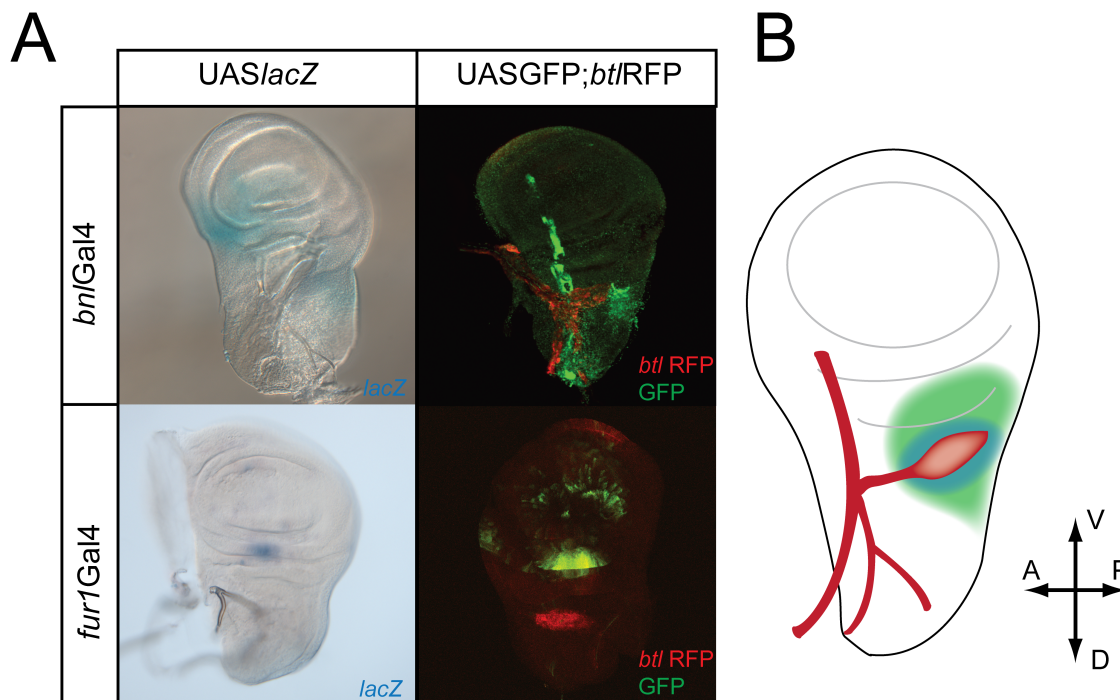


**Figure 5: *bnlGal4* and *fur1Gal4* drive expression in the wing imaginal disc**

**(A) Left column:**  $\beta$ Gal expressed in the wing imaginal disc by *bnlGal4* and *fur1Gal4*.  $\beta$ Gal expression is visualised by X-Gal staining. **Right column:** GFP expressed by *bnlGal4* and *fur1Gal4*. Air sac primordium (ASP) is labelled in red by the *btl*-RFPmoesin construct in which RFPmoesin is expressed under the control of the *btl* promoter. **(B)** Schematic drawing of the wing imaginal disc including trachea and ASP (red) and presumptive expression domain of *bnl* (green) and *fur1* (blue). Note: Both Gal4 lines express markers at the presumptive location of the air sac primordium.

This could mean that *bnl* and *fur1* are not expressed in the same region of the wing disc. But the result could also be explained by the fact that in contrast to the *bnl* Gal4 line the *fur1* Gal4 line does not drive expression in the pattern of the *fur1* gene at least in the wing disc. The visualization of *fur1* expression via the *fur1* Gal4 line simply might be incomplete. An alternative explanation could be the rather short live time of the GFP

used as the reporter. Since it is unclear when exactly Bnl processing might be needed during larval development the exact time point was probably missed by analyzing the expression pattern rather late.

These problems could be resolved with more direct staining techniques like immunostaining or *in situ* hybridization. Since the attempt to produce a functional peptide antibody against Fur1 was unsuccessful an *in situ* hybridization of *fur1* was carried out using a modified approach involving the treatment of the imaginal disc with a xylene-ethanol mixture and acetone (Nagaso et al. 2001). The results showed the expression of *fur1* mRNA in the expected area underneath the air sac, suggesting the presence of the Fur1 protein in this area as well (Figure 6).

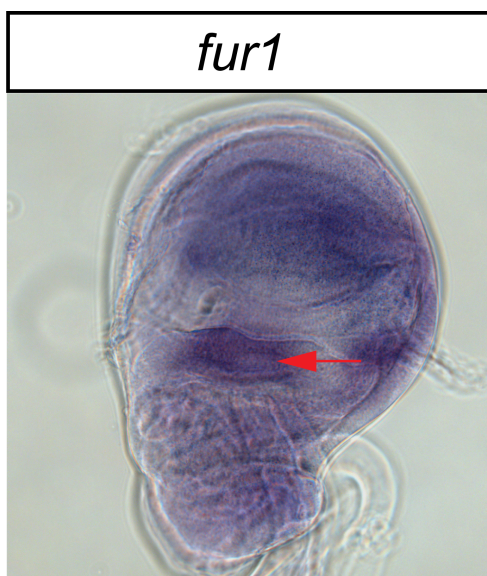


**Figure 6: Detection of *fur1* mRNA in the wing imaginal disc.**

*In situ* hybridisation shows *fur1* mRNA in the expected area underneath the ASP, suggesting the co-localisation of the Fur1 protein (red arrow).

The *in situ* experiment suggested a co-localization of *fur1* and *bnl* within the wing imaginal disc, thus enabling Bnl processing by Fur1 in the wing disc. However, the data derived by *in situ* hybridisation need further confirmation with the additional visualization of the air sac. Nevertheless, it seemed reasonable to assume a co-localisation of Bnl and Fur1, which would enable the proteolytic processing of Bnl by Fur1 within the wing disc.

### 3.1.2 Furin-mediated processing of Bnl is necessary for the formation of the air sac

The presence of Bnl and Fur1 in the wing disc alone allows no conclusion about the biological relevance of Furin-mediated processing of Bnl during air sac formation. To test for the importance of Bnl processing during this process Fur1 activity was inhibited within the wing disc and air sac formation used as biological read out for Bnl activity.

A widely used method of determining the importance of the activity of a protease is the use of a specific inhibitor in comparison to the original experiment. Fortunately in the case of Fur1 a small peptide inhibitor, called Alpha1-antitrypsin variant Portland ( $\alpha$ 1-PDX), is available (Benjannet et al. 1997; Jean et al. 1998; Molloy et al. 1999).  $\alpha$ 1-PDX is a selective and potent inhibitor of the SPC family of proteases. It was engineered from a natural occurring mutation of the human  $\alpha$ 1- anti trypsin protease,  $\alpha$ 1- anti trypsin Pittsburgh. It achieves its inhibitory function through a minimal Furin consensus motive in its reactive site and has been shown to inhibit Furin activity both in cell culture and *Drosophila* embryos (Benjannet et al. 1997; Koledachkina 2010).

Three Gal4 lines were used to express  $\alpha$ 1-PDX in different locations and strength within the wing disc. UAS GFP was used to determine the expression pattern of the different driver lines. While 29BDGal4 showed a strong expression in the whole wing pouch and in the distal region of the hinge region of the wing disc (Figure 7), C765Gal4 showed the strongest expression in the central region of the wing pouch and weaker expression levels dorsal and ventral of it (Figure 7). Both 29BDGal4 and C765Gal4 drive expression in the area underneath the forming air sac, while MS1096Gal4 is driving expression only in the wing pouch and thus shows no overlap in expression with *bni* (Figure 7). Therefore, expression of  $\alpha$ 1-PDX using this driver lines 29BDGal4 and C765Gal4 should inhibit Bnl processing whereas MS1096Gal4 should not. Thus if Bnl processing is essential, expression of the inhibitor using 29BDGal4 and C765Gal4 should inhibit the formation of the air sac whereas MS1096Gal4 should not. In addition to an UAS $\alpha$ 1-PDX construct for the overexpression of the Furin inhibitor the *btl*/RFPmoesin construct was used to enable the assessment of the air sac. Additional transmitted light pictures are shown to prove that the air sac and the overlaying trachea were not removed during preparation.

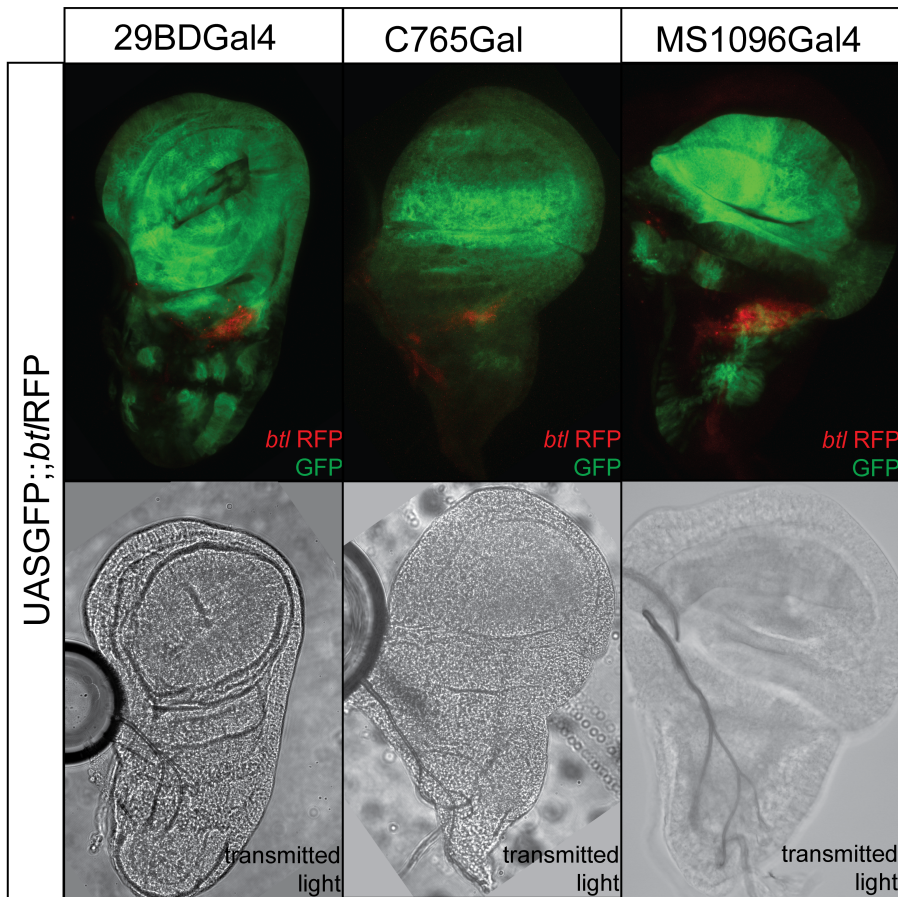


**Figure 7: Expression domain of Gal4 driver lines in the wing imaginal disc.**

**Upper row:** GFP (green) expressed in the wing imaginal disc controlled by 29BDGal4, C765Gal4 and MS1096Gal4. Air sac primordium (ASP) is labelled in red by the *btl*-RFPmoesin construct. **Lower row:** Corresponding transmitted light pictures to show that the ASP was not removed during preparation. Note: Two of the tested lines show clear expression in the area underneath the ASP (29BDGal4 and C675Gal4), while the third line is not (MS1096Gal4).

The expression of  $\alpha$ 1-PDX with 29BDGal4 and C765Gal4 resulted in the complete loss of the air sac while expression with MS1096Gal4 wing discs with an air sac (Figure 8). Inhibition of the Furin protease activity therefore is sufficient to suppress the Bnl-dependent outgrowth of the air sac (Figure 8). This indicates that Bnl processing is needed for air sac formation and its necessity is not limited to embryonic development.

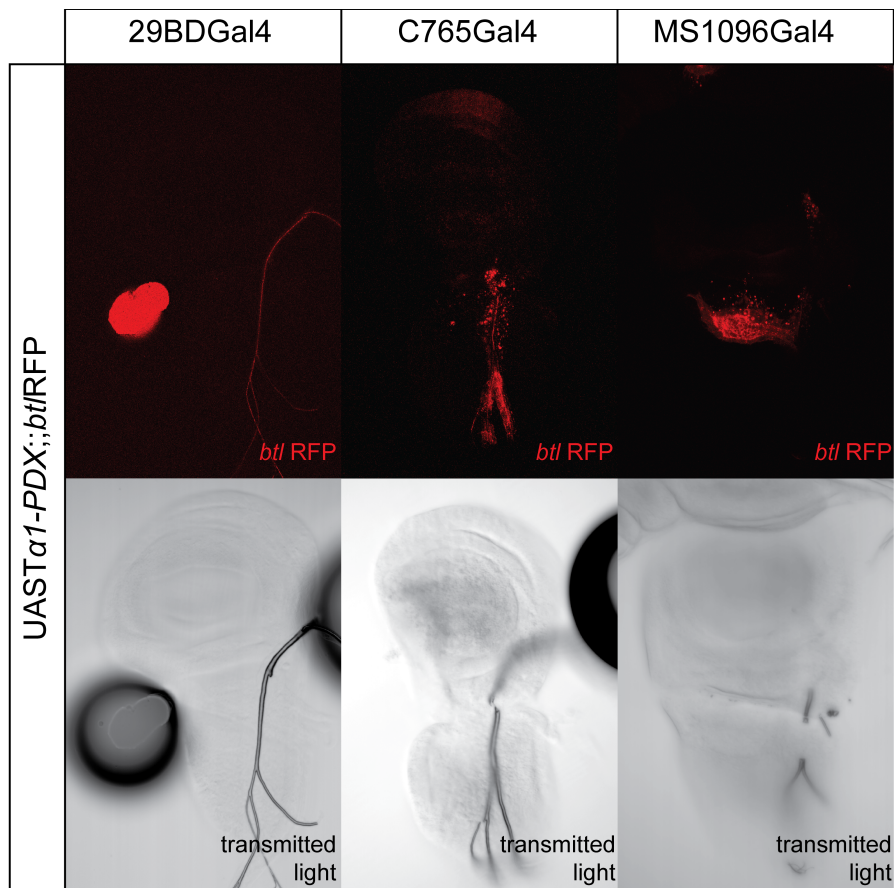


**Figure 8: Inhibition of ASP formation by  $\alpha$ 1-PDX expression**

**Upper Row:** Fur1 activity is inhibited through expression of its inhibitor  $\alpha$ 1-PDX driven by three different Gal4 lines (29BDGal4, C765Gal4 and MS1096Gal4). Air sac primordium (ASP) is labelled in red by the *btl*-RFPmoesin construct. **Lower Row:** Corresponding transmitted light pictures prove that the ASP was not removed during preparation. Note: Expression of  $\alpha$ 1-PDX in the area (with the Gal4 lines 29BDGal4 and C765Gal4) of the ASP prevents its formation, while expression of  $\alpha$ 1-PDX in the ventral pouch region (with MS1096Gal4) does not inhibit formation of the ASP.

### 3.1.3 Bnl processing in the dorsal terminal trachea

#### 3.1.3.1 *Furin processing is needed for the formation of TTBs at the dorsal connectives*

The experiments with the air sac showed that Bnl processing is crucial for developmental processes beyond the embryonic stages and indicated that it might be needed for all Bnl-dependent processes during larval development. To confirm this result in a second larval model, the formation of ternary trachea at dorsal branch was investigated. The model, established by Jarecki et al., (1999) involves the quantification of the thick terminal branches (TTBs) of the dorsal branch of the third segment in

wandering stage larvae (Figure 9A). It was shown that the number of TTBs functions as a direct read out for the strength of Bnl signalling.

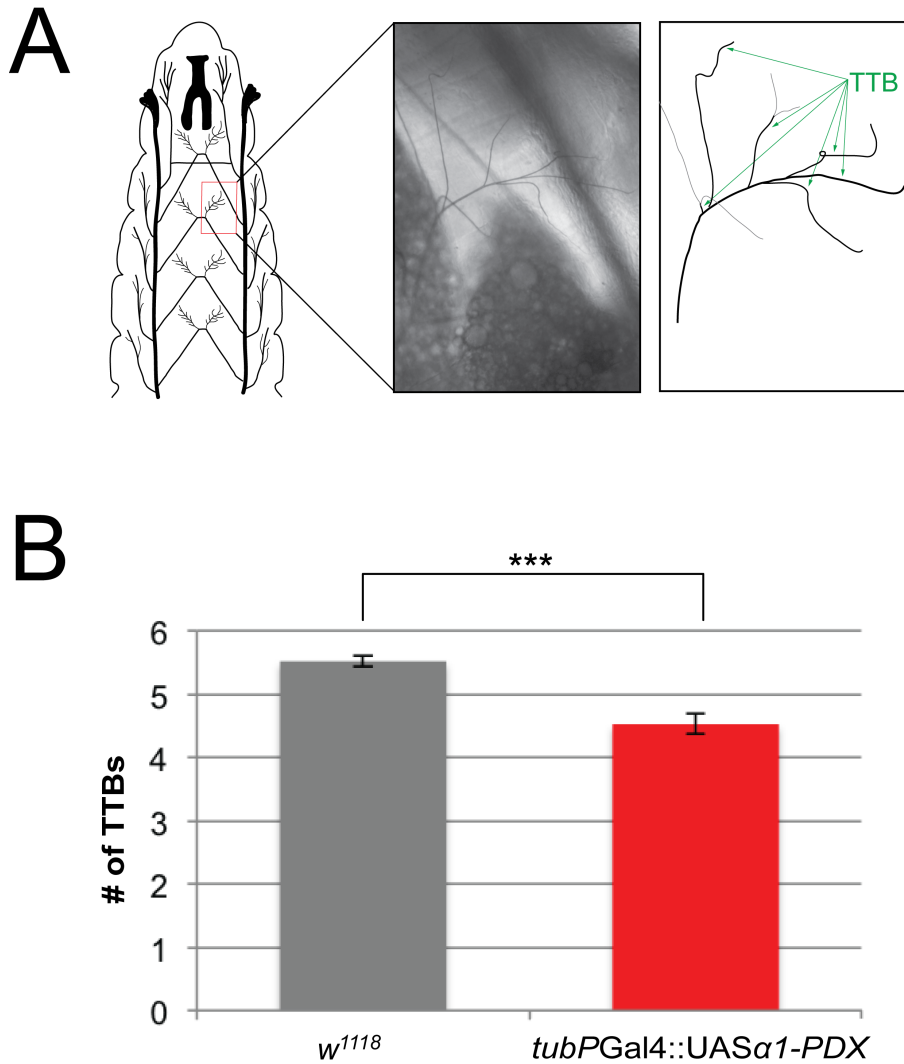


**Figure 9: Inhibition of terminal trachea growth through inhibition of Furins.**

**(A)** Schematic drawing (dorsal view) of the anterior half of a 3<sup>rd</sup> instar larva with the 3<sup>rd</sup> segment dorsal branch highlighted (red box). Magnification of the 3<sup>rd</sup> segment dorsal branch shows the terminal trachea and schematic drawing highlighting the thick terminal trachea (TTBs) (green arrows). **(B)** Quantification of dorsal branch TTBs in 3<sup>rd</sup> instar larvae. Inhibition of Furin by expression of  $\alpha$ 1-PDX through the constitutive driver line *tubPGal4*. p-values:\*\*\*<0.0001 (Wilcoxon-Mann-Whitney Test) Error bars depict standard error. Note: Inhibition of Furin activity through ubiquitous expression of  $\alpha$ 1-PDX leads to a significant decrease in the number of dorsal branch TTBs compared to the *w<sup>1118</sup>* control line.

If the formation of the terminal branches in the larvae is not only dependent on Bnl expression, but on Fur1-dependent processing as well, inhibition of Fur1 activity should result in a decreased number of TTBs. To determine if this assumption is correct  $\alpha 1$ -PDX was expressed using the ubiquitous driver line *tubGal4*. The TTBs were counted in wandering stage larvae and compared to  $w^{1118}$  larvae of the same age. The conduction of the experiment showed that inhibition of Fur1 results in a significant reduction in the number of TTBs compared to  $w^{1118}$ . While the  $w^{1118}$  control has 5.5 TTBs  $\alpha 1$ -PDX expression leads to about 4.5 TTBs (Figure 9B). This experiment revealed that Fur1 inhibition results in an altered tracheal network.

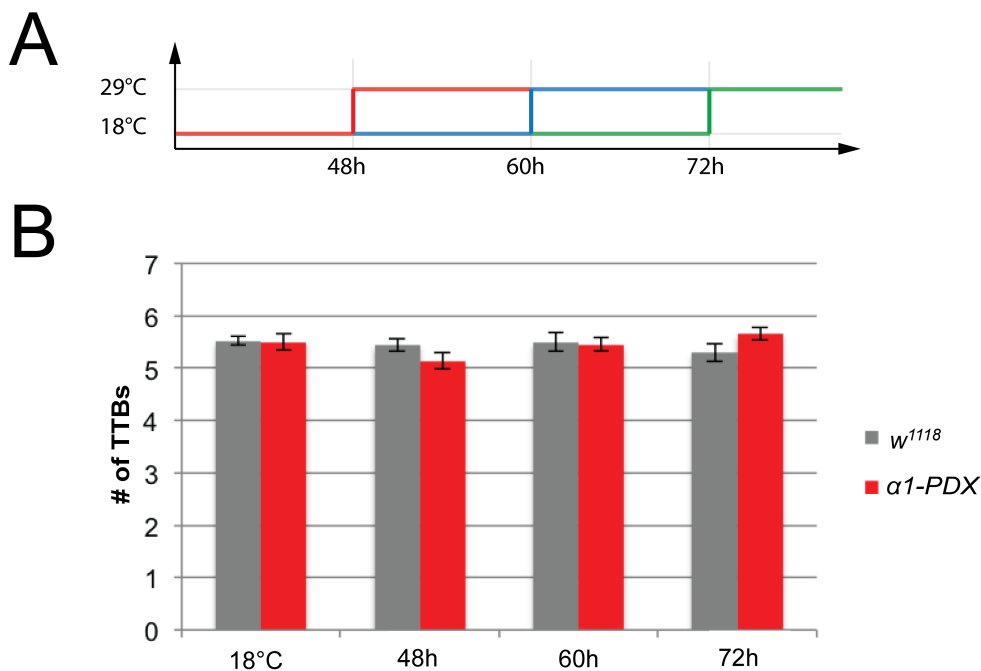


**Figure 10: Determination of the critical period for Furin-mediated cleavage during larval development.**

**(A)** Schematic representation of the time points used for the temperature shift experiments. Expression of the gene of interest was initiated 48h, 60h and 72h after egg laying by shifting the larvae from the restrictive temperature (18°C) to the permissive temperature (29°C). During the restrictive temperature the Gal4 repressor Gal80 is expressed and prevents the expression of the gene of interest, which is under the control of the UAS. At the permissive temperature Gal80<sup>ts</sup> becomes inactive and therefore allows the expression of the gene of interest. **(B)** Quantification of TTBs in 3<sup>rd</sup> instar larvae with a different onset of  $\alpha 1$ -PDX expression through the temperature sensitive constitutive driver line *tubPGal80<sup>ts</sup>; tubPGal4* and temperature shifting. Error bars depict standard error. Note: Inhibition of Furin activity by the expression of  $\alpha 1$ -PDX from 48h after egg laying results a decreased number of TTBs comparable to expression throughout the whole embryonic and larval development.

However, with the experimental setup used it is unclear if this alteration of TTBs is the result of Fur1 inhibition in the larva or a secondary consequence of the *tubGal4* induced  $\alpha$ 1-PDX expression during the embryonic development. To eliminate this uncertainty the Gal80 expression system (Luo 1999; Suster et al. 2004) was used to express  $\alpha$ 1-PDX specifically during larval development. To achieve this aim expression of  $\alpha$ 1-PDX was initiated 48h, 60h and 72h after egg laying (Figure 10A) by a temperature shift to the permissive temperature of 29°C. This experimental setup not only allowed to determine if Bnl processing is needed during larval development, but it also enabled the identification of the sensitive period for Bnl signalling for the growth of the dorsal TTBs. Starting expression of  $\alpha$ 1-PDX from 48h after egg laying resulted in a reduction of TTBs, whereas expression at later stages had no effect. However, even the reduction of 48h expression is not statistically relevant. Further experiments are needed to obtain statistically significant results and to determine the sensitive period for Bnl signalling closer.

Taken together Fur1-dependent processing of Bnl is required for Bnl signalling during the formation of TTBs and the air sac in larval development, thus suggesting that Bnl-processing is needed for Bnl activation consistently throughout embryonic and larval development.

### *3.1.3.2 Furin-mediated processing of Bnl is rate-limiting for the formation of dorsal TTBs*

Investigation of Bnl processing by Fur1 using the specific inhibitor  $\alpha$ 1-PDX showed that it is crucial for activity of Bnl during larval development. However, the results did not allow the conclusion that Fur1-mediated processing represents a novel regulatory mechanism for the temporal and spatial control of Bnl signalling in *Drosophila*. Fur1 could function as a general processing enzyme in cells secreting Bnl similar to the signal peptide protease in the ER. If Fur1-mediated processing truly represents a regulatory mechanism it should be possible to identify Bnl-dependent processes that can be stimulated upon Fur1 (over-) expression and to identify Bnl-expressing tissues in which Bnl is not processed due to the absence of Fur1.



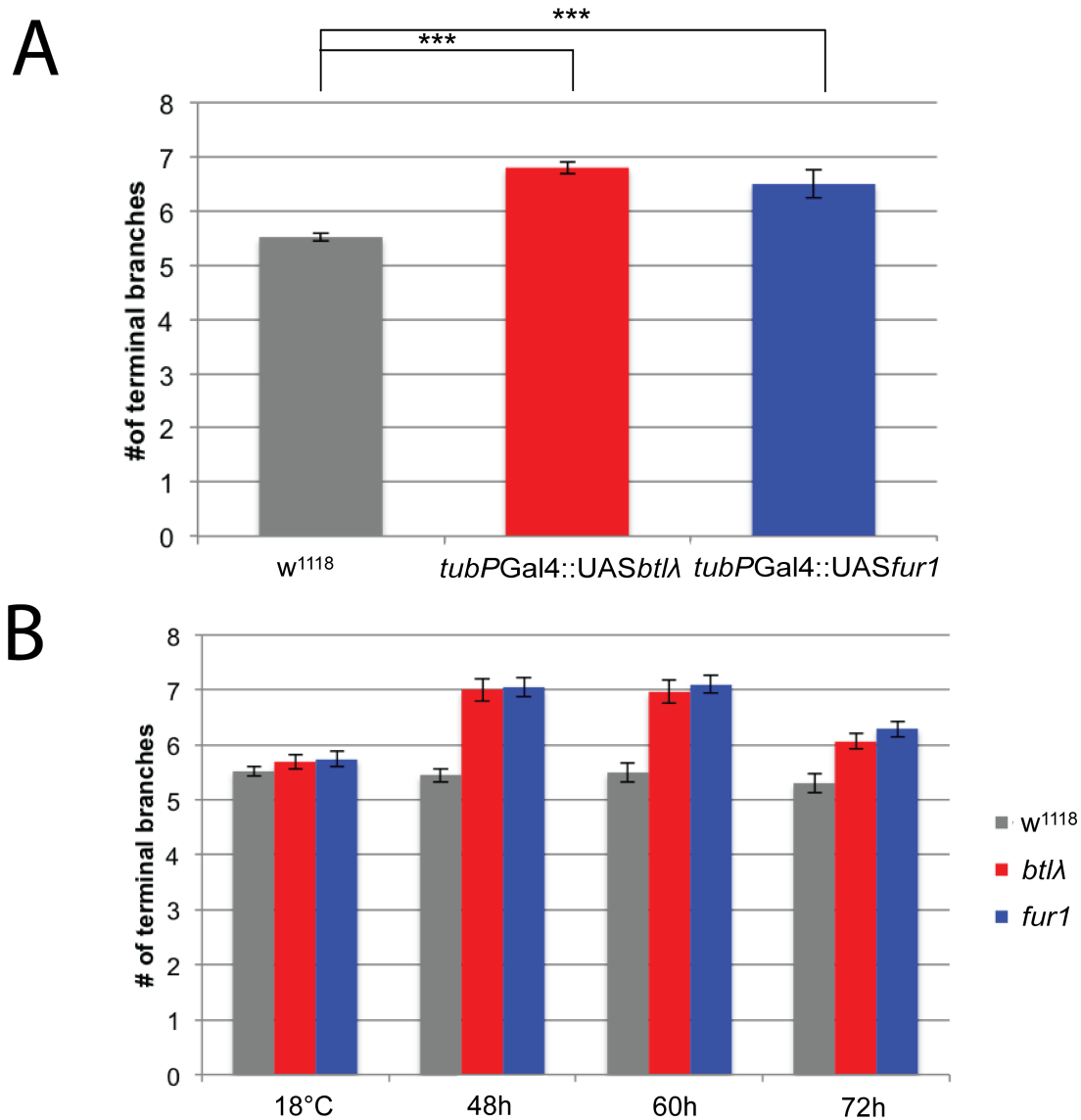


**Figure 11: Increase of terminal trachea growth through increased Fur1 activity.**

**(A)** Quantification of TTBs in 3<sup>rd</sup> instar larvae. Expression of *fur1* and the constitutive active *btl-λ* using the constitutive driver line *tubPGal4*. The use of the constitutive active receptor Btl-λ leads to continuous FGF signalling. It is used to establish the maximum activity of the Btl receptor, which is compared to the effect caused by overexpression of *fur1* to estimate its strength. Note: The overexpression of *fur1* results in a similar increase in the number of TTBs as the expression of *btl-λ*. **(B)** Quantification of TTBs in 3<sup>rd</sup> instar larvae with a different onset of *fur1* and *btlλ* expression through the temperature sensitive constitutive driver line *tubPGal80<sup>ts</sup>;tubPGal4* and temperature shifting. p-values: \*\*\*<0.0001 (Wilcoxon-Mann-Whitney Test). Error bars depict standard error. Note: Expression of *fur1* and *btlλ* from 48h after egg laying results an increased number of TTBs comparable to expression throughout the whole embryonic and larval development.

To test if *fur1* expression represents the rate-limiting step of Bnl signalling the formation of the dorsal ternary branches was used as a model. The expression of constitutive active form of the receptor Btl- $\lambda$  was sufficient to generate up to 7 TTBs (Figure 11A (Lee et al. 1996)). The inability to generate higher numbers of TTBs using the constitutive active form of the receptor Btl- $\lambda$  is suggesting that the natural limitations of the model are reached. On the other hand, ubiquitous expression of Bnl during larval development resulted in a drastic increase of ternary branches in the larvae similar to the effect of *bni* expression in late embryonic development (Sutherland et al. 1996; Jarecki et al. 1999). However, Bnl overexpression results in such a dramatic tracheal phenotype that the larvae die. Only larvae in which overexpression of *bni* was started at 72h after egg laying resulted in surviving 3<sup>rd</sup> instar larvae.

The experiments using *tubGal4* revealed that overexpression of *fur1* during development increased the number of TTBs to the same extent that was seen when the constitutive active receptor Btl- $\lambda$  was expressed (Figure 11A). In both cases the number of TTBs at the dorsal connective was increased from about 5.5 in the wild-type situation to about 7 TTBs. These experimental results suggest that 7TTBs seems to be the maximal effect that can be achieved by enhanced Bnl signalling.

However, based on the use of the *tubGal4* driver line it could not be excluded that embryonic expression of Fur1 caused the effect. To exclude an effect of embryonic expression *fur1* was specifically expressed during larval development using the Gal80 system to restrict the expression of the gene of interest temporally (Lee and Luo 1999; Suster et al. 2004). To identify the critical period expression was induced 48h, 60h and 72h after egg laying by the shift to the permissive temperature. The results of this experiment have shown (Figure 11B) that the onset of *fur1* expression during 2<sup>nd</sup> instar causes similar effects as the ubiquitous expression using the *tubGal4* driver line (Figure 11A). In contrast expression starting in 3<sup>rd</sup> instar larvae after 72h resulted in only weak induction of additional TTBs. These results show that TTBs formation can be induced by Fur1-mediated Bnl-processing during the 2<sup>nd</sup> instar, which is strongly supporting the model that Fur1 mediated processing functions indeed as novel rate-limiting regulatory mechanism in Bnl-signalling.

In a second approach non-tracheated larval tissues were tested for their expression of Bnl and Fur1. In this approach tissues that do express *bni* but do not attract trachea were identified. The idea behind that approach was that in these tissues the potential absence of *fur1* expression might inhibit Bnl signalling. Several non-tracheated larval tissues were found including the fat body, heart and some imaginal discs. Here, two

tissues were studied in detail that showed mutual exclusive expression of *fur1* and *bnl* respectively.

Investigation of the salivary gland revealed that this tissue shows *fur1* expression, but is lacking *bnl* expression. Since Bnl is crucial for the formation of the larval tracheal network (Jarecki et al. 1999; Centanin et al. 2008) no trachea grow into the salivary gland (Figure 12). Ectopic expression of Bnl in the salivary gland, using the driver line 71bGal4, was able to recruit trachea into this tissue, thus demonstrating the importance of Bnl signalling for this process (Figure 12).

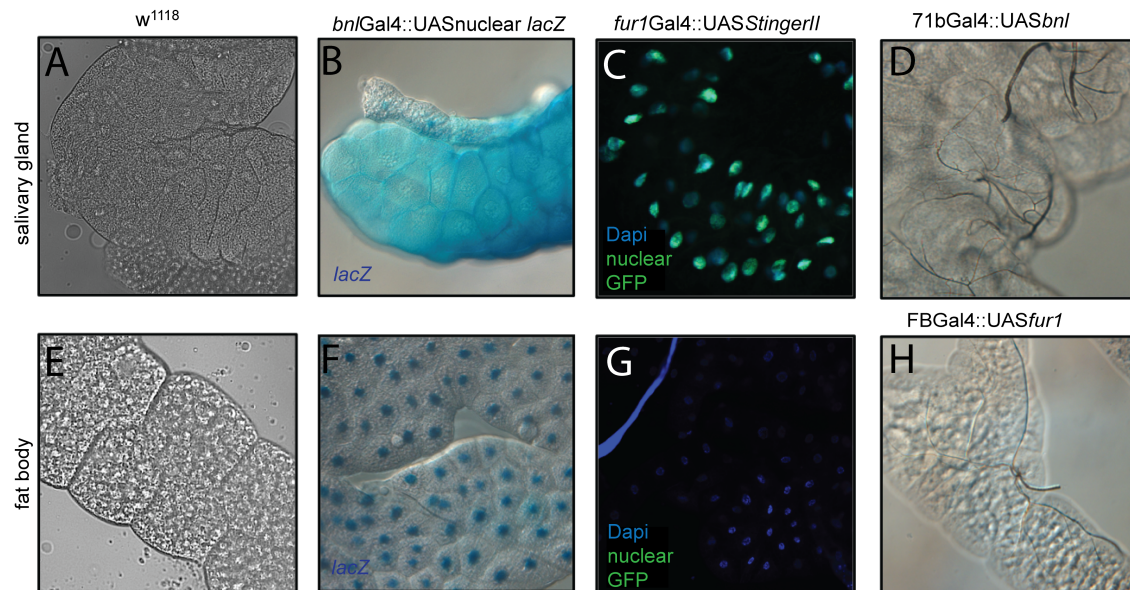


**Figure 12: Fur1-mediated processing of Bnl is the rate-limiting step in Bnl signalling.**

Transmitted light pictures of the  $w^{1118}$  (A) salivary gland and (E) fat body. *lacZ* expression induced by *bnlGal4* in the salivary gland (B) and the fat body (F). *lacZ* is visualised by X-Gal staining. Nuclear GFP is expressed by *fur1Gal4* in the salivary gland (C) and the fat body (G). Nuclei are visualised by DAPI staining to control for nuclear localisation of GFP. Transmitted light pictures of (D) the salivary gland expressing *bnl* using 71BGal4 and (H) the fat body expressing *fur1* using FBGal4. Note: The presence of *bnl* in the fat body is not sufficient to attract trachea. In the salivary gland expression of *fur1* could be detected, while *bnl* was absent, resulting in the lack of trachea within the tissue. Ectopic expression of *bnl* within the salivary gland and *fur1* within the fat body results in the attraction of trachea.

The fat body on the other hand expresses *bnl* as shown here using a GAL4 driver lines inserted in the gene and also by detection of the mRNA (Jarecki et al. 1999). This tissue surprisingly does not attract trachea even though Bnl is present. This fact is especially interesting for this work, since it suggests that the presence of Bnl is crucial but not sufficient to attract trachea without Fur1-mediated processing. Indeed, *fur1* is not expressed in the fat body (Figure 12). To finally test for the rate-limiting effect of

Fur1 for Bnl signalling Fur1 was ectopically expressed in the fat body using the fatbody-specific driver line FBGal4. The expression of *fur1* within the fatbody was sufficient to attract trachea thus proving the rate-limiting effect of Fur1 processing for Bnl signalling activity.

Taken together, the results described above show that Fur1-mediated processing of Bnl is indeed crucial for tracheal modelling in larvae, thereby proving its necessity beyond embryonic development. Additionally the increase of TTBs by the overexpression of *fur1* is shedding light on the nature of Fur1-mediated processing. If Fur1 was acting as a general processing enzyme for Bnl an increased amount of Fur1 should not influence the number of terminal trachea. However, the presented results clearly show that an increase in *fur1* expression starting from the 2<sup>nd</sup> instar larvae is sufficient to induce additional TTBs to the same extend overexpression of a constitutively active form of the Btl receptor. This rate-limiting role of Fur1-mediated processing was also shown for the fatbody. Taken together the experiments above show that both the temporal and spatial expression pattern of Fur1 is limiting for processes controlled by Bnl signalling. Thus Fur1-mediated processing of Bnl is indeed representing a novel regulatory mechanism for Bnl signalling.

#### **3.1.4 Fur1-mediated processing during hypoxia**

The tracheal network that is used in all insects to supply tissues with oxygen is patterned by hardwired development to achieve the stereotypic patterning of the major tracheal branches mostly during embryogenesis (Ghabrial et al. 2003; Uv 2003). However, it has been shown that this patterning is also partially controlled by the oxygen concentration of the environment, which is implemented via Bnl signalling (Jarecki et al. 1999; Centanin et al. 2008). This sensitivity of the tracheal network to oxygen conditions leads to an increase of terminal branches in hypoxia, while hyperoxia leads to a decrease in the number of terminal branches (Jarecki et al. 1999; Centanin et al. 2008). However oxygen conditions do not seem to influence the expression of *bni* and only weakly affect the expression levels of the Btl receptor within the tracheal system (Jarecki et al. 1999; Centanin et al. 2008) Since Bnl signalling is highly dependent on Fur1-mediated processing during embryonic development and larval modelling of the tracheal network a regulatory function of Bnl-processing due to oxygen levels in the environment seems to be a possibility as well.

### 3.1.4.1 Tracheal remodelling due to hypoxia

To investigate the dependency of hypoxia-related tracheal modelling the effect of different oxygen concentrations on trachea formation was first tested in the  $w^{1118}$  control strain. This was done by raising 0-6 h old embryonic collections of  $w^{1118}$  in standard food vials in controlled oxygen environment. The selected oxygen conditions are based on formerly conducted hypoxia studies (Jarecki et al. 1999; Centanin et al. 2008), in which 5% oxygen was chosen for hypoxic and 60% oxygen for hyperoxic conditions. The  $w^{1118}$  offspring was kept in normoxic, hypoxic or hyperoxic conditions until late wandering stage 3<sup>rd</sup> instar, when the larvae were collected and the number of TTBs at the dorsal connective was determined. Since raising larvae in hypoxic conditions leads to an early abandoning of the food a tight control of the time point of analysis was crucial to ensure that all larvae had reached the 3<sup>rd</sup> instar wandering stage and observed phenotypic changes are due to changes of oxygen concentration and not caused by different developmental stages of the tested larvae.

The analysis of the tracheal network under the described conditions showed that the formation of the larval tracheal system is dramatically influenced by the oxygen conditions in which the larvae were raised. Larvae raised in hypoxia showed increased numbers of TTBs while hyperoxia had the opposite effect (Figure 13 A-C). Additionally to the effect on the number of TTBs the oxygen conditions also had an influence on the morphology of the TTBs and the formation the fine trachea that grow towards the target tissues. High oxygen conditions not only led to the formation of fewer but also thinner TTBs and additionally resulted in the formation of fewer fine trachea. In agreement with these findings hypoxia led to the formation of thicker TTBs and to a dramatic increase of fine trachea. Furthermore, the fine trachea are not only increased in number but also showed a change in morphology, resulting in curled trachea and corkscrew-like structures.

The quantitative analysis of the TTBs showed that the number of terminal trachea are increased to an average of 7,1 TTBs in hypoxic conditions compared to 5.5 TTBs during normoxia, while hyperoxia decreased the number of TTBs to an average of 4.9 TTBs, which roughly coincides with the results published by Centanin et al. (2008). However the average number of TTBs during hypoxia was a bit smaller than the 8.7 TTBs of Centanin et al. (2008). Besides reproducing results of former published studies of hypoxia the yielded numbers also reproduced the results of the loss- and gain-of-function of *Fur1* described before (Figure 9 and Figure 11), thus suggesting that the natural limitations of the model are limited to the range of approximately 5 to 7 TTBs.

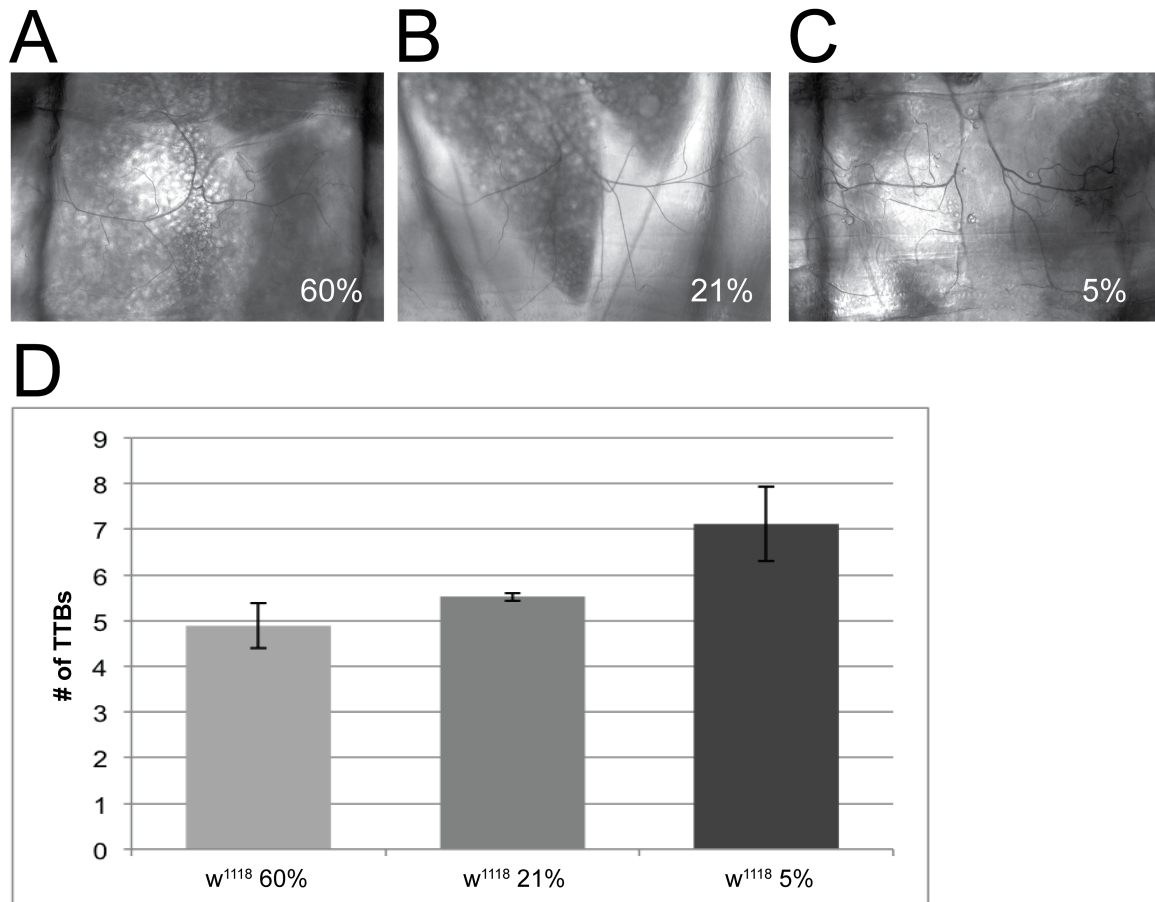


**Figure 13: Effects of oxygen conditions on larval terminal trachea formation.**

Transmitted light pictures of 3rd instar *w<sup>1118</sup>* larvae raised in (A) hypoxia (5% O<sub>2</sub>) (B) normoxia (21% O<sub>2</sub>) and (C) hyperoxia (60% O<sub>2</sub>). (D) Quantification of TTBs in 3<sup>rd</sup> *w<sup>1118</sup>* instar larvae raised in different oxygen conditions. Note: Formation of terminal trachea is dependent on oxygen concentration the larva raised in.

#### 3.1.4.2 *Fur1* processing is involved in tracheal modelling due to hypoxia

After confirming and quantifying the effect of oxygen on the formation of the larval tracheal network the possible involvement of Fur1-mediated processing in the regulation of tracheal remodelling during hypoxia was further investigated. To test the effect of Fur1-mediated processing an approach was chosen in which the effect of the oxygen concentration on the tracheal network should be counteracted through increased or decreased Fur1 activity. For this purpose Furin was overexpressed during hyperoxia to raise the number of TTBs during the oxygen-mediated decrease of TTBs, while the activity of Furin was inhibited through either expression of  $\alpha$ 1-PDX or *fur1*RNAi.

The analysis of larvae in which Fur1 was overexpressed during hyperoxia revealed that increased Fur1 activity was indeed able to raise the number of TTBs during low oxygen conditions. While hyperoxia led to an average of 4.9 TTBs additional overexpression of Fur1 raised the number of TTBs to 6.2, thus exceeding the number of TTBs in normoxia, almost up to the number of TTBs that was seen for Fur1 gain-of-function in normoxia (Table 1). This relatively strong increase in TTBs can be explained by the large amount of Fur1 in the gain of function situation compared to the very low levels of endogenous Fur1. These results showed that enhanced Fur1-mediated processing is sufficient to raise the number of TTBs during hyperoxia, thus suggesting that the adaption of the tracheal network to the oxygen content of the environment might be Fur1 regulated.

	Hypoxia (5%O <sub>2</sub> )	Normoxia (21%O <sub>2</sub> )	Hyperoxia (60%O <sub>2</sub> )
<i>w<sup>1118</sup></i>	7,1 TTBs	5,5 TTBs	4,9 TTBs
<i>tubPGal4::UASTfur1</i>		increased #TTBs (6,5TTBs)	increased # TTBs (6,2TTBs)
<i>tubPGal4::UAST α1-PDX</i>	lethal	reduced # TTBs (4,8TTBs)	
<i>tubPGal4::UASTfur1 RNAi</i>	lethal		

**Table 1: Influence of Fur1 activity on the number of TTBs during different oxygen conditions.**

Quantification of TTBs in 3<sup>rd</sup> instar larvae raised in different oxygen conditions. Larvae analysed were from the *w<sup>1118</sup>* control strain or expressing *fur1*, the Furin inhibitor  $\alpha$ 1-PDX or *fur1*RNAi with the ubiquitous *tubPGal4* line. Note: *fur1* expression during hyperoxia raises the number of TTBs, while decreased Fur1 activity during hypoxia is lethal.

When Furin activity was inhibited by the expression of the  $\alpha$ 1-Pdx inhibitor during hypoxia using the strong ubiquitous *tubGal4* driver line it resulted in lethality during 1<sup>st</sup> larval instar and thus no 3<sup>rd</sup> instar larvae could be obtained. Since remodelling of the tracheal network is needed during hypoxia antagonizes a shortage of oxygen within the larval tissues, the reduction of in the number of trachea by the high level expression of the  $\alpha$ 1-Pdx inhibitor during hypoxia might have led to a critical shortage of oxygen within the larval tissues which induced lethality before reaching the 3<sup>rd</sup> larval instar. However, since Furin-mediated processing is known to be needed for other developmental processes as well (e.g. activation of Dpp (Künnapu et al. 2009)), the induction of

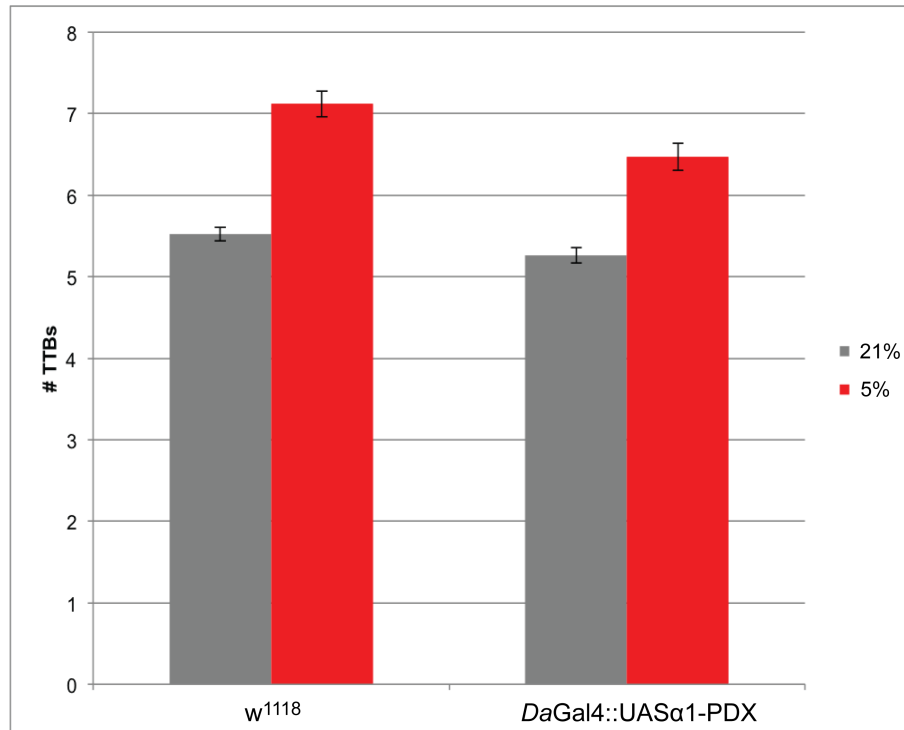
lethality under hypoxic condition could also be due to an interference of Furin processing with changes of larval development under hypoxia independent of Bnl processing.

To test if the strong overexpression of the  $\alpha$ 1-Pdx inhibitor was the cause for the lethality the weaker *daughterless* Gal4 (*daGal4*) driver line was utilized for the expression of  $\alpha$ 1-PDX during hypoxia to induce a milder phenotype, which might lead to viable 3<sup>rd</sup> instar wandering stage larvae. If Fur1-mediated activation of Bnl is responsible for the increased formation of trachea during hypoxia the analysis of these larvae should reveal a reduced number of TTBs. If these larvae show no alteration of the tracheal network other than the effect of the hypoxia this on the other hand would suggest that the inhibition of Furin activity is lethal due to interference with other developmental processes.

Expression of  $\alpha$ 1-PDX with *daGal4* indeed resulted in viable 3<sup>rd</sup> instar wandering stage larvae with an average number of 6,5 TTBs, which is an intermediate between the 7,1 TTBs seen for *w<sup>1118</sup>* larvae in hypoxia and the 5,3 TTBs in larvae derived from the same cross that were raised in normoxia (Figure 14). Since only relatively few larvae could be recovered by this approach it can be assumed that only larvae with a mild reduction of TTBs survived the treatment and the effect of  $\alpha$ 1-PDX during hypoxia is possibly stronger than the analysis of the surviving larvae suggests.

Taken together these results suggest that inhibition of Furin activity is able to decrease the number of TTBs during hypoxia, while raised amounts of Fur1 are able to raise the number of TTBs during hyperoxia. These findings suggest that Fur1-mediated processing of Bnl might be involved in the remodelling of the tracheal network in larvae during changed oxygen conditions. An alternative hypothesis would be that Fur1 regulated Bnl signalling is only an additional process involved in the regulation of tracheal growth in larvae next to a currently unknown regulatory process used to adjust the tracheal network to the oxygen concentration in the environment. However, Furin processing cannot be fully confirmed as the regulatory process during hypoxia by the collected data so far.





	Normoxic (21%O <sub>2</sub> )	Hypoxic (5%O <sub>2</sub> )
<b>W<sub>1118</sub></b>	5.6TTBs	7.1TTBs
<b>DaGal4::UASα1-PDX</b>	5.3TTBs	6.5TTBs

**Figure 14: Expression of  $\alpha$ 1-PDX with *daGal4* results in viable 3<sup>rd</sup> instar larvae.**

Quantification of TTBs in 3<sup>rd</sup> instar larvae raised in hypoxia (5% O<sub>2</sub>) and normoxia (21% O<sub>2</sub>). Larvae analysed originate from the *w<sup>1118</sup>* control strain or are expressing the Furin inhibitor  $\alpha$ 1-PDX using the weaker ubiquitous driver line *daGal4*. Note: Overexpression of  $\alpha$ 1-PDX with *daGal4* during hypoxia leads to the reduction of TTBs in surviving larvae.

## 3.2 Processing of Pyramus and Thisbe

The *Drosophila* FGF family contains two additional FGFs beside Bnl, Pyramus (Pyr) and Thisbe (Ths). These two genes originate from recent gene duplication and encode for FGFs with a FGF domain close to the N-terminus that shows a high degree of conservation to vertebrate FGF8. However, similar to the situation in Bnl, both Pyr and Ths carry large additional sequences C-terminal to the FGF domain.

In case of Bnl former studies by Tatyana Koledachkina (2010) suggested that not only the additional domains of Bnl are removed by the Fur1 protease, but also that the

processing is necessary to achieve an active form of Bnl and are essential for the development of the tracheal network in the embryo. Based on the huge sequence addition that show no homology to vertebrate FGF8 it was suggested that proteolytic processing of the two FGF8 homologues Pyr and Ths might play an important role for the activation of these two ligands as well. Furthermore, it was of interest if the FGF8-like ligands Pyr and Ths would be processed by the same protease Fur1 as shown for the FGF10 homologue Bnl.

Additionally former published data suggests that Pyr and Ths are also proteolytically cleaved and that the cleavage might constitute a regulatory mechanism for these ligands as well (Tulin and Stathopoulos 2010). Pyr and Ths have shown to be cleaved into smaller fragments, both in cell culture and in the embryo, resulting in the release of an active N-terminal fragment including the FGF-domain that is secreted in cell culture. *In vivo* experiments with truncated constructs also showed an increased activity in a gain-of-function assay, if the used truncated constructs are similar in size similar to the detected N-terminal fragments (Tulin and Stathopoulos 2010).

### 3.2.1 Pyr and Ths are cleaved in cell culture

To initially investigate if Pyr and Ths were proteolytically processed as well, *Drosophila* Kc cells were transiently transfected with Pyr and Ths constructs and analysed via Western Blotting. The constructs used for transfection were engineered to enable differentiation between the full-length protein and processed fragments by adding tags to the N- and C-terminus. The resulting fusion proteins consist of the Wingless signal peptide, followed by the EGFP ORF, Pyr or Ths without their signal peptide and STOP codon fused to a 10x Myc tag on the C-terminus (Figure 15A). For the expression a vector with an ubiquitin promotor was used, which allows the constitutive expression in intermediate amounts in *Drosophila* cells. In addition, a double-tagged version of Bnl was used as a control. The cells were transferred 48 hours after transfection into serum free medium to enable the detection of the secreted FGFs in the cell medium (2.1.2.5

As expected the transfection of the double-tagged Bnl resulted in the processing of Bnl as revealed by a 60kDa N-terminal fragment that could be detected using the GFP-antibody in the cell culture supernatant. Also in the case of Pyr and Ths, GFP tagged proteins could be detected in the cell supernatant (Figure 15B). Based on the calculated molecular weight, the detectable fragments seem to originate from processing, thereby removing C-terminal part of the proteins. A further indication of proteolytic processing of Pyr and Ths is the finding that the observed fragments were only detectable with the anti GFP antibody that is directed against the N-terminal tag of the constructs, but could

not be detected by the anti Myc antibody detecting C-terminal Myc tag as would be expected by the uncleaved protein. In the case of Pyr a 95kDa and for Ths a 55kDa fragment, including the EGFP tag, was repeatedly detected in the supernatant with the GFP antibody suggesting that these two FGF are cleaved approximately around aa 550 in Pyr and aa 180 in Ths and subsequently secreted into the supernatant of the cell culture (Figure 15C).

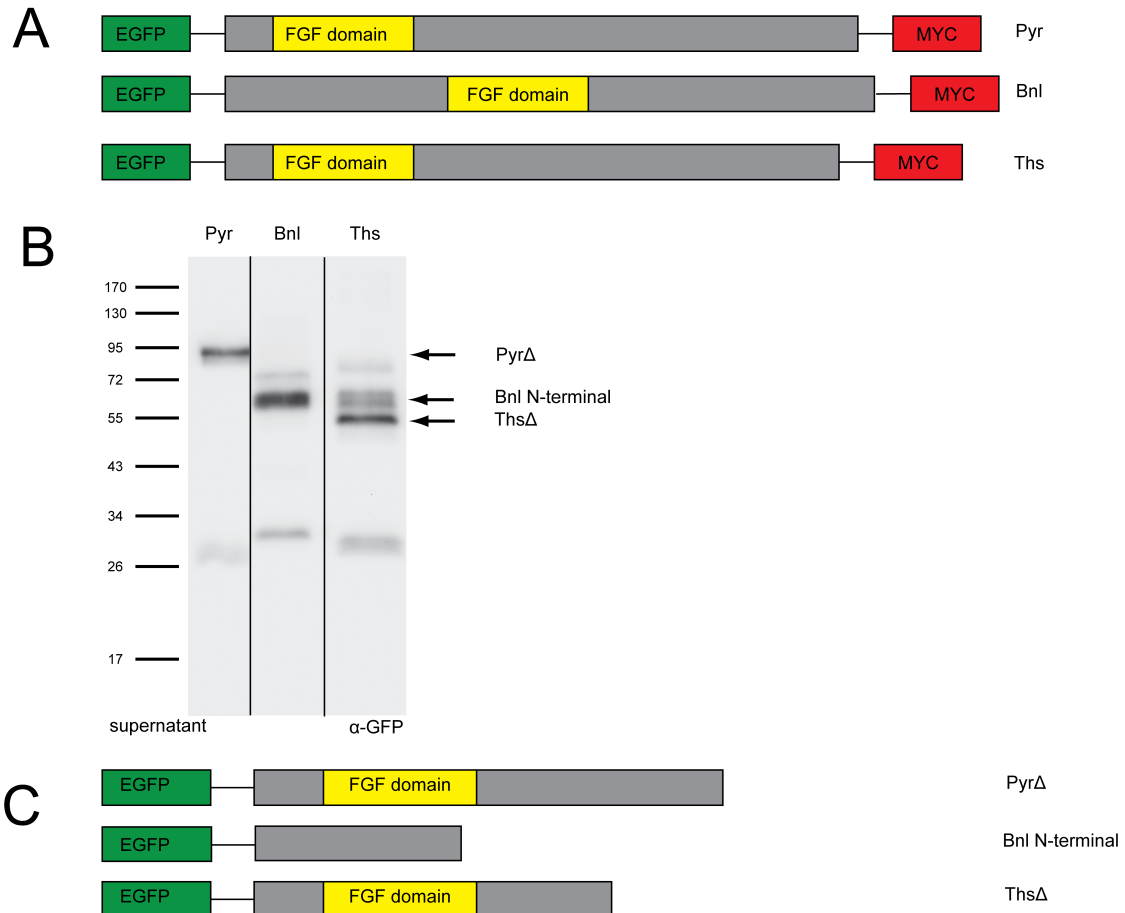


**Figure 15: All *Drosophila* FGFs are cleaved in cell culture.**

**(A)** Schematic drawing of the EGFP- and MYC tagged FGF constructs. **(B)** Western blot analysis of the tagged FGF constructs in cell supernatants using anti-GFP antibody which detects N-terminal cleavage products. Cleaved N-terminal fragments are named and marked by a black arrow. An untransfected specimen was used as mock to exclude unspecific bands. **(C)** Schematic drawing of the detected cleaved fragments with estimated approximate cleavage sites in Pyr and Ths. Note: All *Drosophila* FGFs are proteolytically processed resulting in the detection of smaller N-terminal fragments in cell culture supernatants.

However, the conducted experiments showed that due to glycosylation Bnl is appearing to have a larger than calculated molecular weight on SDS-Page (Koledachkina 2010). Therefore it is possible that the observed apparent molecular weights in the Western Blot likely cannot be used to directly calculate the area of cleavage within Pyr and Ths as well. Noticeably, the full-length fragment could not be detected in the supernatant leading to the conclusion that Pyr and Ths are cleaved completely before secretion or that the secreted full-length proteins are unstable.

### 3.2.2 Conservation of Furin cutting sites in Pyr and Ths

#### 3.2.2.1 *Pyr and Ths contain Furin cutting sites conserved within Drosophila melanogaster FGFs*

After demonstrating the cleavage of Pyr and Ths into smaller fragments the aa sequence two mesodermal *Drosophila* FGFs was screened for Fur1 minimal cutting sites (R-X-X-R). This approach revealed that Pyr contains minimal Furin sites at aa 294-297 (Pyr FS1), 313-316 (Pyr FS2), 351-354 (Pyr FS3), 366-369 (Pyr FS4), 428-434 (Pyr FS5) and 647-650 (Pyr FS6) (Figure 16), whereby Pyr FS5 is consisting of a doubled minimal Furin site (R-R-K-R-D-R-R) similar to the preferred cutting sites of Fur1 in Bnl (Koledachkina 2010). Additionally, cleavage at Pyr FS5 would result in a protein fragment in close proximity of the estimated size based on the observed GFP tagged N-terminal fragment Pyr delta with an apparent molecular weight of 95 KDa. Ths contains minimal Furin sites at the positions aa 94-97 8 (Ths FS1), aa327-330 (Ths FS2) and 651-654 Ths FS3) (Figure 16). Noticeably Ths FS1 is located inside the FGF domain, which would result the functional inactivation of Ths via Fur1 processing and thereby would comprise an additional layer of regulation for FGF signalling. More precisely it would be possible that Furin-mediated processing would result in the activation of Pyr and in the inactivation of Ths.

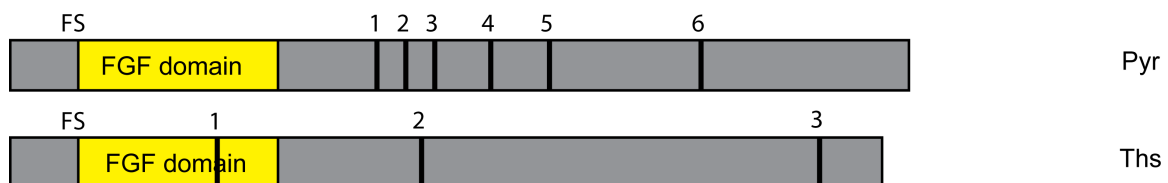


**Figure 16: Furin cutting sites in Pyr and Ths**

Schematic representation of the Furin cutting sites and their approximate location within Pyr and Ths.

### 3.2.2.2 Pyr and Ths contain Furin cutting sites partially conserved within other *Drosophilids*

The conservation of Furin cutting sites throughout all *Drosophila melanogaster* FGFs is pointing to the possibility of Furin-mediated processing as a general mechanism for FGF signalling in other *Drosophilids* than *Drosophila melanogaster*. To further investigate the significance of Furin cleavage sites in Pyr and Ths the evolutionary conservation within the FGF homologues from other *Drosophilids* was analysed by *in silico* sequence comparison. This approach revealed that most Fur1 cutting sites are highly conserved throughout the tested *Drosophilid* species, especially in the case of Pyr. Of special interest is the conservation of Pyr FS3, which is almost perfectly conserved within all tested specimen with the exception of *Drosophila erecta* that has a conservative exchange of the first arginine to lysine. Additionally the double Furin cutting site Pyr FS5, which is especially reminiscent of the preferred cutting sites in Bnl, is conserved in all tested homologues except for *Drosophila sechellia*, which is only 379aa long and thus is missing almost the complete C-terminal half of the *Drosophila melanogaster* Pyr.

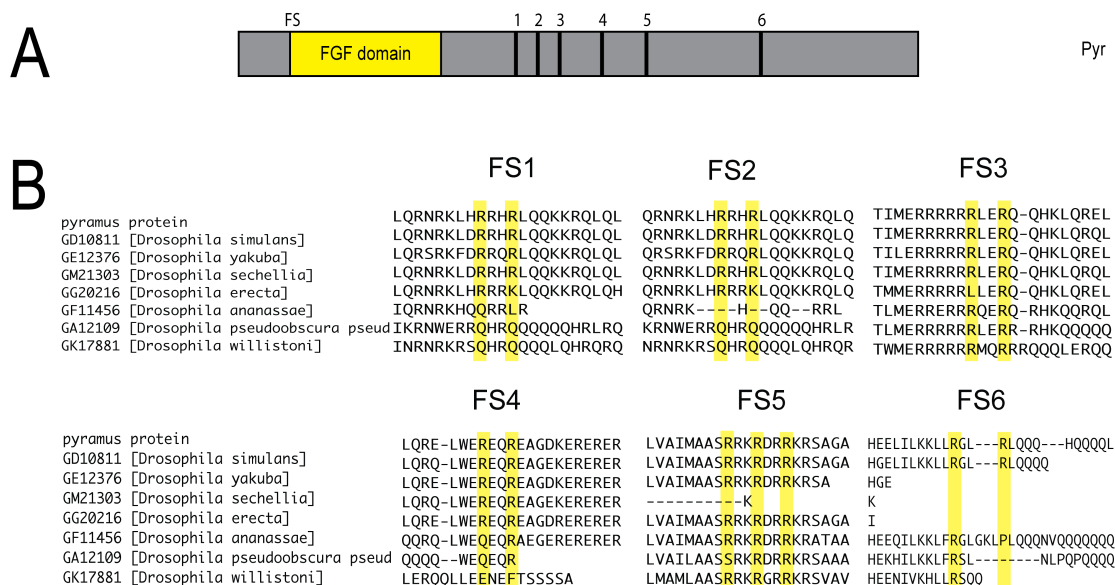


**Figure 17: Pyr contains Furin cutting sites conserved within *Drosophilid* species**

(A) Schematic representation of *Drosophila melanogaster* Pyr including the Furin sites (FS). (B) Comparison of the six FS from the alignment of *Drosophilid* Pyr homologues. The positions of the arginines of the FS are marked in yellow. Note: With the exception of Pyr FS6 all furin cutting sites are partially conserved within the *Drosophilids*. PyrFS3 and Pyr FS5 are conserved almost perfectly.

The sequence alignment of Ths on the other hand showed far less conservation of the Furin cutting sites, with only Ths FS2 being conserved in seven out of ten *Drosophilids*. Conservation of Furin cutting sites FS3 and FS5 in the *Drosophilid* homologues of Pyr is supporting the model that at least Pyr might be cleaved by Furin proteases, while the low conservation of the of the Furin cutting sites in the Ths homologues is pointing against Furin-mediated processing as a regulatory mechanism for all *Drosophila* FGFs. Nevertheless the necessity of Furin-mediated processing for the signalling of Pyr and Ths through the Htl receptor still remains a possibility. Therefore further experiments were performed to investigate if the identified and at least partially conserved Furin cutting sites are used *in vivo*.

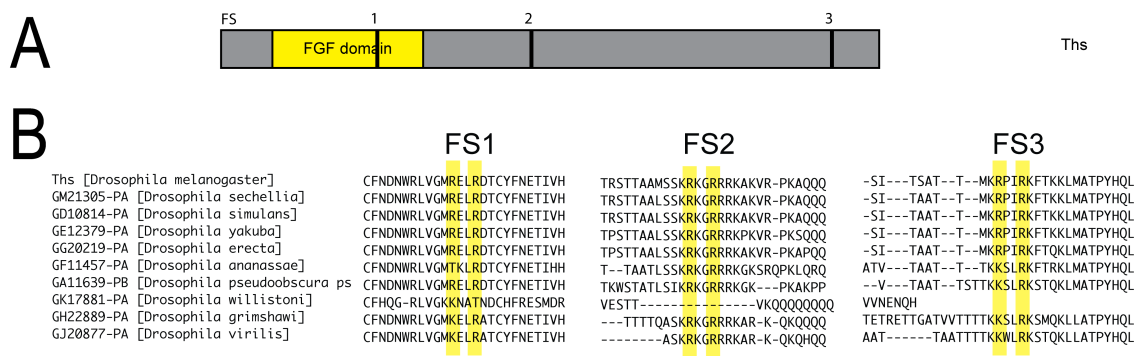


**Figure 18: Ths contains Furin cutting sites conserved within *Drosophilid* species**

(A) Schematic representation of *Drosophila melanogaster* Ths including the Furin cutting sites (FS). (B) Comparison of single FS from the alignment of *Drosophilid* Ths homologues. The positions of the arginines in the FS are marked in yellow. Note: Furin cutting sites show less conservation in Ths than in Pyr. Ths FS2 is the best conserved site with seven out of ten homologues carrying the Furin cutting site.

### 3.2.3 Relevance of Furin cutting sites for the proteolytic processing of Pyr and Ths

To determine if Pyr and Ths are indeed cleaved by a Furin protease the specific inhibitor  $\alpha$ 1-PDX (Benjannet et al. 1997; Koledachkina 2010) was used as its inhibitory function was used before in cell culture and *in vivo*. Therefore a  $\alpha$ 1-PDX containing construct under the control of a constitutive ubiquitin promotor was co-expressed with either tagged Pyr or Ths in *Drosophila* cell culture and subsequently analysed via Western Blot. If Furin is responsible for the cleavage of Pyr or Ths  $\alpha$ 1-PDX expression should prevent the cleaving into the 95kDa Pyr fragment or the 55kDa Ths fragment respectively and the full size fragment should appear in the probe prepared from the cultured cells that will be used additionally to the supernatant in this case.

### 3.2.3.1 Inhibition of Fur1 is not preventing cleavage of Pyr

To investigate the cleavage of Pyr and Tbs independent from possible degradation in the cell supernatant both the supernatant and the cell lysates of *Drosophila* Kc-cells were analysed. Pyr expression revealed the same 95kDa fragment in the cell lysate that was already detected in the supernatant, thus suggesting that Pyr is cleaved within the cells before secretion (Figure 19B). However the detection of the C-terminal fragment using the anti-Myc antibody was unsuccessful, which indicates that the C-terminal product might be already instable within the expressing cells. Since Pyr is cleaved before secretion the effect of the co-expression of Furin protease inhibitor  $\alpha$ 1-PDX was investigated only in cell lysates to avoid potential additional unspecific cleavage in the supernatant.

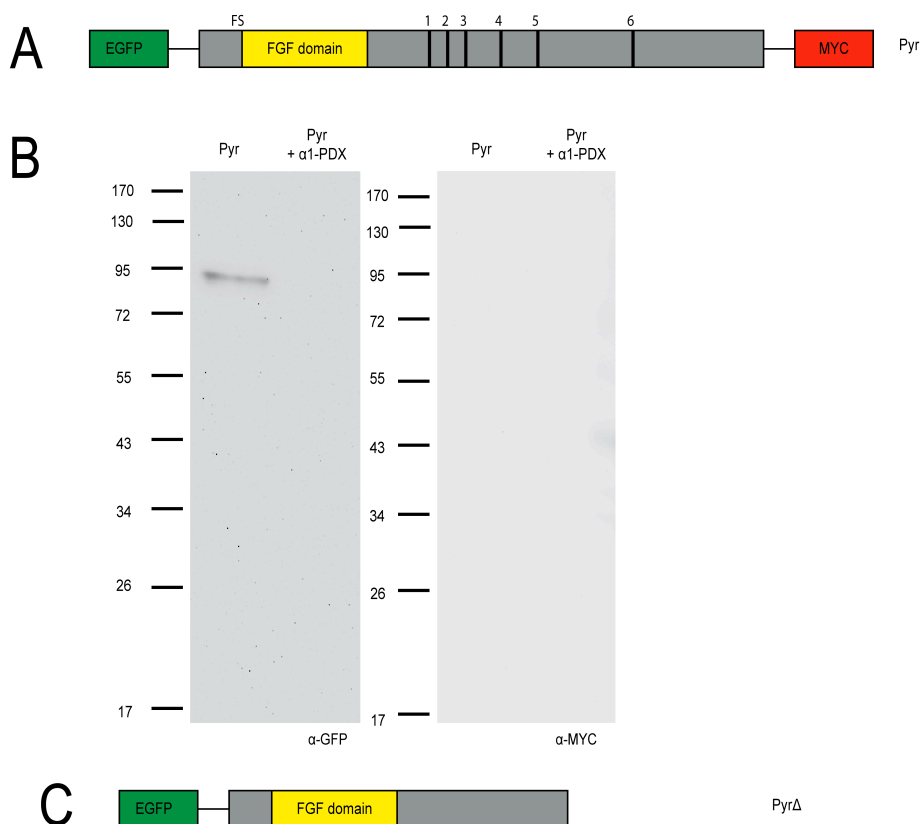


**Figure 19: Co-expression of Pyr and  $\alpha$ 1-PDX**

**(A)** Schematic drawing of the EGFP- and MYC tagged Pyr construct including the position of Furin cutting sites. **(B)** Western blot analysis of the EGFP- and MYC tagged Pyr construct with or without co-expression of the Furin inhibitor  $\alpha$ 1-PDX in cell lysates. N-terminal fragments are detected with the anti-GFP antibody, while C-terminal fragments are detected with the anti-MYC antibody. **(C)** Schematic drawing of the detected cleaved N-terminal fragment with the estimated cleavage site. Note: Inhibition of Furin inhibits the formation of the cleaved N-terminal Pyr fragment but full length Pyr is not detectable.

Co-expression of  $\alpha$ 1-PDX and Pyr prevented the detection of the 95kDa protein band, corresponding to the N-terminal cleavage product, suggesting that a Furin protease might indeed be involved in the formation of this fragment. However in this case an increase in the amount of uncleaved Pyr would be expected. Yet the uncleaved Pyr could neither be detected with the anti-GFP nor with the anti-MYC antibody. Therefore the expression of  $\alpha$ 1-PDX is either affecting the stability of the cleaved fragment or alternatively the uncleaved full-length Pyr is unstable within the cell resulting in the degradation of the protein when cleavage is blocked.

### 3.2.3.2 *Inhibition of Furin is not explicitly verifying Furin-mediated cleavage of Ths*

The corresponding analysis of Kc-cell lysates, expressing the double-tagged Ths construct, showed a band at a molecular weight of 55kDa corresponding to a cleaved N-terminal fragment also shown in the cell supernatant (Figure 15) proving that also Ths is cleaved within the cell before its secretion. However, detection with the anti-Myc antibody revealed an additional 170kDa protein band, presumably representing the uncleaved double-tagged full-length Ths protein. Surprisingly the anti-GFP antibody cannot detect the full-length Ths protein, suggesting that the responsible epitope is not accessible. However the molecular weight of uncleaved Ths was calculated *in silico* to be 83kDa. Including the molecular weight of the tags that were used in this approach the full-length protein should have a molecular weight of approximately 130kDa. This dramatic difference in size of Ths determined by *in silico* analysis versus the detected protein on the SDS-Page could correlate to secondary protein modifications like glycosylations since both Ths and Pyr show multiple O- and N-glycosylation sites. Alternatively the observed 170kDa band might represent a Ths dimer.

In contrast to Pyr, N- and C-terminal cleavage fragments of Ths could be detected in cell lysates by their Tags. Additional to the earlier identified 55kDa N-terminal Ths fragment that was detected with the anti-GFP antibody an approximately 130kDa C-terminal cleavage fragment was detected using the anti-Myc antibody. Both of these fragments might together form the full size fragment, which is only detectable by its C-terminal Myc tag.

The co-expression of  $\alpha$ 1-PDX resulted in a reduction in the signal strength of these two fragments. However, no increase in the amount of the full size protein was detected in the presence of  $\alpha$ 1-PDX using the anti-Myc antibody. In contrast, the total amount of protein was reduced as a consequence when  $\alpha$ 1-PDX was overexpressed, possibly indicating the long time treatment of cells with the inhibitor  $\alpha$ 1-PDX affects cell viability.



Taken together the addition of  $\alpha$ 1-PDX is neither proving a Furin-specific cleavage of Ths or Pyr nor is it excluding a role of Furin proteases in Pyr and Ths processing.

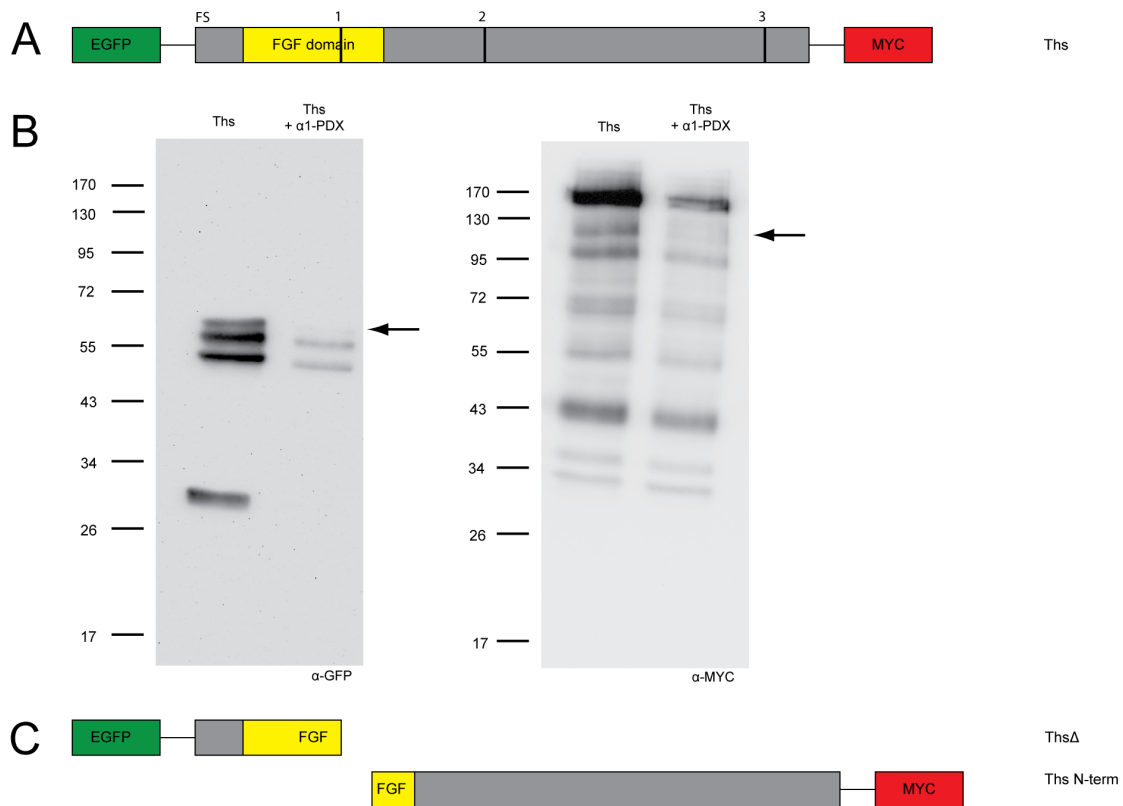


**Figure 20: Co-expression of Ths and  $\alpha$ 1-PDX**

(A) Schematic drawing of the EGFP- and MYC tagged Ths construct including the position of the Furin cutting sites. (B) Western blot analysis of the EGFP- and MYC tagged Ths construct with or without co-expression of the Furin inhibitor  $\alpha$ 1-PDX in cell lysates. N-terminal fragments are detected with the anti-GFP antibody, while C-terminal fragments are detected with the anti-MYC antibody. Black arrows highlight bands that are absent when  $\alpha$ 1-PDX is co-expressed. (C) Schematic drawing of the detected cleaved fragments estimating the approximate cleavage site. Inhibition of Fur1 inhibits the formation of two possibly corresponding Ths fragments. Note: Transfection of  $\alpha$ 1-PDX prevents the formation of a N- and C-terminal cleavage fragment each.

### 3.2.4 Biological effect of Pyr and Ths processing

The conducted cell culture experiments were suggesting the involvement of Furin in the processing of the two FGF8 homologues. To test the importance of Furin-mediated processing independently the effect of the inhibition of Furin proteases for Pyr and Ths activity was analysed *in vivo* during embryonic development.

The observed processing of Pyr and Ths should have an effect on the biological activity the FGF8 homologues as shown before for Bnl (Koledachkina 2010). Pyr and Ths activate the FGFR Htl, which in turn controls the movement of the mesodermal cells, the specification of the pericardial cells (Gryzik and Müller 2004; Kadam et al. 2009; Klingseisen et al. 2009; McMahon et al. 2010) and the caudal visceral mesoderm formation (Mandal et al. 2004); (Kadam et al. 2012; Reim et al. 2012). Therefore these tissues can be used as readout for the activity of the Htl receptor. If cleavage is of importance for the activity of Pyr and Ths the inhibition of the cleavage should result in a reduction of their biological activity. To identify an effect of Furin-mediated processing on Pyr and Ths in the embryo the number of Eve-expressing pericardial cells of stage 11 embryos were chosen as model. In each hemisegment the activation of the Htl receptor is needed to specify two eve-expressing progenitor cells, which subsequently give rise to three eve-expressing founder cells. Two of these eve-positive cells will form pericardial cells, while the last eve-positive cell will give rise to a somatic muscle (Buff et al. 1998; Carmena et al. 1998). It was shown before that these most dorsally localized eve-expressing cells are highly sensitive to changes in the amount of Pyr and Ths expression (Gryzik and Müller 2004; Stathopoulos 2004; Kadam et al. 2009; Klingseisen et al. 2009; Tulin and Stathopoulos 2010). Therefore, the number of the Eve-expressing cells seemed to be a highly sensitive and quantifiable system to analyse Pyr and Ths activity.

#### *3.2.4.1 Inhibition of Furin-mediated processing affects the formation of Eve-positive cells*

In order to test if Furin-mediated processing has any influence on the activity of Pyr and Ths the Furin inhibitor  $\alpha$ 1-PDX was expressed in the embryo with the help of the *KrGal4* driver line. This driver line is inducing expression in the centre of the embryo with the strongest expression in the hemisegments 5+6, which are located at the posterior end of the embryo during full germ band elongation in stage 11. Thus the flanking hemisegments are unaffected and serve as an internal control.

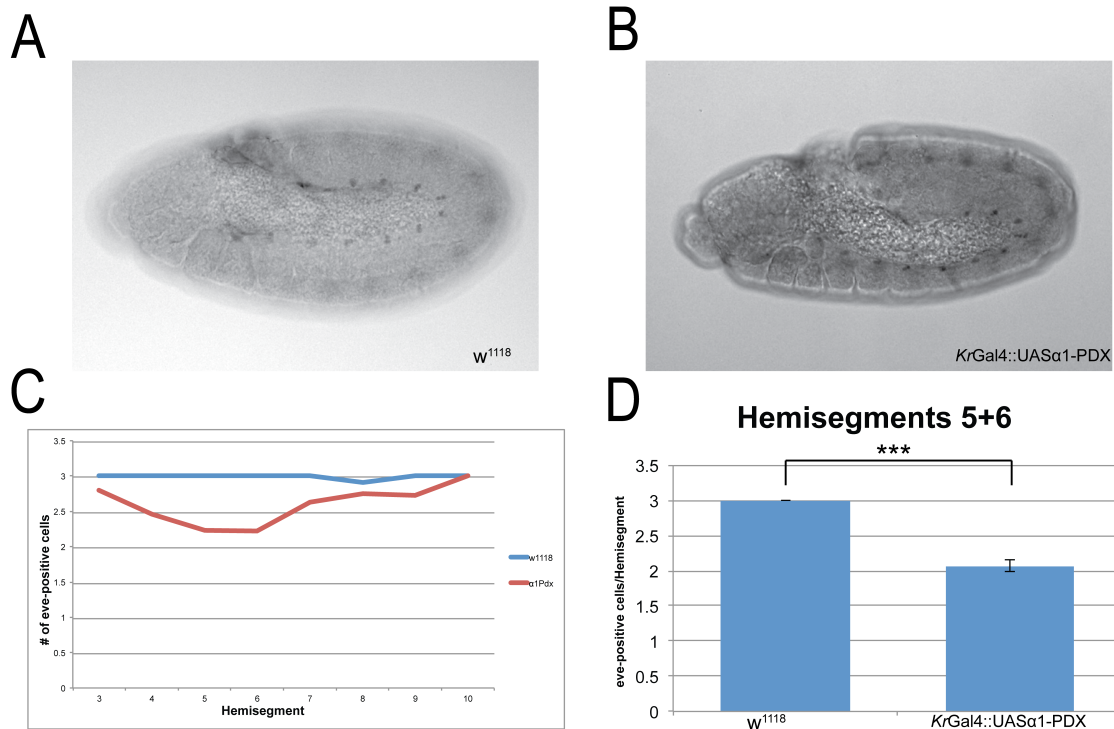


**Figure 21: Inhibition of Furin in the embryo**

Immunostaining against Eve on stage 11 embryos: (A) *w<sup>1118</sup>*, (B) embryo with expression of  $\alpha$ 1-PDX controlled by the *KrGal4* driver line. (C) Quantification of Eve-positive cells per hemisegment in stage 11 embryos (*w<sup>1118</sup>* control line and *KrGal4::UAS $\alpha$ 1-PDX*). (D) Comparison of the average number of Eve-positive cells in the hemisegments 5 and 6. p-value: \*\*\*<0.0001 (Wilcoxon-Mann-Whitney test). Error bars are depicting the standard error. Note: Expression of  $\alpha$ 1-Pdx in the *Kr* domain leads to a significant decrease in the number of Eve-positive cells in the hemisegments 5 and 6.

If Fur1-mediated processing is affecting the activity of the FGF8-homologues the expression of  $\alpha$ 1-PDX should result in a reduced number of Eve-positive cells similar to the *pyr* and the *pyr* and *ths* double mutants (Kadam et al. 2009; Klingseisen et al. 2009), while the flanking segments should be unaffected. In the segments expressing  $\alpha$ 1-PDX a reduced number of Eve-positive cells was observed. The reduction was most severe in the hemisegments 5 and 6, which are positioned in the centre of the *Kr*-expression domain. Furthermore, as expected the hemisegments 1-2 and 9-10 are unaffected (Figure 21C). Therefore, to facilitate a quantitative comparison the average number of Eve-positive cells in hemisegment 5 and 6 was used. Compared to *w<sup>1118</sup>* control embryos the inhibition of the Furin protease by  $\alpha$ 1-PDX resulted in a significant reduction from three in wild type to two Eve-positive cells. Thus showing a role of Furin-mediated processing on the formation of Eve-positive cells and thereby confirming the results of the cell culture experiments. However, the rather weak reduction in the

number of Eve-expressing cells indicates that either the inhibition of Furin proteases is only partial or alternatively the processing of Pyr and Ths is not absolutely required for the generation of an active form of these FGF8-homologues. Furthermore, the experimental design does not allow to exclude that the inhibition of Furin proteases affects the number of Eve-expressing dorsal mesodermal cells by a mechanism independent of the FGF8-homologues like the regulation of an unrelated factor such as Dpp which was shown to be processed by furins as well (Künnapu et al. 2009).

#### 3.2.4.2 *Mutation of Furin cleavage sites in Pyr and Ths results in minor biological effects*

The inhibition of Furin proteases by  $\alpha$ 1-PDX indicated both in cell culture expression experiments as well as in the *in vivo* analysis of the Eve-positive cells that Furin proteases might be involved in the processing of Pyr and Ths. An alternative strategy to confirm the involvement of Furin proteases is the mutation of identified cutting sites to render the resulting protein uncleavable. Since the minimal cutting motif of the Fur1 protease is well described (Molloy et al. 1992; Thomas 2002) this approach was used to produce versions of Pyr and Ths that are no longer cleavable by Furin proteases.

A site directed mutagenesis approach was employed to mutate all Furin cutting sites (FS) in a sequential fashion starting with the first FS and adding one furin site at a time per construct, resulting in a total number of 6 constructs for Pyr and 3 constructs for Ths. This progressing approach was chosen to avoid the use of an alternative cutting site after the mutation of the normally used cutting site. To prevent cleavage the arginines of the R-X-X-R motif were substituted with glycine (Table 2 and Table 3). The necessary point mutations were introduced with a site-directed mutagenesis approach using primers that carry the desired modification and the method described in 2.1.1.8.

In order to compare the biological activity of wild type cleavable Pyr and Ths with the variants that cannot be cleaved by Furin proteases *in vivo*, transgenic flies lines with UAS constructs carrying the wild type forms and mutated versions of both Pyr (Pyr MFS1-3, Pyr MFS1-5) and Ths (Ths MFS1-3) were generated. If the mutation of the putative cutting sites is preventing either the activation or inactivation of Pyr or Ths, the non-cleavable versions of Pyr and Ths should have a different activity than the wild type proteins. To analyse the activity of the FGF8-homologues in a gain-of-function experiment *in vivo* the number of Eve-positive cells were used as read out. These Eve-positive cells are increased dramatically when Pyr and Ths were overexpressed in the *Kr*-expression domain (Tulin and Stathopoulos 2010).

	Furin cleavage sites (FSs)	Mutated Furin sites (MFSs)
<b>Pyr FS1</b>	RKLHRRHRLQQK	RKLHGRHGLQQK
<b>Pyr FS2</b>	QQQRRRQRQYGT	QQQRGRQGQYGT
<b>Pyr FS3</b>	RRRRRLERQQHK	RRRRGLEGQQHK
<b>Pyr FS4</b>	ELWEREQREAGD	ELWEGEQGEAGD
<b>Pyr FS5</b>	MAASRRKRDRRKRSAG	MAASRRKGDRRKGSAG
<b>Pyr FS6</b>	KKLLRGLRLQQQ	KKLLGGLGLQQQ

**Table 2: Furin cutting sites in Pyr**

Furin cutting sites are highlighted in blue, introduced point mutations in red.

	Furin cleavage sites (FSs)	Mutated Furin sites (MFSs)
<b>Ths FS1</b>	LVGMRELRDTCY	LVGMGELGDTCY
<b>Ths FS2</b>	MSSKRKGRRKA	MSSKGKGRRKA
<b>Ths FS3</b>	TTMKRPIRKFTK	TTMKGPIRKFTK

**Table 3: Furin cutting sites in Ths**

Furin cutting sites are highlighted in blue, introduced point mutations in red.

Embryos expressing wild type Pyr within the *Kr* central domain show an increased average number of Eve-positive cells of approximately 5 in the hemisegments 5 and 6 in the case of Pyr and approximately 6 in the case of Ths. However, in some hemisegments the number of Eve-positive cells was elevated to up to 12 in comparison to 3 in wild type embryos. These results confirmed that overactivation of Htl signalling results in a boosting effect on the formation of Eve-expressing heart progenitor cells as shown by Tulin and Stathopoulos (2010).

However, Ths and Pyr containing mutations in the putative Furin cutting sites showed an only marginal reduction in the number of Eve-positive precursor cells in comparison to the wild type proteins. The expression of Ths MFS1-3, which carries mutations in all Furin-cleavage sites, induced 5 Eve-positive cells whereas the expression of wild type Ths induced 6. Similarly, the mutation of Furin cleavage sites 1-3 in Pyr elevated the number of Eve-positive precursor cells to 5 thereby matching the effect of the wild type Pyr. The mutation of Furin-sites 1-5 on the other hand resulted in a reduced activity resulting in 3.8 Eve-positive cells.

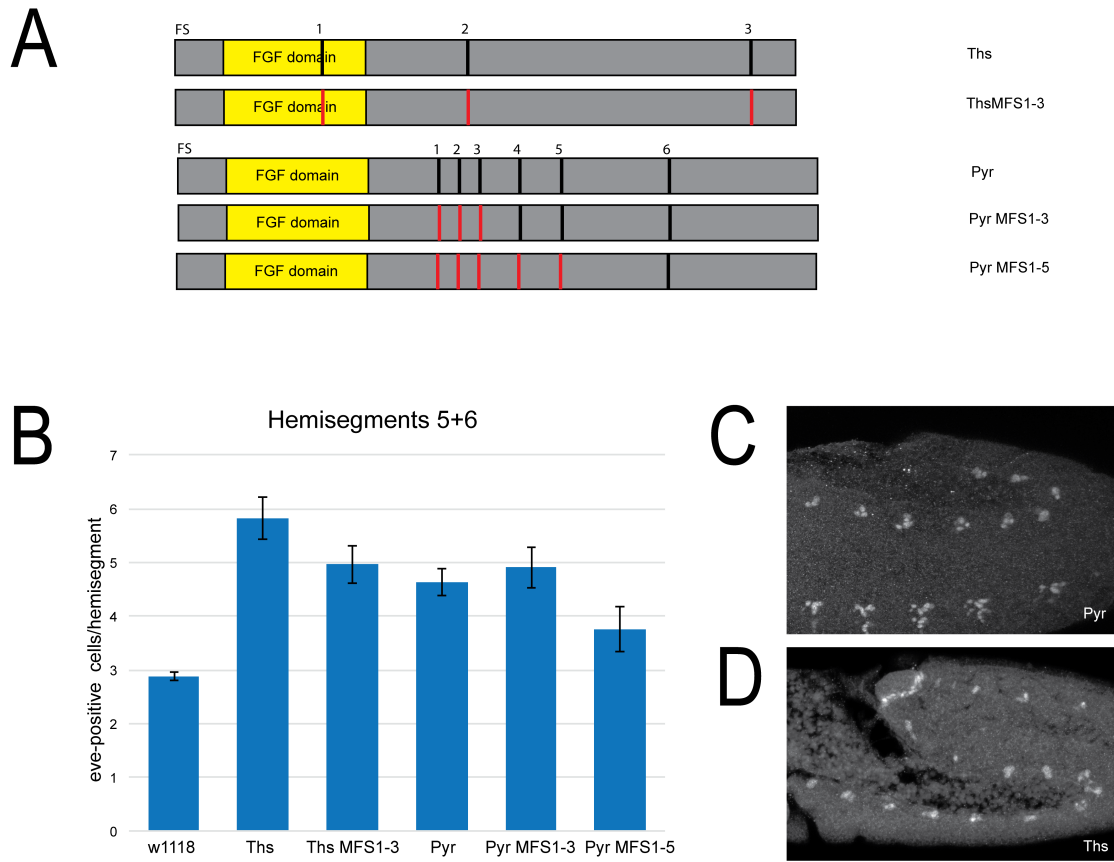


**Figure 22: Biological effect of mutated Furin cleavage sites**

(A) Schematic drawing of the FGF constructs including positions of Furin cutting sites. Mutated cutting sites are depicted in red. (B) Quantification of the Eve-positive cells in the hemisegments 5 and 6. Used embryos were expressing wild type FGFs or FGFs with mutated furin sites (MFS). Immunostaining against Eve on stage 11 embryos: (C) overexpression of Pyr, (D) overexpression of Ths. Note: Overexpression of all tested Pyr and Ths variants leads to an increase of Eve-positive cells in the hemisegments 5 and 6. Mutation of the furin cleavage sites leads to a small reduction in TTB number compared to the wildtype version of Pyr and Ths.

These results could either suggest that the Furin sites are not used for processing of Pyr and Ths or that processing of Pyr and Ths is not required for receptor activation. A third explanation would be that the strong overexpression of the non-cleavable forms of Pyr and Ths might lead to Htl receptor activation although the activity of the not processed variants might be reduced. Therefore, further experiments had to be conducted in order to investigate Furin-mediated cleavage of Pyr and Ths directly.

### 3.2.5 Processing of Pyr and Ths is not Fur1-mediated

#### 3.2.5.1 Mutation of Furin cleavage sites is not preventing cleavage in cell culture

Based on the inconclusive results from the *in vivo* analysis the Ths and Pyr variants with the mutated furin cleavage sites were tested in cell culture to determine if the mutation of the Furin sites prevents the cleavage of Pyr and Ths. For this purpose double-tagged Pyr and Ths with mutated Furin cleavage sites in a sequential fashion, adding one mutation at a time, were tested for processing in cell culture (Figure 23).

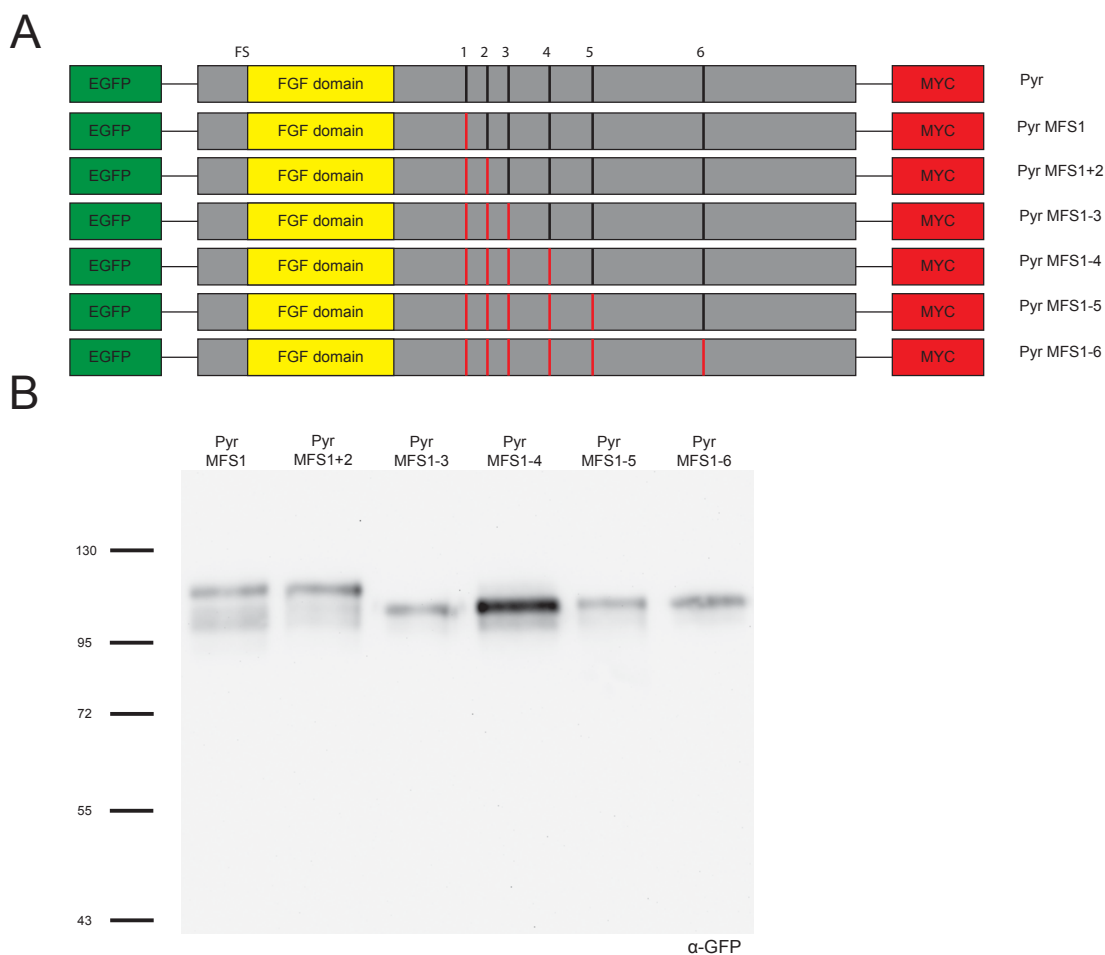


**Figure 23: Role of Furin cutting sites for the processing of Pyr**

(A) Schematic drawing of the EGFP- and MYC tagged Pyr constructs including Furin cutting sites. Mutated Furin cutting sites (MFS) are marked in red. (B) Western blot analysis of the expressed EGFP- and MYC tagged Pyr constructs in cell supernatants. Western blots were treated with the anti-GFP antibody. Note: Mutation of Pyr FS1 results in a double band that is lost when Pyr MFS3 is introduced in addition.

If Furin is indeed mediating the cleavage of Pyr and Ths the sequential mutation of the cutting sites should result in the inhibition of the processing and therefore recover the full-length proteins. However, it cannot be excluded that the mutation of the cleavage site leads to the processing at a more C-terminal Furin site, which would result in the generation of a longer protein fragment.

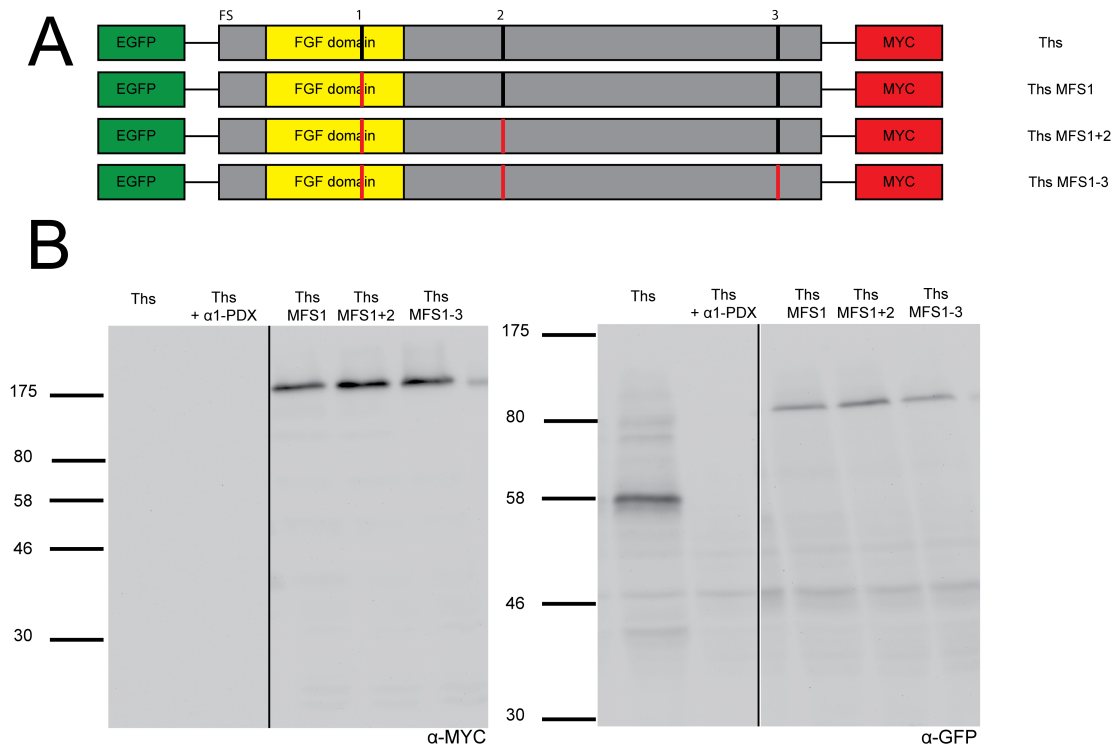


**Figure 24: Role of Furin cutting sites for the processing of Ths**

(A) Schematic drawing of the EGFP- and MYC tagged Ths constructs including Furin cutting sites. Mutated Furin cutting sites (MFS) are marked in red. (B) Western blot analysis of the expressed EGFP- and MYC tagged Ths constructs in cell lysates. Western blots were treated with the anti-GFP antibody and the anti-MYC antibody. Note: Mutation of Ths FS1 leads to the inhibition of cleavage and the accumulation of the uncleaved protein in cell extracts.

The experiments shown in (Figure 23B) revealed that all mutated Pyr variants were still cleaved into the 90kDa EGFP-tagged N-terminal fragment that can be detected when wild type Pyr is cleaved. However, an interesting observation made in this context was the appearance of a double band of the 90kDa fragment that appears when Pyr FS1 was mutated alone or together with the FS2. This could imply that the mutation of Pyr FS1 might block cleavage resulting in the alternative cleavage at Pyr FS3. However, the additional mutation of Pyr FS3 reversed this effect and all subsequent mutations showed the N-terminal 90kDa fragment as well. Thus the mutation of Pyr FS1 possibly affects the mobility of the protein indirectly by a potential secondary protein modification or a structural change in the Pyr protein rather than blocking the processing of Pyr.



Taken together the mutation of the Furin cleavage sites in Pyr alone or in combination did not prevent the cleavage of the protein, proving that cleavage of Pyr is not carried out by a Furin protease. The results obtained in cell culture and the observed small differences in the activity of wild type Pyr and Pyr with mutated Furin cleavage sites *in vivo* (Figure 22) strongly suggest that Pyr is proteolytically processed by another currently unknown protease.

Similar to the results obtained for Pyr the inhibition of the Furin protease via the use of the inhibitor  $\alpha$ 1-PDX in cell culture (Figure 19) and in the gain-of-function analysis *in vivo* (Figure 22) did not lead to the clear results necessary to validate a role of Furin proteases for the processing of Ths. Therefore double-tagged Ths variants with sequentially mutated Furin cleavage sites were also tested in cell culture and their cleavage analysed in Western Blots (Figure 24).

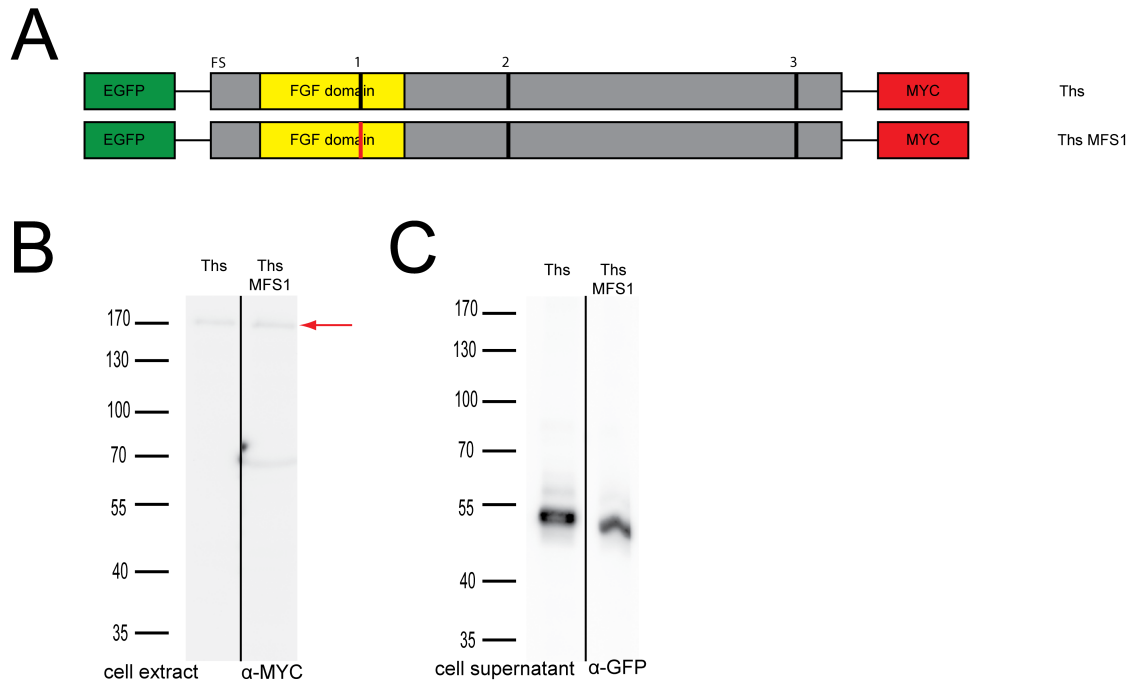


**Figure 25: Ths MFS1 is cleaved and secreted**

(A) Schematic drawing of the EGFP- and MYC tagged Ths constructs including Furin cutting sites. Mutated Furin cutting sites (MFS) are marked in red. (B+C) Western blot analysis of the expressed EGFP- and MYC tagged Ths constructs (B) in the cell extract and (C) in cell supernatants. Proteins were detected using (C) anti-GFP antibody and (B) the anti-MYC antibody. A red arrow marks uncleaved Ths protein. Note: Mutation of Ths MFS1 is not preventing cleavage and secretion of Ths.

This approach revealed that both, the inhibition of the Furin protease by  $\alpha$ 1-PDX and the mutation of the cutting sites, led to the inhibition of cleavage in Ths in cell extracts.

Interestingly already the mutation of the first cutting site (Ths FS1), which is located within the FGF domain, was sufficient to inhibit the proteolytic cleavage completely. As a result the full-length Ths protein could be detected with antibodies against the N-terminal EGFG-Tag and the C-terminal MYC-Tag in the cell extract. This result suggests that the first Furin cleavage site is indeed used for the proteolytic processing of Ths by a Furin protease. However wild type Ths could be detected neither as cleaved 55kDa fragment nor as full-length protein within the cell extracts. This result is in accordance with earlier experiments that showed that wild type Ths could only be detected as cleaved fragment in cell supernatants (2.1.2.5). The absence uncleaved Ths in cell extracts would therefore indicate that the secretion of Ths is highly efficient, leaving hardly any protein in cell extracts. Furthermore, since only processed Ths can be detected in the cell supernatant, Ths must be entirely processed during or after the secretion from the cells. If this explanation were correct the mutation of Ths FS1 would affect the secretion of Ths and thus indirectly prevent the subsequent proteolytic processing.

This hypothesis was tested by the expression of the wild type Ths and Ths carrying a mutation in the first Furin cleavage site (Ths MFS1) in cell culture and the analysis of both the cell extracts and the supernatant. In the supernatant only the cleaved 55kDa fragment was detected both in the wild type Ths and in Ths MFS1. However, in the cell extracts full-length Ths is detectable in small amounts when the Ths MFS1 was transfected and also in case of the wild type Ths (Figure 25B).

These results exclude Fur1 as the protease involved in the cleavage of Ths, thus suggesting that Fur1-mediated cleavage is exclusive to Bnl and not presenting an overall mechanism for all FGFs in *Drosophila melanogaster*. Furthermore, the experiment showed that wild type Ths is hardly detectable in cell extracts neither as uncleaved nor as a cleaved protein thus supporting the model that Ths is unstable in the cellular context and that is completely processed during or after its secretion. However, the first cleavage site seems to have an effect on the stability of Ths within the cells.

### **3.2.6 Identification of the Pyr cleavage site**

#### *3.2.6.1 Mapping of the Pyr cleavage site*

After excluding Furin proteases as candidates for Pyr and Ths processing it was essential to map the cleavage position in detail to obtain a first hint for the identification of the protease involved. The N-terminal cleavage product of wild type Pyr had a

molecular weight of approximately 95kDa including EGFP in SDS gels. This would indicate a cleavage site between aa 500 and 600. However, the full-length protein showed a dramatic increase in the molecular weight compared to the size calculated for its aa sequence. Taking this into consideration a systematic series of C-terminally truncated double-tagged Pyr variants were cloned (Figure 26A) and tested in cell culture and Western blot of the supernatants as described before. The cleavage of the double-tagged variants should result in an EGFP tagged N-terminal fragment and a MYC tagged C-terminal fragment. Variants that are truncated beyond the cleavage site would no longer be cleaved and should be detectable with antibodies against both tags. The loss of a tag through cleavage will result in an additional decrease in molecular weight compared to the double-tagged constructs.

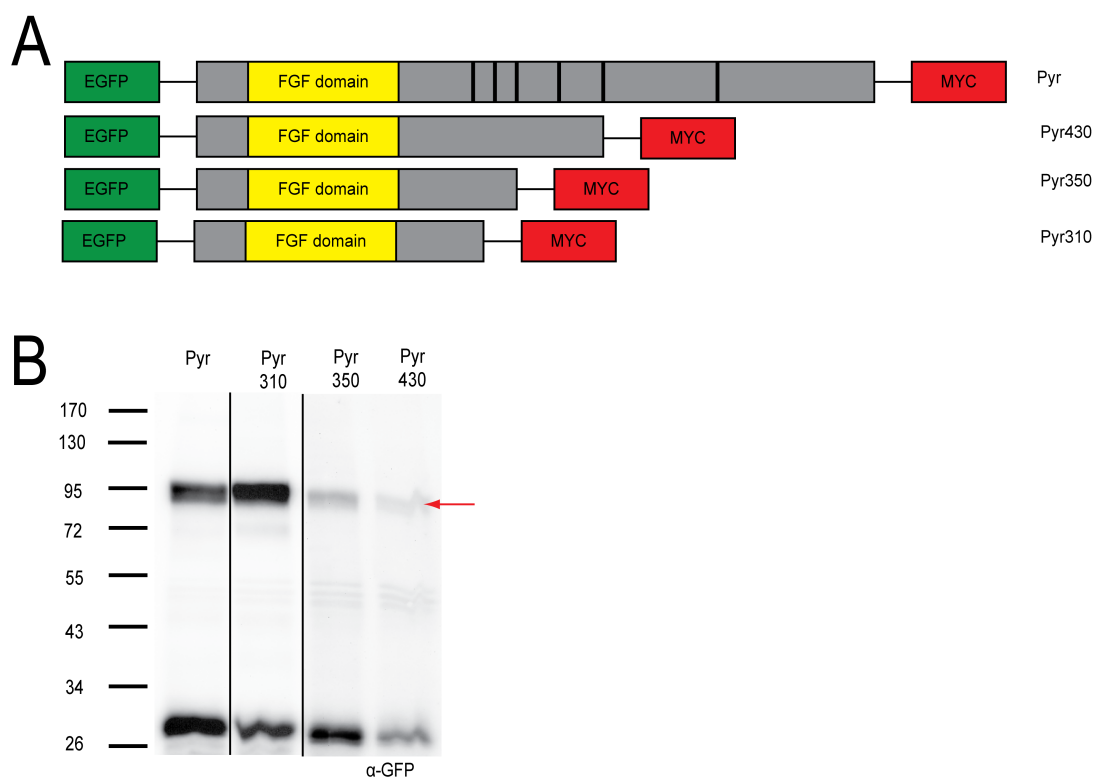


**Figure 26: Mapping of the Pyr cutting site by C-terminally truncated constructs**

(A) Schematic drawing of the EGFP- and MYC tagged Pyr truncation constructs. (B) Western blot analysis of the expressed EGFP- and MYC tagged Pyr truncation constructs in cell supernatants. Proteins were detected using anti-GFP antibody. The red arrow indicates cleaved fragments. The additional band with a molecular weight of about 30kDa represents presumably EGFP. Note: All truncated constructs are cleaved.

A first set tested included constructs with truncations reaching from aa310 to aa430. All of these constructs were cleaved resulting in the 95kDa N-terminal fragment (Figure 26B). Therefore, the cleavage site must be located even further N-terminal. These findings indicate that Pyr is post-translationally modified in its N-terminal half, which causes a dramatic shift in its molecular weight in SDS-gels.

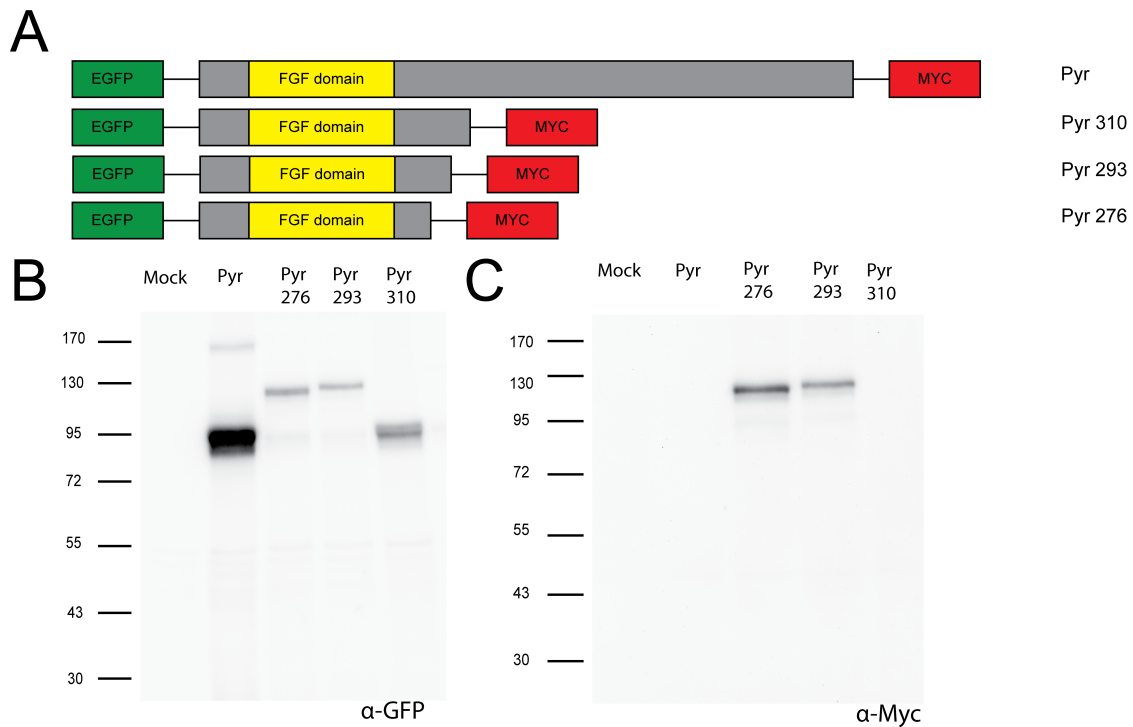


**Figure 27: Mapping of the Pyr cutting site by C-terminally truncated constructs**

(A) Schematic drawing of the EGFP- and MYC tagged Pyr truncation constructs. (B+C) Western blot analysis of the expressed EGFP- and MYC tagged Pyr truncation constructs in cell supernatants. Proteins were detected using anti-GFP antibody (B) and anti-MYC antibody (C). Note: Pyr310 is cleaved, while shorter constructs remain uncleaved and therefore can be detected with the anti-MYC antibody.

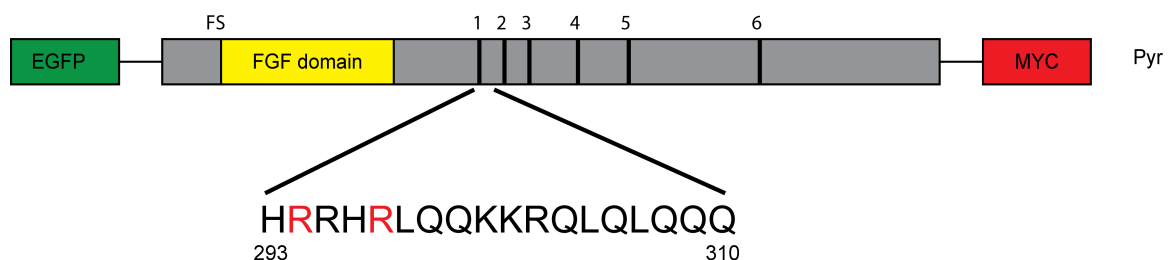


**Figure 28: Presumptive Pyr cleavage site**

Schematic drawing of Pyr with the amino acid sequence of the cleavage site between aa293 and aa310. Pyr FS1 is marked red.

A second set of truncated constructs, containing constructs with truncations as small as 276 aa, revealed that the cutting site is located in the area between aa293 and aa310 (Figure 27B and C). The experiment showed that constructs smaller than 310 aa remained uncleaved and can be clearly detected with antibodies against the N-terminal and C-terminal tag while Pyr310 is cleaved into the 95kDa fragment as shown before for wild type Pyr. Taken together the cutting site has to be positioned in the sequence that distinguishes these two constructs from each other, which is the area from aa293 and aa310.

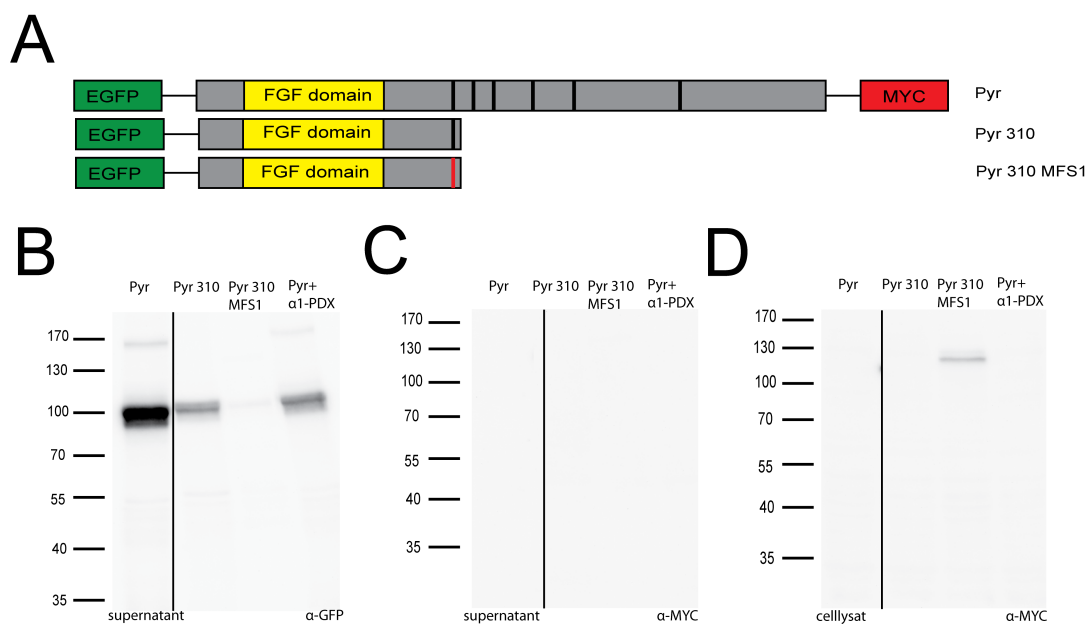


**Figure 29: Role of Pyr FS1 for the processing and secretion of Pyr**

(A) Schematic drawing of the EGFP- and MYC tagged Pyr truncation constructs including Furin cutting sites. Mutated Furin cutting sites (MFS) are marked in red. (B+C) Western blot analysis of the overexpressed EGFP- and MYC tagged Pyr constructs in cell supernatants and (D) cell lysate. Proteins were detected using the anti-GFP antibody (B) and anti-MYC antibody (C,D). Note: Mutation of Pyr FS1 in the truncated Pyr310 leads to an inhibition of cleavage and of secretion and therefore accumulation of the protein within the cell.

The inspection of the aa sequence between aa293 and aa310 revealed that Pyr FS1 is positioned in the area of question (Figure 28). Since, the mutation of this cleavage site in the Pyr full-length protein resulted in the appearance of an additional band (Figure 23) it seemed possible that Pyr is cleaved in a sequential fashion by more than one protease and Fur1 processing only takes place after initial cutting by another protease. Therefore Pyr FS1 might still be involved in the processing of Pyr. If this is the case mutation of the cutting site in the shorter 310aa construct (Pyr310MFS1) might inhibit

the cleavage of the truncated variant but not in the full-length Pyr. When this construct was generated and tested as described it appeared that this protein variant could no longer be detected in the supernatant like the Pyr310 construct it is based on, but remained uncleaved within the cells (Figure 29). However, it remained unclear if the protein is no longer secreted because it is not cleaved, or if it is not cleaved because it is no longer secreted.

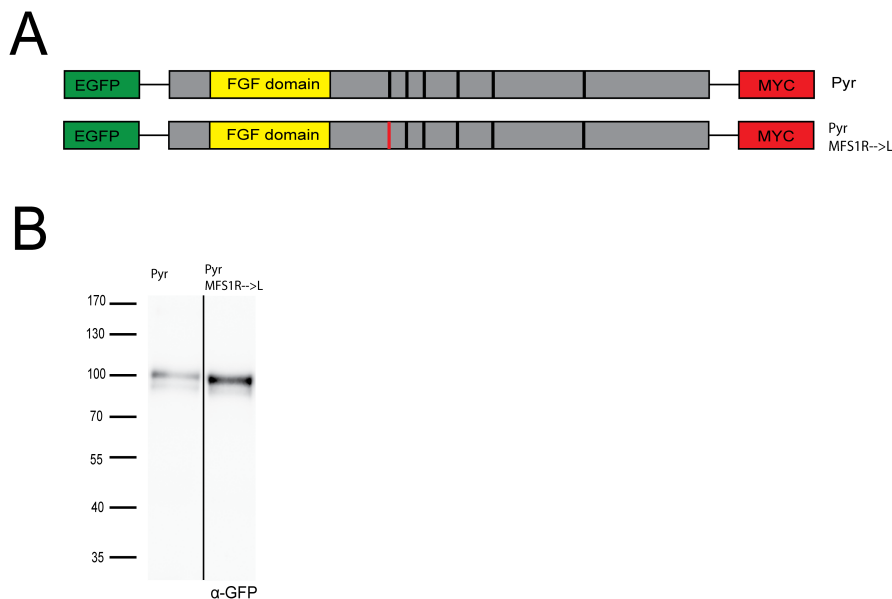


**Figure 30: Mutation of Pyr FS1 is not preventing cleavage of Pyr**

(A) Schematic drawing of the EGFP- and MYC tagged Pyr truncation constructs including Furin cutting site. Mutated Furin cutting sites (MFS) are marked in red. (B) Western blot analysis of the overexpressed EGFP- and MYC tagged Pyr constructs in cell supernatants. Proteins were detected using the anti-GFP antibody. Note: The preservation of the original charge in the mutation of Pyr MFS1 leads to cleavage of Pyr.

One possible explanation why the mutation of the first Furin cleavage site was preventing the secretion of the protein might be that the change in charge in the domain affects the cleavage as the two arginines in the Furin cleavage motif (R-X-X-R) were mutated into glycines. Alternatively, the change in charge could directly affect the secretion and thereby affect subsequent cleavage of Pyr. To prevent Furin-mediated processing without a change of the charge, the two arginines were substituted with lysines (PyrMFS1 R→K), a positively charged amino acid that nevertheless blocks Furin-mediated cleavage. When this version of the truncated Pyr310 protein was tested for cleavage, it showed that the preservation of the protein's distribution of charge was sufficient to restore both the processing of the protein and its secretion. Hence, the mutation of the FS was not directly responsible for rendering the protein no longer cleavable. This experiment ultimately excludes a role of Furin in processing of Pyr.

Furthermore, these results support the model that the charge of the amino acid sequence surrounding the cleavage site is essential for target recognition of the protease responsible for Pyr cleavage. Alternatively the charge could be required for the transport of Pyr into subcellular domain, where the protease is localized.

### 3.2.6.2 Deletion of presumptive Pyr cutting site is not preventing cleavage

To prove independently that the cutting site is positioned between aa293 and aa310 the sequence was deleted in the Pyr full-length protein. This deletion should prevent the cleavage of Pyr if the identified region is required for cleavage of the full-length protein. The described deletion was achieved with the same method as the site-directed mutagenesis, described in 2.1.1.8. In addition, a second deletion from aa277 to aa309 (Pyr $\Delta$ 277-309) was generated to cover the possibility that prior to the cutting site a specific recognition site was of importance.

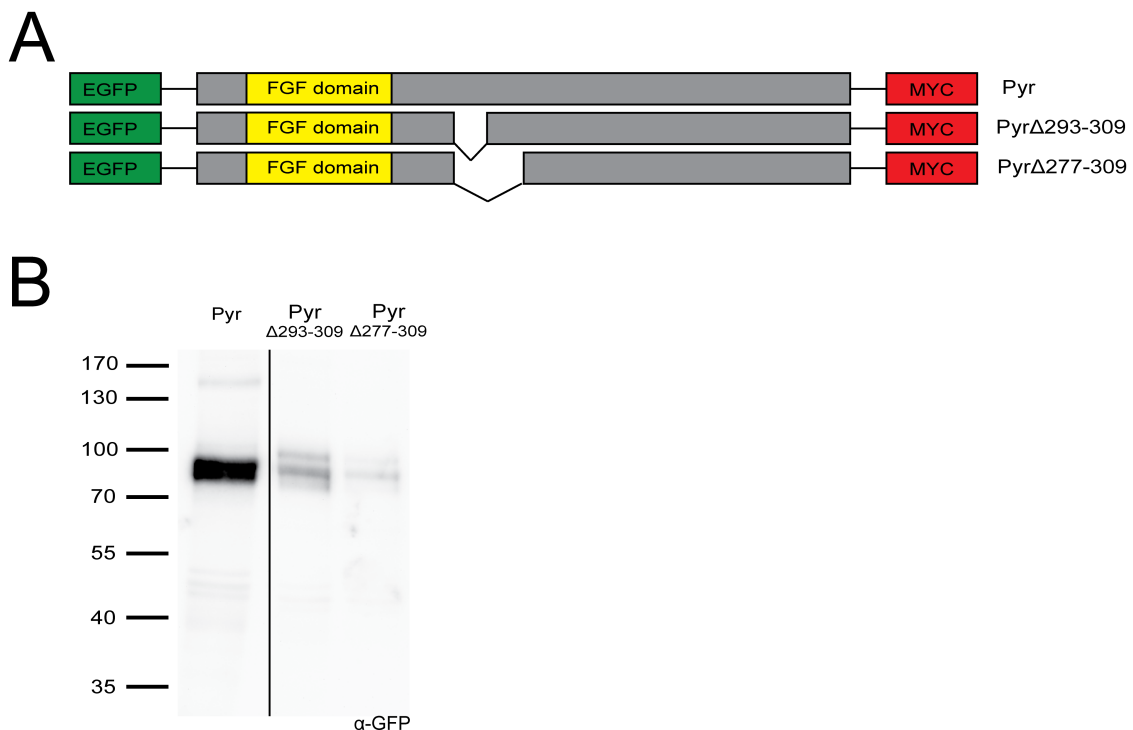


**Figure 31: Necessity of the presumptive cleavage site for the processing of Pyr**

(A) Schematic drawing of the EGFP- and MYC tagged Pyr deletion constructs. (B) Western blot analysis of the overexpressed EGFP- and MYC tagged Pyr deletion constructs in cell supernatants. Proteins were detected using anti-GFP antibody. Note: Deletion of the presumptive cleavage sites does not prevent processing of Pyr.

The test of these two constructs revealed that the deletion of the sequence in question was not sufficient to prevent the cleavage of full-length Pyr. However, the deletion of the mapped cleavage region resulted in the appearance of an additional N-terminal fragment with a slightly higher molecular weight for both deletion constructs (Figure 31). Such an additional band was also detected before in the full-length Pyr carrying a mutated FS1, which is located within the deleted sequence (Figure 23). An explanation for this result could be that the cleavage of Pyr between aa293 and aa310 is not determined by a specific target sequence but rather by protein folding, which might expose this domain for cleavage independent of its aa sequence. Therefore the sequence change due to the deletion or mutation of the FS1 might change the running behaviour on a SDS gel by a change of charge in the protein to form the detected additional band.

Although the truncation constructs revealed a clear result and the molecular weight fits the observed size of the cleaved fragment of wild type Pyr, It remains unclear if Pyr is cleaved between aa293 and aa310. Furthermore, the mapping did not reveal the cutting motif of a characterized protease. Hence it remains unclear which protease is responsible for the processing of Pyr and by what possible recognition site it is recruited.

### **3.2.7 Identification of the Ths cleavage site**

#### *3.2.7.1 Mapping of the Ths cleavage site*

After excluding Furin as the protease in question, the cutting site was mapped for Ths in the same way as it was done for Pyr (Figure 26 and Figure 27). A series of truncated constructs was cloned including constructs as short as 130aa. As the FGF domain in Ths is positioned between aa32 to aa137, the aa130 construct is not carrying the full FGF domain and was thought to function as the end point for the truncation series as the resulting protein would be functionally inactive (Figure 32).



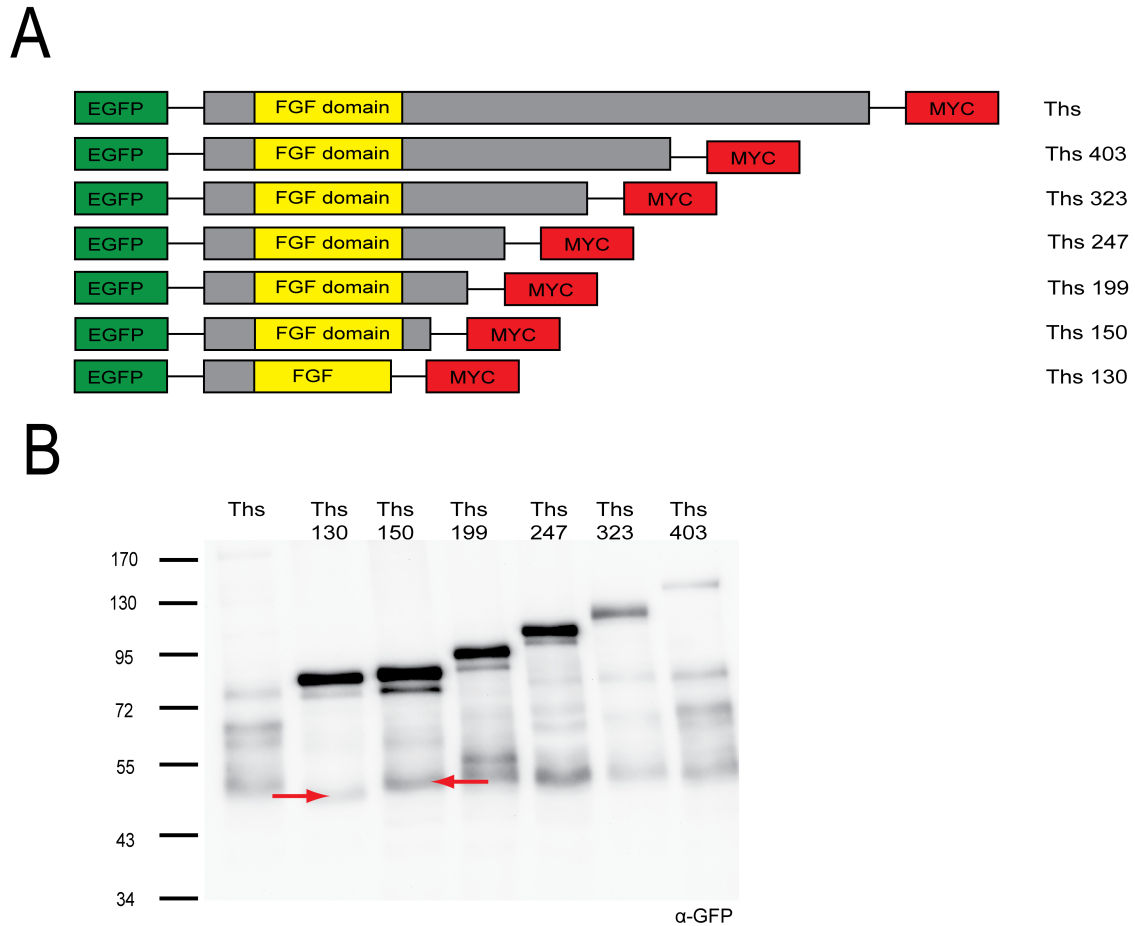


**Figure 32: Mapping of the Ths cutting site by C-terminally truncated constructs**

(A) Schematic drawing of the EGFP- and MYC tagged Ths truncation constructs.

(B) Western blot analysis of the overexpressed EGFP- and MYC tagged Ths truncation constructs in the cell supernatant. N-terminal fragments were detected with the anti-GFP antibody. Red arrows indicate different size of the Ths cleavage product. Note: All Ths truncation constructs are only partially cleaved. Ths130 is producing a N-terminal fragment of different molecular weight than the larger truncation constructs, indicating that Ths130 might not be cleaved.

When the truncated Ths proteins were tested on a Western blot it became apparent that all truncation variants tested resulted in the detection of at least two protein bands with the anti-GFP antiserum. The larger of the two bands was also detectable with the Myc antibody (not shown) and thus represents the uncleaved truncated Ths variants. This was further supported by the increase in molecular weight with the increase of length of the tested truncation construct. Therefore only a portion of the Ths variants is cleaved which could be caused by the strong overexpression or directly by the C-terminal truncations. The smaller band of 55 kDa was independent of the size of the tested variant and corresponds to the cleaved N-terminal fragment of 55 kDa that was

detected in wild type Ths. The detection of the uncleaved and the cleaved N-terminal fragments within the cell culture supernatant suggests that the tested C-terminally truncated constructs are only partially cleaved in Kc cells. However, in the Ths 130 construct the band is not only weaker but also runs at slightly different molecular weight suggesting that this band is not corresponding to the N-terminal cleavage product detected for the wild type Ths. Thus Ths150 was cleaved, while in Ths 130 the cleavage seemed to be affected.

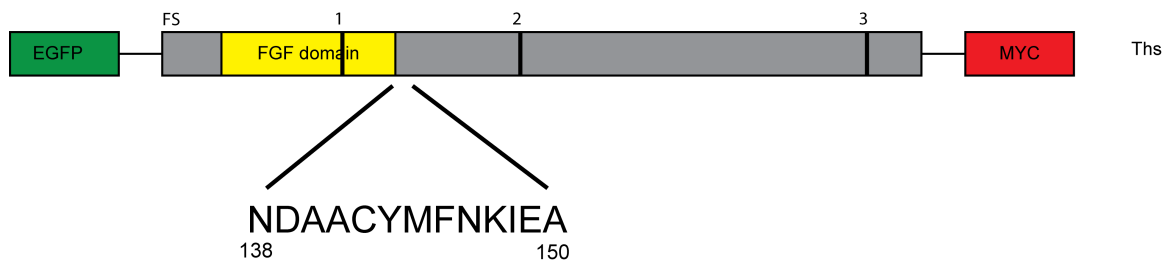


**Figure 33: Presumptive Ths cleavage site**

Schematic drawing of Ths with the amino acid sequence of the cleavage site between aa138 and aa150

### 3.2.7.2 Deletion of the presumptive Ths cutting site is preventing cleavage

The analysis of Ths truncation constructs indicated that the cleavage occurs most likely between the FGF domain and the mapped area, which would be in the area between aa138 and aa150. However, since all truncated constructs were only partially cleaved, a full-length construct of Ths with an internal deletion of aa 140 to 150 was generated and tested to investigate if the identified cleavage region is essential for cleavage of the full length Ths protein as well. The deletion was chosen to include the mapped area, while allowing for some distance to the FGF domain to ensure the functionality of the protein. When this deletion construct was expressed in cell culture only the full-length Ths was detectable in both the cell lysate and the cell supernatant. Thus although the results of the truncated variants left some doubts the identified stretch between aa 140 and 150 is the target for cleavage in full length Ths. If all former results are taken together it is very likely that the Ths cutting site is contained within the aa141-150 and therefore was mapped successfully in this work.

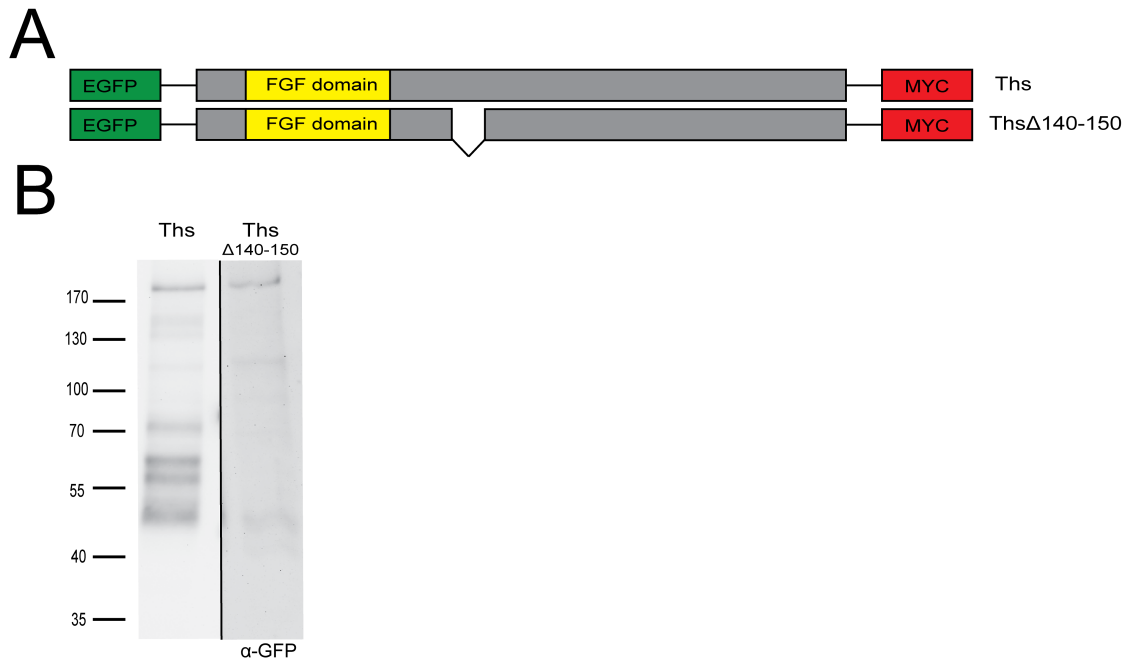


**Figure 34: Necessity of the presumptive cleavage site for the processing of Ths**

(A) Schematic drawing of the EGFP- and MYC tagged Ths deletion constructs. (B) Western blot analysis of the overexpressed EGFP- and MYC tagged Ths deletion constructs of cell supernatant. Proteins were detected using anti-GFP antibody. Note: Deletion of the presumptive cutting site prevents cleavage of Ths leads to the accumulation of the full-size protein.

## 4 Discussion

FGF signalling is essential for a vast amount of processes throughout development and during adulthood. They play major roles for developmental processes like mesoderm induction, gastrulation, midbrain-hindbrain patterning and the formation of limbs and bones (Niswander et al. 1993; Shiang et al. 1994; Crossley et al. 1996; Reifers et al. 1998; Ciruna and Rossant 2001; Thisse and Thisse 2005). During adulthood FGFs continue to function in tissue homeostasis and wound healing, while misregulation of FGF signalling can lead to the formation of tumours and contribute to other human diseases (Coumoul and Deng 2003; Chen and Deng 2005; Eswarakumar et al. 2005; Thisse and Thisse 2005). Thus tight regulation of these highly dynamic and potent growth factors is of major importance.

Most of the known 24 vertebrate FGFs are relatively small proteins with a molecular mass of 17-34kDa, while in *Drosophila* all three FGF ligands have a much larger predicted molecular mass of approximately 80kDa (Sutherland et al. 1996; Ornitz and Itoh 2001). While vertebrate and *Drosophila* FGF show homologies within the FGF domain, *Drosophila* FGFs have large additional domains with no sequence homology and of currently unknown function. In the case of the FGF10 homologue Bnl these additional domains are both N- and C-terminal of the FGF domain (Sutherland et al. 1996), whereas the FGF8 homologues Pyr and Ths both have a large C-terminal domain (Gryzik and Müller 2004; Stathopoulos 2004).

Recently Tatyana Koledachkina (2010) demonstrated that the *Drosophila* FGF ligand Bnl is cleaved at multiple sites releasing of approximately 34kDa, which roughly resembles the size and composition of its vertebrate homologue FGF10 (Min et al. 1998). This processing is essential for the activation of Bnl and crucial for the patterning of the embryonic development of the trachea. In the study presented here the use of Furin-mediated processing as an activation mechanism for Bnl could be demonstrated to take place beyond embryonic development. The analysis of two commonly used models for Bnl signalling in the larva, the formation of terminal branches at the dorsal connective of the tracheal network and the formation of the air sac of the wing imaginal disc, showed that Furin-mediated processing of Bnl is crucial also during larval development. Further analysis of Bnl signalling in the larva showed that Fur1-mediated processing is the rate-limiting step of Bnl signalling in at least two larval processes. This result suggests that Furin-mediated processing composes a novel regulatory mechanism to a greater subset or even of all Bnl-dependent processes.

This work further demonstrated that the cleavage of Bnl is no exception and that all three *Drosophila* FGF are cleaved into smaller proteins that roughly resemble the size of their vertebrate homologues. Similar to Bnl the large additional domains with no homology to their vertebrate homologue and known function are removed in Pyr and Ths. While Bnl is cleaved both C- and N-terminal, Pyr and Ths are cleaved exclusively C-terminal.

Although both FGF-8 homologues contain multiple Furin cutting sites, some of which are even conserved throughout the *Drosophilids*, analysis in cell culture and *in vivo* showed that Pyr and Ths are cleaved by a different protease. Neither the use of the Furin-specific peptide inhibitor  $\alpha$ 1-PDX (Benjannet et al. 1997; Jean et al. 1998; Molloy et al. 1999) nor the mutation of the identified Furin cutting sites prevented the cleavage of Pyr and Ths. Subsequently the cutting sites in both proteins were mapped by the use of truncated constructs to a 10 or 17 amino acid sequences respectively, which hopefully will help to discover the responsible protease in the future. Furthermore, it has to be investigated if cleavage of Pyr and Ths is necessary for their activation in the same fashion as in the case of Bnl. However, published data is pointing towards this possibility (Tulin and Stathopoulos 2010).

#### **4.1 Fur-mediated processing is used to regulate Bnl signalling during larval terminal branch formation**

The proteolytic processing of Bnl has been shown to be crucial for its function during the embryonic development (Koledachkina 2010). The activation of Bnl is achieved by the removal of its large N- and C-terminal domains by the Fur1 protease, which releases a much smaller fragment with a strong similarity in size and sequence to its vertebrate homologue FGF10. Only this Bnl biologically active fragment has been shown to be responsible for the patterning of the tracheal network during embryonic development (Koledachkina 2010). However, preceding studies have shown that the role of Bnl signalling is not confined to embryonic development, but also plays an active role during larval development (Jarecki et al. 1999; Sato and Kornberg 2002; Centanin et al. 2008; Roy and Kornberg 2011). In this context Bnl is likewise working as a chemoattractant for tracheal cell expressing the FGFR Btl and thereby inducing differentiation and migration (Sutherland et al. 1996; Ribeiro et al. 2002).

The dorsal branch TTBs within the 3<sup>rd</sup> segment of the 3<sup>rd</sup> instar larva has been used as a model to investigate Bnl signalling in the *Drosophila* larva (Jarecki et al. 1999; Centanin et al. 2008). Its terminal branches have a characteristic branching behaviour, typically with a main branch ramifying into several straight TTBs with a diameter over

1mm. These TTBs then project and ramify into even thinner extensions into the target cells. Overexpression of a constitutive active form of Btl within the tracheal network leads to an increased number of TTBs, which led the investigating parties to the conclusion that Bnl signalling is a major factor for terminal branch formation during larval development (Jarecki et al. 1999; Centanin et al. 2008). However former studies concerning Bnl signalling in the larva utilize the Gal4 system, which is driving expression throughout all *Drosophila* development including embryonic stages (Brand and Perrimon 1993; Jarecki et al. 1999; Sato and Kornberg 2002; Centanin et al. 2008). Thus the data created by this approach cannot distinguish if the observed effect is due to Bnl signalling in larva or a secondary effect caused by changes of the embryonic development. Thus it cannot be distinguished if the observed effect is due to Bnl signalling in larva or a secondary effect caused by changes of the embryonic development by the data created by this approach. Additionally it allowed to determine the time window of Bnl function during the formation of the ternary branches at the dorsal connectives. A temperature-sensitive Gal80 was used to initially repress Gal4 activity and hence preventing the expression of the gene of interest, which is under control of the UAS (Lee and Luo 1999; Suster et al. 2004). Thus the expression of the gene of interest can be controlled by a change in temperature. This technique allowed the expression of the gene of interest solely during larval development with no expression during the embryonic development. The use of the Gal80ts system confirms that the effect of Furin-mediated processing on Bnl signalling is not confined to embryonic development. Furthermore temperature shifts at multiple time points identified the 2<sup>nd</sup> larval instar to be essential for Bnl-regulated trachea growth. This result suggests that the growth of the trachea system during larval development is not a uniform process but rather has certain periods when defined developmental processes like the formation of new ternary branches are determined. However, the observed requirement of Bnl-signalling during 2<sup>nd</sup> instar does not exclude additional functions during 3<sup>rd</sup> instar larvae as only the formation of the dorsal TTBs was analysed. Therefore, Bnl may still regulate the elongation of fine ternary branches of the trachea towards their growing target tissues in 3<sup>rd</sup> instar larvae.

In summary, this work demonstrates for the first time that the observed effect of Bnl signalling on formation of the larval tracheal network is indeed a larval effect and not a remnant of embryonic development. It allowed the identification of the 2<sup>nd</sup> larval instar as the period requiring Bnl signalling for the formation of novel ternary branches. Furthermore, it proved that Furin-mediated processing is essential for Bnl activity also beyond embryonic development.

## **4.2 Formation of the adult air sac during larval development is dependent on Fur-mediated processing of Bnl**

Another Bnl-dependent process that was investigated in this work is the formation of the wing imaginal disc ASP that gives rise to the air sac in the thorax of the adult animal. Air sacs are hollow, air filled structures that supply the brain and major muscles of the adult with oxygen (Cohen 1993). The formation of these air sacs starts during late larval development and continues throughout the pupal development until it forms the adult structure. The formation of the wing disc ASP has been shown to be guided by Bnl signalling (Sato and Kornberg 2002; Roy and Kornberg 2011). Taking into consideration that Fur1-mediated processing was crucial for all tested Bnl-dependent processes; it seemed reasonable to test if Fur1-mediated processing of Bnl is necessary for ASP formation. To test this hypothesis  $\alpha$ 1-PDX was used to inhibit Fur1 activity within the wing imaginal disc. Inhibition of Fur1 activity in the presumptive area of Bnl expression within the wing disc led to an absence of the ASP. Therefore the Fur1-mediated processing of Bnl is essential for the formation of the ASP. These findings are compliant with former experiments that showed the necessity of Fur1-mediated processing for all former tested Bnl-dependent processes.

To further investigate the role of Bnl processing and verify its necessity for all Bnl-dependent processes further experiments have to be conducted in future. Possible experiments for this purpose would be for example the investigation the influence of Fur1-mediated processing of Bnl during later developmental stages such as in the pupa or during adulthood. Proof of the necessity of Fur1-mediated processing during these stages would allow for the conclusion that Bnl signalling is regulated by Fur1 throughout the whole live cycle of *Drosophila* and possibly confirm Fur1 processing as a regulatory mechanism for all Bnl signalling.

## **4.3 Remodelling of the larval tracheal network during hypoxia is regulated by Furin proteases**

Adequate supply of all tissues with oxygen is a basic need of all animals and the necessity to cover this need lead to the development of elaborate organ systems to ensure proper oxygen supply. The lung and blood vessel of the vertebrates and the tracheal system of the insects are particularly successful examples of systems that capture and transport oxygen. These systems typically respond to environmental or local oxygen conditions with alterations of the respiratory system to ensure the

coverage of this basic need. Both in vertebrates and insects the alteration of the respiratory system is mediated by HIFs. During hypoxia HIFs alter gene expression to recruit more extensions of the oxygen supply system into the oxygen-deprived tissue (Nagao et al. 1996; Wenger 2002).

In *Drosophila* the molecular mechanism for this adaptation is thought to be based on Bnl signalling. A comparison of Bnl protein levels in larvae raised under different oxygen conditions shows that hypoxia increases the amount of Bnl protein by 2-fold compared to normoxic conditions (Jarecki et al. 1999). However, in this experiment only the unprocessed full-length Bnl was investigated which does not allow any conclusions about the amounts of the active processed form of Bnl. Additionally increased amounts of Btl RNA could be detected, suggesting that an increased number of receptors could be involved as well (Centanin et al. 2008). While this theory sounds reasonable it remains unclear how this accumulation of Bnl is controlled and if the amount of Btl protein is increased at all. Thus the molecular mechanism underlying the adaptation of the tracheal network to the oxygen concentration in the environment is still not fully understood.

During this work first experiments to explore the role of Bnl processing during hypoxia were conducted. Therefore *fur1* gain-of-function and *fur1* loss-of-function experiments were conducted during hyperoxia and hypoxia to investigate the role of Fur1-mediated processing for oxygen-dependent remodelling of the tracheal network. The results of these experiments showed that the adjustment of Bnl processing is able to counteract the effects of environmental oxygen concentration on the formation of terminal trachea. To achieve this Bnl processing was intensified by *fur1* overexpression during hyperoxia, which lead to a raised number of TTBs as expected. Inhibition of Bnl processing by expression of  $\alpha 1$ -PDX or *Fur1* RNAi during hypoxia resulted in lethality during late embryonic or early larval development. Therefore Fur1-mediated Bnl processing seems to have a major influence on tracheal remodelling due to environmental oxygen conditions. Bnl processing either could be directly involved in the hypoxia response of the tracheal network or influencing the ramification of the tracheal network independently from the oxygen content of the environment.

The use of a weaker driver line, resulting in the expression of a smaller amount of  $\alpha 1$ -PDX, enabled the survival of a small number of larvae during hypoxia. In these larvae the number of TTBs was reduced compared to w1118 larvae in hypoxia indicating that indeed a reduction of Furin activity can inhibit ternary tracheal outgrowth during hypoxia. These results suggest that the enhanced terminal trachea formation, due to increased Furin activity, is indeed of major importance for the survival of larvae during



hypoxia. Moreover this correlation would imply that the larvae that survived the treatment were suffering from mild defects due to partial Fur1 inhibition. In this case the defect would be obscured by lethality. Therefore the true effect of Fur1 is most likely larger than the defects that were observed here. Taken together these findings suggest that Fur1-mediated processing of Bnl is indeed the molecular mechanism that controls tracheal adaption during hypoxia. However, the experimental design does not allow to exclude that the Furin activity affects the tracheal adaptation upon changes in the oxygen concentration indirectly through the regulation of a yet unknown factor important for tracheal outgrowth.

Two possible explanations could be applied to explain the lethality of decreased Fur1 activity during hypoxia. Since the increased number of trachea during hypoxia are needed to insure an adequate supply of oxygen in the larvae the decrease of terminal trachea growth by the inhibition of Bnl-processing might result in a critical shortage of oxygen, finally resulting in the death of the larvae. However, the results do not allow to rule out that the induced lethality was caused by a completely unrelated process regulated by Furin proteases. For example, it was shown Fur1 activity is required for processes other than Bnl signalling, including Dpp signalling (Künnapu et al. 2009). The disruption of these processes might impair the fitness of the larvae or independently cause the lethality. However, in this case it is unclear why the reduction of Furin activity causes lethality only under hypoxic conditions.

To finally prove the hypothesis that Furin-mediated processing is essential for the adjustment of the tracheal network further experiments are required. The analysis of Bnl processing in larvae raised in different oxygen conditions using Western blots should reveal if Bnl cleavage is regulated under different oxygen concentrations. If Fur1-mediated Bnl processing is regulating the number of TTBs during hypoxia, the ratio between cleaved and uncleaved Bnl should be tipped in favour of the cleaved protein. During hyperoxia on the other hand the full-length protein should accumulate with only small amounts of the cleaved protein. This analysis is of special importance, as Jaerecki et al. showed that full-length Bnl is detectable in Western Blots from in larval extracts and that its amount accumulates during reduced oxygen supply (Jaerecki et al. 1999). Unfortunately the Western Blot depicting this increase shows only the full-length protein and does not allow any conclusion about the ratio of cleaved versus uncleaved protein. Thus it is unclear if the observed increase in the amount of uncleaved protein is caused by an increase in expression or reflects the inhibition of Bnl processing in hypoxia (Jaerecki et al. 1999). Based on the results shown here an increased rate of Bnl

processing would be expected. This would indicate that the increased amount of uncleaved Bnl is indeed reflecting an increase in *bnl* expression.

Additionally the mechanism underlying the control of Furin activity upon changes in oxygen concentration is of great interest. Analysis via quantitative RT-PCR will determine changes in the amount of *fur1* mRNA. One would expect the raise of *fur1* mRNA if Fur1 is mediating the tracheal remodelling during hypoxia. Furthermore, it would be of interest to investigate if also *bnl* mRNA levels are upregulated based on the findings of Jaerecki et al. (1999) who discovered that hypoxia is elevating the amount of full-length Bnl protein.

Alternatively, the activity of the Furin protease could be regulated by a change of its subcellular localization. The localization of Furin within the cell has been described as highly dynamic as it has been shown to rapidly cycle between the *trans*-Golgi network, the cell surface and the endosomal compartment (Molloy et al. 1994; Molloy et al. 1999). Human Furin is known to catalyze processing of multiple signalling factors within the *trans*-Golgi network (Thomas 2002). However, it was also suggested that Furin proteases are active at the cell surface. Bnl cleavage is occurring before it can be detected in the cell supernatant. However, it is unclear if Bnl is processed within the *trans*-Golgi or at the surface of the secreting cells. Additionally studies in human fibrosarcoma cells have shown that hypoxia enhanced the re-localization of Furin from the *trans*-Golgi to the cell surface, which in turn enhances cancer cell invasion (Arsenault et al. 2012). Therefore one would presume that Fur1 might undergo the same re-localization from the *trans*-Golgi to the cell surface in *Drosophila* during hypoxia. To investigate the localization of Fur1 in *Drosophila* a GFP-tagged Fur1 construct has been generated and sent for injection into *Drosophila* embryos to obtain transgenic fly lines. These transgenic fly lines will enable to determine if Fur1 localization is indeed regulated in an oxygen concentration-dependent fashion in *Drosophila* and will hopefully help to establish the subcellular location of Bnl processing.

To investigate the role of Bnl signalling during hypoxia and larval development in more depth the examination of the remaining larval tracheal network could be of interest as well. Especially the ganglionic branch has been shown to be susceptible to morphological changes due to Bnl signalling and changes in oxygen supply. Both overexpression of Btl within the trachea and hypoxia cause the ganglionic branch to adopt a ringlet-shaped appearance instead of their regular straight shape (Centanin et al. 2008; Misra 2014). Therefore the duplication of this hypoxia-related phenotype by *fur1* overexpression would also confirm the connection between Bnl processing and

tracheal remodelling during hypoxia and thus point towards Fur1 as regulator of the process in an independent experimental setup.

#### **4.4 Fur1-mediated processing is the rate-limiting step of Bnl signalling**

Proteases are not limited to regulation in order to fine-tune their activity, but often are themselves major components of regulatory mechanisms. They can for example control the level of activity in signalling pathways (Ehrmann and Clausen 2004). In this context proteolysis is used to remove regulatory proteins or modify regulatory proteins to achieve an active state or alter their existing function (Ehrmann and Clausen 2004). For instance the activity of NF- $\kappa$ B (also known as Relish) is tightly controlled by its negative regulator Cactus. Only upon degradation of Cactus NF- $\kappa$ B can enter the nucleus and function as a transcription factor (Geisler et al. 1992).

In case of Bnl proteolytic cleavage has an activating function (Koledachkina 2010). Its core domain is released by Fur1-mediated cutting in order to achieve an active state of Bnl and thereby activate the interconnected signalling pathway. But even though Fur1-mediated processing has shown to be of great importance for Bnl signalling formerly produced data did not allow to conclude if Fur1 functions as a novel regulatory mechanism or cleavage represent a general processing mechanism like the signal peptide protease. Therefore we strive to answer the question if Fur1 is a general processing enzyme, involved in the maturation of Bnl protein or if it represents a novel key regulatory component.

This thesis provides the information that was needed to clarify the relationship between Fur1-mediated processing and Bnl signalling. If Fur1 was indeed a simple processing factor the inhibition of Fur1 activity should result in a decrease number of TTBs. The increase of Fur1 activity on the other hand should have no influence whatsoever. Experiments using the formation of additional terminal branches as a model show that Fur1 processing has the characteristics of a real regulatory process in Bnl signalling. The experimental data shows that inhibition of Fur1 processing resulted in a decrease in dorsal branch terminal trachea as expected. However, an increased amount of Fur1 in the larva resulted in an increased number of the dorsal branch TTBs up to the natural limits of the model. This quantitative data proofs that Fur1-mediated processing is indeed a novel mechanism involved in the regulation of Bnl signalling.

Additional experiments show that Fur1 expression not only affects Bnl signalling in a quantitative manner but that Fur1 expression can be the key regulator for Bnl activity in certain tissues as well. The analysis of tissue-specific expression show that presence of both Bnl and Fur1 are needed qualitatively to attract trachea into a tissue. In the salivary gland, in which Fur1 is expressed but Bnl is absent, additional expression of *bnl* was sufficient to attract trachea. More importantly, in the non-tracheated fat body, where *bnl* expression could be detected but Fur1 was absent, the expression of *fur1* alone was sufficient to stimulate the growth of trachea into the tissue. Therefore Fur1-mediated processing of Bnl is not only a new regulatory process for Bnl signalling, but represents at least in some tissues a qualitative rate-limiting step.

The study of literature concerning the cleavage of vertebrate FGFs shows that proteolytic processing does not seem to be a common feature in the signalling of vertebrate FGFs. Nevertheless proteolytic processing is able to provide effective temporal regulation in addition to the spatial control provided by the expression pattern of FGFs. Previous investigation of *Xenopus leavis* FGF3 had shown, similar to the situation in Bnl, a C- and N-terminal cleavage by an unknown protease, possibly by a member of the SPC family (Kiefer et al. 1993; Antoine et al. 2000). Additional evidence for the cleavage of FGFs comes from the study of the mouse FGF4, which is processed in the N-terminal region of the protein (Kosaka et al. 2009). Also human FGF23 is cleaved in the C-terminal region by an unidentified protease. However, cleavage occurs at a minimal Furin cutting site, which suggests the involvement of Furin. FGF23 gain of function is associated amongst other diseases with autosomal dominant hypophosphatemic rickets. This disease has been found to have its basis in a loss of the minimal furin site, suggesting the cleavage is required for the inhibition of FGF23 activity (Shimada et al. 2001; White et al. 2001; Benet-Pages et al. 2004). Lately Tatyana Koledachkina (2010) was able to demonstrate that Furin-mediated processing of human FGF10 is, analog to its *Drosophila* homologue Bnl, necessary for the activity of the protein.

To supplement the findings concerning the influence of Fur1-mediated processing on the formation of the tracheal network further experiments are planned in future. Since the necessity of Fur1-mediated processing in the larva has been researched only indirectly, via phenotypical changes during *fur1* gain-of-function and expression of  $\alpha$ -PDX, direct proof for Bnl processing has yet to be produced. For that purpose the processing of Bnl will be analyzed via Western blot in larvae with enhanced or inhibited Fur1 activity.

## 4.5 All *Drosophila* FGFs are processed

Pyr and Ths control the movement of mesodermal cells (Stathopoulos 2004; Wilson et al. 2005; McMahon et al. 2008; Kadam et al. 2009), the differentiation of the pericardial cells (Stathopoulos 2004; Wilson et al. 2005; McMahon et al. 2008; Kadam et al. 2009; Klingseisen et al. 2009), migration of the caudal visceral mesoderm (CVM) (Mandal et al. 2004; Kadam et al. 2012; Reim et al. 2012) and glial differentiation, migration and axonal wrapping in the eye imaginal disc (Franzdottir et al. 2009) via the activation of the FGFR Heartless.

Conducted experiments proved that both FGF8 homologues are cleaved releasing N-terminal fragments of approximately 60kDa for Pyr and 20kDa for Ths, including the FGF- domain. These results corresponded roughly to the findings of Tulin et al. (2010). The discovery of Furin cutting sites suggested that Fur1 might be involved in the proteolysis of Pyr and Ths as shown for Bnl (Koledachkina 2010) and hence Furin-mediated processing might comprise a general regulatory mechanism for FGF signalling in *Drosophila*. This model was further supported by the observation that at least some of the Furin minimal cleavage motifs are conserved in most *Drosophilids*. Furthermore, some of the potential cleavage site appeared to be a combination of two motifs in close proximity, which were shown to be the target for Bnl processing (Koledachkina 2010). However, further research disproved the involvement of Furin proteases in the proteolytic processing of Pyr and Ths. The proteolysis of both proteins could not be prevented by the co-expression of a specific Furin inhibitor or by the mutation of the Furin cutting sites thus providing the evidence that Pyr and Ths are not cleaved by Furin and hence Furin-mediated processing is not constituting a general regulatory mechanism for FGF signalling in *Drosophila*.

Surprisingly the expression of the Furin inhibitor  $\alpha$ 1-PDX had an effect on the formation of the Eve-positive pericardial and muscle precursor cells, which were used as a read out for Htl signalling. This is quite unexpected considering that Fur1-mediated cleavage of Pyr and Ths can be excluded. However, based on the dorsal position within the mesoderm the formation of these cells might be depending on Dpp signalling, which in turn requires Furin-mediated processing for its activation (Künnapu et al.; 2009). Thus one possible explanation for the effect  $\alpha$ 1-PDX on Eve-positive cell formation is the disturbance of Dpp signalling, rather than the inhibition of Htl signalling, due to the inhibition of Furin by  $\alpha$ 1-PDX.

After disproving Furin-mediated processing of Pyr and Ths further experiments were conducted in order to determine the exact position of processing. Since modifications of

Pyr and Ths caused a shift in the running behaviour of the detected fragments in SDS protein gels it was impossible to identify the cleavage sites of the two proteins just based on their apparent molecular weight. The use of truncated constructs on the other hand was successfully applied to narrow the position of the cutting site down to a sequence of 17aa for Pyr and 10aa for Ths.

Proteases can be specific for very specific target sequences confining them to a relatively small subset of substrates or highly promiscuous enabling a high number of substrates (Ehrmann and Clausen 2004). The more promiscuous proteases, like trypsin or lysin, usually bind to single amino acids in the substrate and hence are only specific for that residue (Keil 1992; Olsen et al. 2004; Rodriguez et al. 2008), while highly specific proteases like thrombin or the TEV protease bind to specific multi aa sequences enabling them to engage in highly specific cleavage events (Carrington and Dougherty 1988; Kostallas et al. 2011). Therefore, the high specificity of some proteases can facilitate the identification of the protease involved in the cleaving of a substrate through the analysis of the substrates aa sequence. However when the sequence of the putative cutting sites of Pyr and Ths and their surroundings were analysed *in silico* to determine the involved proteases this effort remained unsuccessful.

To evaluate the influence of Pyr and Ths cleavage on the biological function the construction of transgenic lines containing truncated constructs of Pyr and Ths, representing the size of the cleaved proteins, are in planning. The biological activity of these constructs will be evaluated using the eve expressing cells gain-of function assay (Kadam et al. 2009; Tulin and Stathopoulos 2010). The formation of three eve expressing cells per hemisegment strongly depends on FGF signalling. Thus the observation and quantification of these cells can be used as readout for the activity of the FGF signalling pathway. If the truncated constructs of Pyr and Ths are indeed active, an increased number of eve expressing cells would be expected due to the stronger than usual activation of the FGF signalling pathway. Additionally the influence of the truncated constructs on the formation of other structures, like the gut musculature and glia formation of the eye imaginal disc (Franzdottir et al. 2009), would be interesting to study. With this approach it should be possible to create an extensive picture of the biological function of the processing of the FGF8 homologues.

## 4.6 Differential functions of Pyr and Ths

As described above Pyr and Ths support mesoderm formation by signalling through the FGFR Heartless. While Pyr and Ths have very similar function not all of these functions rely on Pyr and Ths in equal measure (Kadam et al. 2009; Klingseisen et al. 2009).

While this is depicted in their differential expression pattern, the differential function of these two signalling factors seems not to rely on the expression pattern alone. More likely Pyr and Ths, although most likely derived from an ancient gene duplication (Gryzik and Müller 2004; Stathopoulos 2004), have evolved to serve different functions. Pyr is more essential for the migration of the mesoderm and differentiation of pericardial cells and the dorsal muscles, whereas these tissues are hardly affected in *ths* mutant embryos (Klingseisen et al. 2009; Tulin and Stathopoulos 2010). In contrary, mesoderm spreading relies on both Pyr and Ths (Kadam et al. 2009; Klingseisen et al. 2009). To understand how Pyr and Ths exactly play these divergent roles, even though they share the same receptor and have a mostly overlapping expression pattern, it is tempting to speculate that there are additional mechanisms that regulate signalling of the two FGF ligands. Processing of Pyr and Ths by different proteases would represent a possible regulatory mechanism to achieve differential signalling of the two factors through the same receptor. The identification of the cleaving proteases would represent valuable insight into the mechanism through which differential signalling of Pyr and Ths is achieved.

The experimental data provided by this study is encouraging the hypothesis that Pyr and Ths are cleaved by different proteases. Mapping of the cutting sites in Pyr and Ths shows that Pyr and Ths are cleaved in different positions of the protein. Pyr is cleaved in the C-terminal half of the protein, resulting in an N-terminal fragment of approximately 60kDa. Ths on the other hand is cleaved much further N-terminal, straight after the FGF domain, resulting in a small N-terminal fragment of around 20kDa. *In silico* analysis of the cutting sites and their surrounding area showed no similarities within the amino acid sequence that would reveal the nature of the protease. However analysis of the amino acid sequence and subsequent experimental verification revealed that charged residues at the Pyr cutting site are crucial for its cleavage.

Additionally secretion is also prevented by the removal of the charged amino acids at the presumptive cleavage site of Pyr, suggesting a connection between proteolytic processing and secretion of Pyr. Cleavage of Pyr might be a requirement for secretion of Pyr. Another possible connection would be the processing during secretion, which would reveal the localization of the protease in question.

Furthermore, analysis of a construct with a deletion of the prospective cleavage site showed that deletion of the Pyr cutting site did not prevent cleavage in cell culture and even resulted in the same smaller N-terminal fragment that was observed in the unmodified Pyr. A possible explanation for this behaviour of the Pyr deletion construct would be that the responsible protease does not cleave at a specific amino acid

sequence but rather at a certain position in the folded Pyr protein. Concluding from these findings, the protease cleaving Pyr is most likely depending on charged residues. Subsequent initiation of cleavage at a relative position between the amino acids 293 and 310 is presumably independent of a defined cleavage motif.

Additionally the Western blot data is suggesting that Pyr and Ths are cleaved in different subcellular locations. The Pyr fragment was detectable both in the supernatant and within the cell lysate suggesting intracellular cleaving. Ths however is found cleaved only within the supernatant indicating extracellular cleavage or alternatively cleavage during a late stage of its secretion.

Taken together the data is indicating that Pyr and Ths are cleaved by different proteases, which might comprise different regulatory mechanisms to achieve the temporal and spatial divergent signalling of the two FGF8-homologues Pyr and Ths. This theory is further strengthened by the study of truncated Pyr and Ths constructs, which has shown that cleavage of Pyr and Ths is most likely associated with increased activity of the proteins (Tulin and Stathopoulos 2010). Therefore, processing seems to be essential for the activation of Ths and Pyr. Additionally the requirement of two individual proteases could explain the temporal and spatial divergence of Pyr and Ths signalling during embryonic development simply by distinct expression patterns of the two proteases.

To confirm this hypothesis the proteases cleaving Pyr and Ths have to be identified. One attempt that will be followed in future is based on the knowledge that cutting takes place both in S2- and Kc-cell lines and in early embryos. Comparison of the proteases that are expressed based on Chip-data in all mentioned cases led to a list of candidate proteases. This list of candidates was shortened by excluding components of the proteasom and characterized proteases involved in apoptosis and autophagy. Furthermore, some of the remaining proteases like the Rhomboid family could be excluded based on the cleavage preference within membranes thereby only cleaving transmembrane domains (Lee et al. 2001; Urban et al. 2001). Additionally literature research for proteases that promotes cleavage extracellular or within the secretion pathway can possibly narrow the group of candidates. Preliminary testing of some of the candidates using RNAi driven knock down using maternal Gal4 and the novel TRIP lines (Dietzl et al., 2007; Ni et al., 2008) is ongoing. An alternative way would be the knock down of the candidate proteases in cell culture using Kc-cells that take up RNA molecules without transfection.



The remaining list of candidates will be ordered as mutant or RNAi lines if available and subsequently tested for their influence on Pyr and Ths in early embryos. However, since Pyr has shown to have a greater influence on embryonic development and seems to have the ability to partially substitute for Ths (Kadam et al. 2009; Klingseisen et al. 2009) this test might be specific for the protease cleaving Pyr.

Following the identification of the protease or proteases cleaving Pyr and Ths study of lines mutant for the protease and rescue experiments with truncated constructs can be used to confirm the necessity of the protease for the mesoderm formation and the activity of the truncated proteins.

## Summary and Conclusion

Proteolytic processing is a potent regulatory mechanism of signalling molecules and therefore the processes they are involved in. In this thesis the proteolytic processing of the *Drosophila* FGFs Bnl, Pyr and Ths was investigated. The conducted experiments show that all three FGF ligands undergo proteolytic processing. Processing results in the release of smaller proteins that are subsequently secreted. In the case of Bnl Fur1-mediated processing is crucial for its activity. The data collected in this thesis and further publications are suggesting that this is also the case for Pyr and Ths. However this model has to be verified by future experiments.

Bnl signalling is crucial for the formation of the tracheal network during all stages of *Drosophila* development. It directs migration of the tracheal cells by providing a guidance cue, which leads to the stereotypical patterning of the tracheal network. Fur1-mediated processing is of major importance for tracheal patterning. The inhibition of Fur1 results in phenotypes similar to *bnl* loss-of-function in the embryo. This study shows that Fur1-mediated processing is necessary beyond embryonic development. Fur1 activity is crucial for the formation of the ASP and terminal branches in the larva. Moreover Fur1-mediated processing is the rate-limiting step for all Bnl-dependent processes that were investigated in this study. Additionally the results suggest that Fur1-mediated processing is important for the adaptation of the larval tracheal network to the oxygen content of the environment.

Vascularisation of tumours is of major importance for the development of cancers. It is driven by hypoxia and the need for nutrients. In studies of human cancers it has been shown that Furin proteases are supporting cancer progression by promoting vascularisation. Interestingly the Furin sites found in Bnl are conserved in its human homologue FGF10, which is involved in the formation of vascular networks. In cell culture FGF10 is cleaved by a Furin related protease. Thus Fur1-mediated processing of FGF10 homologues might be conserved as regulatory mechanism beyond *Drosophila* FGF signalling and aid in the regulation of human FGF signalling and its further investigation might aid in the understanding of human tumour formation.

Signalling of Pyr and Ths is crucial for the formation of several mesodermal structures. The results of this study show that Pyr and Ths are cleaved into smaller proteins similar to Bnl. Cleavage removes the extensive C-terminal domains of Pyr and Ths, which is releasing smaller proteins containing the FGF domain and facilitates their secretion. However, mutation of the Furin cutting sites revealed that this process is Furin-independent. Mapping of the actual cleavage site in Pyr and Ths and its deletion further

suggested that the two proteins are cleaved by different proteases. The involvement of different proteases would offer an explanation for their differential biological activity although both activate the same receptor. The identification of the responsible proteases will enable the further examination of the involved regulatory mechanism.

Taken together the experimental evidence from this study shows that proteolytic processing represents a novel rate-limiting step of Bnl-signalling and possibly a novel regulatory mechanism for all *Drosophila* FGF signalling. Moreover Fur1-mediated processing of Bnl is a solid candidate for the regulatory mechanism that controls the changes of the tracheal network in answer to hypoxia, while processing of Pyr and Tbs by different proteases offers an explanation for the differential signalling of two FGF ligands through the same receptor.

# References

- Acevedo, J. M., L. Centanin, et al. (2010). "Oxygen Sensing in Drosophila: Multiple Isoforms of the Prolyl Hydroxylase Fatiga Have Different Capacity to Regulate HIFalpha/Sima." PLoS ONE **5**(8): e12390.
- Achstetter, T. and D. H. Wolf (1985). "Hormone processing and membrane-bound proteinases in yeast." EMBO J **4**(1): 173-177.
- Affolter, M. and E. Caussinus (2008). "Tracheal branching morphogenesis in Drosophila: new insights into cell behaviour and organ architecture." Development **135**(12): 2055-2064.
- Anderson, E. D., J. K. VanSlyke, et al. (1997). "Activation of the furin endoprotease is a multiple-step process: requirements for acidification and internal propeptide cleavage." EMBO J **16**(7): 1508-1518.
- Antoine, M., M. Daum, et al. (2000). "NH2-terminal cleavage of Xenopus fibroblast growth factor 3 is necessary for optimal biological activity and receptor binding." Cell Growth & Differentiation **11**(11): 593-605.
- Armelin, H. A. (1973). "Pituitary extracts and steroid hormones in the control of 3T3 cell growth." Proc Natl Acad Sci U S A **70**(9): 2702-2706.
- Arquier, N., P. Vigne, et al. (2006). "Analysis of the hypoxia-sensing pathway in Drosophila melanogaster." The Biochemical journal **393**(Pt 2): 471-480.
- Arsenault, D., F. Lucien, et al. (2012). "Hypoxia enhances cancer cell invasion through relocalization of the proprotein convertase furin from the trans-golgi network to the cell surface." Journal of Cellular Physiology **227**(2): 789-800.
- Aso, T., K. Yamazaki, et al. (2000). "Drosophila von Hippel-Lindau tumor suppressor complex possesses E3 ubiquitin ligase activity." Biochemical and Biophysical Research Communications **276**(1): 355-361.
- Bacon, N. C., P. Wappner, et al. (1998). "Regulation of the Drosophila bHLH-PAS protein sima by hypoxia: functional evidence for homology with mammalian HIF-1 alpha." Biochemical and Biophysical Research Communications **249**(3): 811-816.
- Beenken, A. and M. Mohammadi (2009). "The FGF family: biology, pathophysiology and therapy." Nature reviews. Drug discovery **8**(3): 235-253.

Beiman, M., B. Z. Shilo, et al. (1996). "Heartless, a Drosophila FGF receptor homolog, is essential for cell migration and establishment of several mesodermal lineages." Genes & Development **10**(23): 2993-3002.

Benet-Pages, A., B. Lorenz-Depiereux, et al. (2004). "FGF23 is processed by proprotein convertases but not by PHEX." Bone **35**(2): 455-462.

Benjannet, S., D. Savaria, et al. (1997). "alpha 1-antitrypsin portland inhibits processing of precursors mediated by proprotein convertases primarily within the constitutive secretory pathway." Journal of Biological Chemistry **272**(42): 26210-26218.

Blaumueller, C. M., H. Qi, et al. (1997). "Intracellular cleavage of Notch leads to a heterodimeric receptor on the plasma membrane." Cell **90**(2): 281-291.

Boilly, B., A. S. Vercoutter-Edouart, et al. (2000). "FGF signals for cell proliferation and migration through different pathways." Cytokine Growth Factor Rev **11**(4): 295-302.

Bottcher, R. T. and C. Niehrs (2005). "Fibroblast growth factor signaling during early vertebrate development." Endocr Rev **26**(1): 63-77.

Brand, A. H. and N. Perrimon (1993). "TARGETED GENE-EXPRESSION AS A MEANS OF ALTERING CELL FATES AND GENERATING DOMINANT PHENOTYPES." Development **118**(2): 401-415.

Bresnahan, P. A., R. Leduc, et al. (1990). "Human fur gene encodes a yeast KEX2-like endoprotease that cleaves pro-beta-NGF in vivo." J Cell Biol **111**(6 Pt 2): 2851-2859.

Brou, C., F. Logeat, et al. (2000). "A novel proteolytic cleavage involved in Notch signaling: the role of the disintegrin-metalloprotease TACE." Mol Cell **5**(2): 207-216.

Buff, E., A. Carmena, et al. (1998). "Signalling by the Drosophila epidermal growth factor receptor is required for the specification and diversification of embryonic muscle progenitors." Development **125**(11): 2075-2086.

Cabernard, C. and M. Affolter (2005). "Distinct Roles for Two Receptor Tyrosine Kinases in Epithelial Branching Morphogenesis in Drosophila." Developmental cell **9**(6): 831-842.

Carmeliet, P. (2003). "Blood vessels and nerves: common signals, pathways and diseases." Nat Rev Genet **4**(9): 710-720.

Carmeliet, P., Y. Dor, et al. (1998). "Role of HIF-1alpha in hypoxia-mediated apoptosis, cell proliferation and tumour angiogenesis." Nature **394**(6692): 485-490.

Carmena, A., B. Murugasu-Oei, et al. (1998). "Inscuteable and numb mediate asymmetric muscle progenitor cell divisions during *Drosophila* myogenesis." Genes & Development **12**(3): 304-315.

Carrington, J. C. and W. G. Dougherty (1988). "A viral cleavage site cassette: identification of amino acid sequences required for tobacco etch virus polyprotein processing." Proc Natl Acad Sci U S A **85**(10): 3391-3395.

Centanin, L., A. Dekanty, et al. (2008). "Cell Autonomy of HIF Effects in *Drosophila*: Tracheal Cells Sense Hypoxia and Induce Terminal Branch Sprouting." Developmental cell **14**(4): 547-558.

Chen, F. and M. A. Krasnow (2014). "Progenitor outgrowth from the niche in *Drosophila* trachea is guided by FGF from decaying branches." Science **343**(6167): 186-189.

Chen, L. and C. X. Deng (2005). "Roles of FGF signaling in skeletal development and human genetic diseases." Front Biosci **10**: 1961-1976.

Ciruna, B. and J. Rossant (2001). "FGF signaling regulates mesoderm cell fate specification and morphogenetic movement at the primitive streak." Developmental cell **1**(1): 37-49.

Clark, I. B., V. Muha, et al. (2011). "Fibroblast growth factor signalling controls successive cell behaviours during mesoderm layer formation in *Drosophila*." Development **138**(13): 2705-2715.

Cohen, S. M. (1993). Imaginal disc development. The Development of *Drosophila melanogaster*. M. Bate. Plainview, NY Cold Spring Harbor Laboratory Press.

Coumoul, X. and C. X. Deng (2003). "Roles of FGF receptors in mammalian development and congenital diseases." Birth Defects Res C Embryo Today **69**(4): 286-304.

Crossley, P. H., S. Martinez, et al. (1996). "Midbrain development induced by FGF8 in the chick embryo." Nature **380**(6569): 66-68.

Crump, C. M., Y. Xiang, et al. (2001). "PACS-1 binding to adaptors is required for acidic cluster motif-mediated protein traffic." EMBO J **20**(9): 2191-2201.

Csiszar, A., E. Vogelsang, et al. (2010). "A novel conserved phosphotyrosine motif in the *Drosophila* fibroblast growth factor signaling adaptor Dof with a redundant role in signal transmission." Mol Cell Biol **30**(8): 2017-2027.

de Bie, I., D. Savaria, et al. (1995). "Processing specificity and biosynthesis of the *Drosophila melanogaster* convertases dfurin1, dfurin1-CRR, dfurin1-X, and dfurin2." Journal of Biological Chemistry **270**(3): 1020-1028.

DeLotto, Y. and R. DeLotto (1998). "Proteolytic processing of the Drosophila Spatzle protein by easter generates a dimeric NGF-like molecule with ventralising activity." Mech Dev **72**(1-2): 141-148.

Dreyfuss, J. L., C. V. Regatieri, et al. (2009). "Heparan sulfate proteoglycans: structure, protein interactions and cell signaling." An Acad Bras Cienc **81**(3): 409-429.

Ehrmann, M. and T. Clausen (2004). "Proteolysis as a regulatory mechanism." Annu Rev Genet **38**: 709-724.

Eriksson, A. E., L. S. Cousens, et al. (1991). "Three-dimensional structure of human basic fibroblast growth factor." Proc Natl Acad Sci U S A **88**(8): 3441-3445.

Eswarakumar, V. P., I. Lax, et al. (2005). "Cellular signaling by fibroblast growth factor receptors." Cytokine & Growth Factor Reviews **16**(2): 139-149.

Ferrara, N., G. Frantz, et al. (2003). "Differential expression of the angiogenic factor genes vascular endothelial growth factor (VEGF) and endocrine gland-derived VEGF in normal and polycystic human ovaries." Am J Pathol **162**(6): 1881-1893.

Fong, G. H. (2008). "Mechanisms of adaptive angiogenesis to tissue hypoxia." Angiogenesis **11**(2): 121-140.

Fortini, M. E. (2002). "Gamma-secretase-mediated proteolysis in cell-surface-receptor signalling." Nature reviews. Molecular cell biology **3**(9): 673-684.

Franzdottir, S. R., D. Engelen, et al. (2009). "Switch in FGF signalling initiates glial differentiation in the Drosophila eye." Nature **460**(7256): 758-U106.

Frasch, M. (1995). "Induction of visceral and cardiac mesoderm by ectodermal Dpp in the early Drosophila embryo." Nature **374**(6521): 464-467.

Fritsch, C., A. Sawala, et al. (2012). "Different requirements for proteolytic processing of bone morphogenetic protein 5/6/7/8 ligands in Drosophila melanogaster." J Biol Chem **287**(8): 5942-5953.

Geisler, R., A. Bergmann, et al. (1992). "cactus, a gene involved in dorsoventral pattern formation of Drosophila, is related to the I $\kappa$ B gene family of vertebrates." Cell **71**(4): 613-621.

Ghabrial, A., S. Luschnig, et al. (2003). "Branching morphogenesis of the Drosophila tracheal system." Annual review of cell and developmental biology **19**: 623-647.

Gisselbrecht, S., J. B. Skeath, et al. (1996). "heartless encodes a fibroblast growth factor receptor (DFR1/DFGF-R2) involved in the directional migration of early mesodermal cells in the Drosophila embryo." Genes & Development **10**(23): 3003-3017.

Gospodarowicz, D. (1974). "Localisation of a fibroblast growth factor and its effect alone and with hydrocortisone on 3T3 cell growth." Nature **249**(453): 123-127.

Gryzik, T. and H. A. J. Müller (2004). "FGF8-like1 and FGF8-like2 Encode Putative Ligands of the FGF Receptor Htl and Are Required for Mesoderm Migration in the Drosophila Gastrula." Current Biology **14**(8): 659-667.

Guha, A. and T. B. Kornberg (2005). "Tracheal branch repopulation precedes induction of the Drosophila dorsal air sac primordium." Developmental Biology **287**(1): 192-200.

Hacker, U., K. Nybakken, et al. (2005). "Heparan sulphate proteoglycans: the sweet side of development." Nature reviews. Molecular cell biology **6**(7): 530-541.

Hacohen, N., S. Kramer, et al. (1998). "sprouty Encodes a Novel Antagonist of FGF Signaling that Patterns Apical Branching of the Drosophila Airways." Cell **92**(2): 253-263.

Halfon, M. S., A. Carmena, et al. (2000). "Ras pathway specificity is determined by the integration of multiple signal-activated and tissue-restricted transcription factors." Cell **103**(1): 63-74.

Hallenberger, S., V. Bosch, et al. (1992). "Inhibition of furin-mediated cleavage activation of HIV-1 glycoprotein gp160." Nature **360**(6402): 358-361.

Hart, K. C., S. C. Robertson, et al. (2000). "Transformation and Stat activation by derivatives of FGFR1, FGFR3, and FGFR4." Oncogene **19**(29): 3309-3320.

Hayflick, J. S., W. J. Wolfgang, et al. (1992). "A unique Kex2-like endoprotease from Drosophila melanogaster is expressed in the central nervous system during early embryogenesis." Journal of Neuroscience **12**(3): 705-717.

Hochachka, P. W., L. T. Buck, et al. (1996). "Unifying theory of hypoxia tolerance: molecular/metabolic defense and rescue mechanisms for surviving oxygen lack." Proc Natl Acad Sci U S A **93**(18): 9493-9498.

Hsouna, A., G. Nallamotheu, et al. (2010). "Drosophila von hippel-lindau tumor suppressor gene function in epithelial tubule morphogenesis." Molecular and Cellular Biology **30**(15): 3779-3794.

Imam, F., D. Sutherland, et al. (1999). "stumps, a Drosophila Gene Required for Fibroblast Growth Factor (FGF)-directed Migrations of Tracheal and Mesodermal Cells." Genetics **152**(1): 307-318.



Inoue, H., H. Nojima, et al. (1990). "High efficiency transformation of Escherichia coli with plasmids." Gene **96**(1): 23-28.

Itoh, N. and D. M. Ornitz (2004). "Evolution of the Fgf and Fgfr gene families." Trends in Genetics **20**(11): 563-569.

Jarecki, J., E. Johnson, et al. (1999). "Oxygen regulation of airway branching in Drosophila is mediated by branchless FGF." Cell **99**(2): 211-220.

Jean, F., K. Stella, et al. (1998). "alpha1-Antitrypsin Portland, a bioengineered serpin highly selective for furin: application as an antipathogenic agent." Proc Natl Acad Sci U S A **95**(13): 7293-7298.

Jiang, B. H., J. Z. Zheng, et al. (1997). "Transactivation and inhibitory domains of hypoxia-inducible factor 1alpha. Modulation of transcriptional activity by oxygen tension." J Biol Chem **272**(31): 19253-19260.

Kadam, S., S. Ghosh, et al. (2012). "Synchronous and symmetric migration of Drosophila caudal visceral mesoderm cells requires dual input by two FGF ligands." Development **139**(4): 699-708.

Kadam, S., A. McMahon, et al. (2009). "FGF ligands in Drosophila have distinct activities required to support cell migration and differentiation." Development **136**(5): 739-747.

Kaelin, W. G., Jr. and P. J. Ratcliffe (2008). "Oxygen sensing by metazoans: the central role of the HIF hydroxylase pathway." Mol Cell **30**(4): 393-402.

Kalus, I., B. Schnegelsberg, et al. (2003). "The proprotein convertase PC5A and a metalloprotease are involved in the proteolytic processing of the neural adhesion molecule L1." J Biol Chem **278**(12): 10381-10388.

Katoh, M. and H. Nakagama (2014). "FGF Receptors: Cancer Biology and Therapeutics." Medicinal Research Reviews **34**(2): 280-300.

Keil, B. (1992). Specificity of proteolysis. Berlin, Germany, Springer-Verlag.

Kiefer, P., M. Mathieu, et al. (1993). "FGF3 FROM XENOPUS-LAEVIS." Embo Journal **12**(11): 4159-4168.

Klambt, C., L. Glazer, et al. (1992). "breathless, a Drosophila FGF receptor homolog, is essential for migration of tracheal and specific midline glial cells." Genes Dev **6**(9): 1668-1678.

Klingseisen, A., I. B. N. Clark, et al. (2009). "Differential and overlapping functions of two closely related Drosophila FGF8-like growth factors in mesoderm development." Development **136**(14): 2393-2402.

Koledachkina, T. (2010). Furin-mediated proteolytic activation of Drosophila FGF homologue branchless. Braunschweig, TU Braunschweig. **Phd**: 115.

Kornberg, S. a. (2002). "FGF is an essential mitogen and chemoattractant for the air sacs of the drosophila tracheal system." Developmental Cell **3**.

Kosaka, N., H. Sakamoto, et al. (2009). "Pleiotropic function of FGF-4: its role in development and stem cells." Developmental dynamics : an official publication of the American Association of Anatomists **238**(2): 265-276.

Kostallas, G., P. A. Lofdahl, et al. (2011). "Substrate profiling of tobacco etch virus protease using a novel fluorescence-assisted whole-cell assay." PLoS ONE **6**(1): e16136.

Kouhara, H., Y. R. Hadari, et al. (1997). "A lipid-anchored Grb2-binding protein that links FGF-receptor activation to the Ras/MAPK signaling pathway." Cell **89**(5): 693-702.

Krejci, P., J. Prochazkova, et al. (2009). "Molecular pathology of the fibroblast growth factor family." Human Mutation **30**(9): 1245-1255.

Krock, B. L., N. Skuli, et al. (2011). "Hypoxia-induced angiogenesis: good and evil." Genes Cancer **2**(12): 1117-1133.

Künnapuu, J., I. Bjorkgren, et al. (2009). "The Drosophila DPP signal is produced by cleavage of its proprotein at evolutionary diversified furin-recognition sites." Proceedings of the National Academy of Sciences of the United States of America **106**(21): 8501-8506.

Kylsten, P. and R. Saint (1997). "Imaginal tissues of Drosophila melanogaster exhibit different modes of cell proliferation control." Dev Biol **192**(2): 509-522.

Laemmli, U. K. (1970). "Cleavage of structural proteins during the assembly of the head of bacteriophage T4." Nature **227**(5259): 680-685.

Lavista-Llanos, S., L. Centanin, et al. (2002). "Control of the hypoxic response in Drosophila melanogaster by the basic helix-loop-helix PAS protein Similar." Molecular and Cellular Biology **22**(19): 6842-6853.

Lee, J. R., S. Urban, et al. (2001). "Regulated intracellular ligand transport and proteolysis control EGF signal activation in Drosophila." Cell **107**(2): 161-171.

Lee, T., N. Hacohen, et al. (1996). "Regulated Breathless receptor tyrosine kinase activity required to pattern cell migration and branching in the Drosophila tracheal system." Genes & Development **10**(22): 2912-2921.

Lee, T. and L. Luo (1999). "Mosaic analysis with a repressible cell marker for studies of gene function in neuronal morphogenesis." Neuron **22**(3): 451-461.

Leptin, M. (1991). "twist and snail as positive and negative regulators during Drosophila mesoderm development." Genes Dev **5**(9): 1568-1576.

Leptin, M. and M. Affolter (2004). "Drosophila Gastrulation: Identification of a Missing Link." Current Biology **14**(12): R480-R482.

Lieber, T., S. Kidd, et al. (2002). "kuzbanian-mediated cleavage of Drosophila Notch." Genes & Development **16**(2): 209-221.

Lin, H. Y., J. Xu, et al. (1998). "Identification of the cytoplasmic regions of fibroblast growth factor (FGF) receptor 1 which play important roles in induction of neurite outgrowth in PC12 cells by FGF-1." Mol Cell Biol **18**(7): 3762-3770.

Lin, X. and N. Perrimon (2000). "Role of heparan sulfate proteoglycans in cell-cell signaling in Drosophila." Matrix Biology **19**(4): 303-307.

Locke, M. (1958). "THE CO-ORDINATION OF GROWTH IN THE TRACHEAL SYSTEM OF INSECTS." Quarterly Journal of Microscopical Science **99**(3): 373-&.

Logeat, F., C. Bessia, et al. (1998). "The Notch1 receptor is cleaved constitutively by a furin-like convertase." Proc Natl Acad Sci U S A **95**(14): 8108-8112.

Luo, L. a. (1999). "Mosaic Analysis with a Repressible Cell Marker for Studies of Gene Function in Neuronal Morphogenesis." Neuron **22**(3): 451-461.

Mahon, P. C., K. Hirota, et al. (2001). "FIH-1: a novel protein that interacts with HIF-1alpha and VHL to mediate repression of HIF-1 transcriptional activity." Genes Dev **15**(20): 2675-2686.

Mandal, L., K. Dumstrei, et al. (2004). "Role of FGFR signaling in the morphogenesis of the Drosophila visceral musculature." Developmental dynamics : an official publication of the American Association of Anatomists **231**(2): 342-348.

Manning, G. and M. Krasnow (1993). Development of the Drosophila tracheal system. The Development of Drosophila melanogaster. M. Bate and A. Arias. Cold Spring Harbor, Cold Spring Harbor Laboratory Press: 609-685.

- McMahon, A., G. T. Reeves, et al. (2010). "Mesoderm migration in *Drosophila* is a multi-step process requiring FGF signaling and integrin activity." Development **137**(13): 2167-2175.
- McMahon, A., W. Supatto, et al. (2008). "Dynamic analyses of *Drosophila* gastrulation provide insights into collective cell migration." Science **322**(5907): 1546-1550.
- McMahon, S., F. Grondin, et al. (2005). "Hypoxia-enhanced expression of the proprotein convertase furin is mediated by hypoxia-inducible factor-1: impact on the bioactivation of proproteins." J Biol Chem **280**(8): 6561-6569.
- Metzger, R. J. and M. A. Krasnow (1999). "Genetic control of branching morphogenesis." Science **284**(5420): 1635-1639.
- Michelson, A. M., S. Gisselbrecht, et al. (1998). "Heartbroken is a specific downstream mediator of FGF receptor signalling in *Drosophila*." Development **125**(22): 4379-4389.
- Min, H., D. M. Danilenko, et al. (1998). "Fgf-10 is required for both limb and lung development and exhibits striking functional similarity to *Drosophila* branchless." Genes Dev **12**(20): 3156-3161.
- Misra, T. (2014). Metabolic control of tracheal branching in *Drosophila*. life science. Zurich, University of Zurich. **PHD**.
- Mohammadi, M., S. K. Olsen, et al. (2005). "Structural basis for fibroblast growth factor receptor activation." Cytokine Growth Factor Rev **16**(2): 107-137.
- Mohammadi, M., J. Schlessinger, et al. (1996). "Structure of the FGF Receptor Tyrosine Kinase Domain Reveals a Novel Autoinhibitory Mechanism." Cell **86**(4): 577-587.
- Molloy, S. S., E. D. Anderson, et al. (1999). "Bi-cycling the furin pathway: from TGN localization to pathogen activation and embryogenesis." Trends Cell Biol **9**(1): 28-35.
- Molloy, S. S., P. A. Bresnahan, et al. (1992). "Human furin is a calcium-dependent serine endoprotease that recognizes the sequence Arg-X-X-Arg and efficiently cleaves anthrax toxin protective antigen." J Biol Chem **267**(23): 16396-16402.
- Molloy, S. S., L. Thomas, et al. (1994). "Intracellular trafficking and activation of the furin proprotein convertase: localization to the TGN and recycling from the cell surface." The EMBO Journal **13**(1): 18-33.
- Muha, V. and H. A. Muller (2013). "Functions and Mechanisms of Fibroblast Growth Factor (FGF) Signalling in *Drosophila melanogaster*." Int J Mol Sci **14**(3): 5920-5937.

Nagao, M., B. L. Ebert, et al. (1996). "Drosophila melanogaster SL2 cells contain a hypoxically inducible DNA binding complex which recognises mammalian HIF-binding sites." FEBS Lett **387**(2-3): 161-166.

Nagaso, H., T. Murata, et al. (2001). "Simultaneous detection of RNA and protein by in situ hybridization and immunological staining." J Histochem Cytochem **49**(9): 1177-1182.

Niswander, L., C. Tickle, et al. (1993). "FGF-4 replaces the apical ectodermal ridge and directs outgrowth and patterning of the limb." Cell **75**(3): 579-587.

Olsen, J. V., S. E. Ong, et al. (2004). "Trypsin cleaves exclusively C-terminal to arginine and lysine residues." Mol Cell Proteomics **3**(6): 608-614.

Ornitz, D. M. and N. Itoh (2001). "Fibroblast growth factors." Genome Biology **2**(3).

Parangi, S., M. O'Reilly, et al. (1996). "Antiangiogenic therapy of transgenic mice impairs de novo tumor growth." Proc Natl Acad Sci U S A **93**(5): 2002-2007.

Parker, M. W., L. M. Hellman, et al. (2010). "Furin processing of semaphorin 3F determines its anti-angiogenic activity by regulating direct binding and competition for neuropilin." Biochemistry **49**(19): 4068-4075.

Pasquato, A. and N. G. Seidah (2008). "The H5N1 influenza variant Fujian-like hemagglutinin selected following vaccination exhibits a compromised furin cleavage : neurological Consequences of highly pathogenic Fujian H5N1 strains." J Mol Neurosci **35**(3): 339-343.

Perkins, L. A., I. Larsen, et al. (1992). "corkscrew encodes a putative protein tyrosine phosphatase that functions to transduce the terminal signal from the receptor tyrosine kinase torso." Cell **70**(2): 225-236.

Petit, V., U. Nussbaumer, et al. (2004). "Downstream-of-FGFR is a fibroblast growth factor-specific scaffolding protein and recruits Corkscrew upon receptor activation." Molecular and Cellular Biology **24**(9): 3769-3781.

Pugh, C. W. and P. J. Ratcliffe (2003). "Regulation of angiogenesis by hypoxia: role of the HIF system." Nat Med **9**(6): 677-684.

Rand, M. D., L. M. Grimm, et al. (2000). "Calcium depletion dissociates and activates heterodimeric Notch receptors." Molecular and Cellular Biology **20**(5): 1825-1835.

Rayburn, L. Y. M., S. P. Choksi, et al. (2002). "Correction of an amontillado (amon) cDNA artifact and identification of single nucleotide polymorphisms in the amon gene." Drosophila Information Service **85**: 23-24.

Reichman-Fried, M., B. Dickson, et al. (1994). "Elucidation of the role of breathless, a Drosophila FGF receptor homolog, in tracheal cell migration." Genes Dev **8**(4): 428-439.

Reifers, F., H. Bohli, et al. (1998). "Fgf8 is mutated in zebrafish acerebellar (ace) mutants and is required for maintenance of midbrain-hindbrain boundary development and somitogenesis." Development **125**(13): 2381-2395.

Reim, I., D. Hollfelder, et al. (2012). "The FGF8-related signals Pyramus and Thisbe promote pathfinding, substrate adhesion, and survival of migrating longitudinal gut muscle founder cells." Developmental Biology.

Reuter, R. and M. Leptin (1994). "Interacting functions of snail, twist and huckebein during the early development of germ layers in Drosophila." Development **120**(5): 1137-1150.

Ribeiro, C., A. Ebner, et al. (2002). "In vivo Imaging reveals different cellular functions for FGF and Dpp signaling in tracheal branching morphogenesis." Developmental cell **2**(5): 677-683.

Ribeiro, C., M. Neumann, et al. (2004). "Genetic Control of Cell Intercalation during Tracheal Morphogenesis in Drosophila." Current Biology **14**(24): 2197-2207.

Rockwell, N. C., D. J. Krysan, et al. (2002). "Precursor processing by Kex2/furin proteases." Chemical Reviews **102**(12): 4525-4548.

Rodriguez, J., N. Gupta, et al. (2008). "Does trypsin cut before proline?" J Proteome Res **7**(1): 300-305.

Roebroek, A. J. M., T. A. Y. Ayoubi, et al. (1995). "The Dfur2 gene of Drosophila melanogaster: Genetic organization, expression during embryogenesis, and pro-protein processing activity of its translational product Dfurin2." DNA and Cell Biology **14**(3): 223-234.

Roebroek, A. J. M., J. W. M. Creemers, et al. (1993). "GENERATION OF STRUCTURAL AND FUNCTIONAL DIVERSITY IN FURIN-LIKE PROTEINS IN DROSOPHILA-MELANOGASTER BY ALTERNATIVE SPLICING OF THE DFUR1 GENE." Embo Journal **12**(5): 1853-1870.

Roy, S. and T. B. Kornberg (2011). "Contact mediated transport of signaling proteins over long distance by Drosophila cytonemes." Molecular Biology of the Cell **22**.

Samakovlis, C., N. Hacohen, et al. (1996). "Development of the Drosophila tracheal system occurs by a series of morphologically distinct but genetically coupled branching events." Development **122**(5): 1395-1407.

Sambrook, J., E. F. Fritsch, et al. (1989). Molecular Cloning: a Laboratory Manual, 2d edition. Cold Spring Harbor Laboratory, Cold Spring Harbor Laboratory.

Sato, M. and T. B. Kornberg (2002). "FGF is an essential mitogen and chemoattractant for the air sacs of the *Drosophila* tracheal system." Developmental cell **3**(2): 195-207.

Schlessinger, J., A. N. Plotnikov, et al. (2000). "Crystal Structure of a Ternary FGF-FGFR-Heparin Complex Reveals a Dual Role for Heparin in FGFR Binding and Dimerization." Molecular Cell **6**(3): 743-750.

Seidah, N. G. (2011). "What lies ahead for the proprotein convertases?" Annals of the New York Academy of Sciences **1220**(1): 149-161.

Semenza, G. L. and G. L. Wang (1992). "A nuclear factor induced by hypoxia via de novo protein synthesis binds to the human erythropoietin gene enhancer at a site required for transcriptional activation." Mol Cell Biol **12**(12): 5447-5454.

Shiang, R., L. M. Thompson, et al. (1994). "Mutations in the transmembrane domain of FGFR3 cause the most common genetic form of dwarfism, achondroplasia." Cell **78**(2): 335-342.

Shimada, T., S. Mizutani, et al. (2001). "Cloning and characterization of FGF23 as a causative factor of tumor-induced osteomalacia." Proc Natl Acad Sci U S A **98**(11): 6500-6505.

Shishido, E., N. Ono, et al. (1997). "Requirements of DFR1/Heartless, a mesoderm-specific *Drosophila* FGF-receptor, for the formation of heart, visceral and somatic muscles, and ensheathing of longitudinal axon tracts in CNS." Development **124**(11): 2119-2128.

Siekhaus, D. E. and R. S. Fuller (1999). "A role for *amontillado*, the *Drosophila* homolog of the neuropeptide precursor processing protease PC2, in triggering hatching behavior." Journal of Neuroscience **19**(16): 6942-6954.

Stathopoulos, A. (2004). "pyramus and thisbe: FGF genes that pattern the mesoderm of *Drosophila* embryos." Genes & Development **18**(6): 687-699.

Sun, X., L. V. Tse, et al. (2010). "Modifications to the hemagglutinin cleavage site control the virulence of a neurotropic H1N1 influenza virus." J Virol **84**(17): 8683-8690.

Suster, M. L., L. Seugnet, et al. (2004). "Refining GAL4-driven transgene expression in *Drosophila* with a GAL80 enhancer-trap." Genesis **39**(4): 240-245.

Sutherland, D., C. Samakovlis, et al. (1996). "branchless encodes a *Drosophila* FGF homolog that controls tracheal cell migration and the pattern of branching." Cell **87**(6): 1091-1101.

Teuchert, M., S. Berghofer, et al. (1999a). "Recycling of furin from the plasma membrane. Functional importance of the cytoplasmic tail sorting signals and interaction with the AP-2 adaptor medium chain subunit." J Biol Chem **274**(51): 36781-36789.

Teuchert, M., W. Schafer, et al. (1999b). "Sorting of furin at the trans-Golgi network. Interaction of the cytoplasmic tail sorting signals with AP-1 Golgi-specific assembly proteins." J Biol Chem **274**(12): 8199-8207.

Thisse, B., M. el Messal, et al. (1987). "The twist gene: isolation of a Drosophila zygotic gene necessary for the establishment of dorsoventral pattern." Nucleic Acids Research **15**(8): 3439-3453.

Thisse, B. and C. Thisse (2005). "Functions and regulations of fibroblast growth factor signaling during embryonic development." Dev Biol **287**(2): 390-402.

Thomas, G. (2002). "Furin at the cutting edge: from protein traffic to embryogenesis and disease." Nature reviews. Molecular cell biology **3**(10): 753-766.

Tulin, S. and A. Stathopoulos (2010). "Analysis of Thisbe and Pyramus functional domains reveals evidence for cleavage of Drosophila FGFs." BMC Developmental Biology **10**(1): 83.

Turk, B., D. Turk, et al. (2012). "Protease signalling: the cutting edge." EMBO J **31**(7): 1630-1643.

Turner, N. and R. Grose (2010). "Fibroblast growth factor signalling: from development to cancer." Nat Rev Cancer **10**(2): 116-129.

Urban, S., J. R. Lee, et al. (2001). "Drosophila rhomboid-1 defines a family of putative intramembrane serine proteases." Cell **107**(2): 173-182.

Uv, A. (2003). "Drosophila tracheal morphogenesis: intricate cellular solutions to basic plumbing problems." Trends in Cell Biology **13**(6): 301-309.

Vincent, S., R. Wilson, et al. (1998). "The Drosophila protein Dof is specifically required for FGF signaling." Mol Cell **2**(4): 515-525.

Walker, J. A., S. S. Molloy, et al. (1994). "Sequence specificity of furin, a proprotein-processing endoprotease, for the hemagglutinin of a virulent avian influenza virus." J Virol **68**(2): 1213-1218.

Wang, G. L. and G. L. Semenza (1993). "General involvement of hypoxia-inducible factor 1 in transcriptional response to hypoxia." Proc Natl Acad Sci U S A **90**(9): 4304-4308.

Wang, Q., M. Uhlirova, et al. (2010). "Spatial Restriction of FGF Signaling by a Matrix Metalloprotease Controls Branching Morphogenesis." Developmental cell **18**(1): 157-164.



Wassarman, D. A., M. Therrien, et al. (1995). "The Ras signaling pathway in Drosophila." Curr Opin Genet Dev **5**(1): 44-50.

Weaver, M. and M. A. Krasnow (2008). "Dual Origin of Tissue-Specific Progenitor Cells in Drosophila Tracheal Remodeling." Science **321**(5895): 1496-1499.

Weiner, M. P., G. L. Costa, et al. (1994). "Site-directed mutagenesis of double-stranded DNA by the polymerase chain reaction." Gene **151**(1-2): 119-123.

Wenger, R. H. (2002). "Cellular adaptation to hypoxia: O<sub>2</sub>-sensing protein hydroxylases, hypoxia-inducible transcription factors, and O<sub>2</sub>-regulated gene expression." FASEB J **16**(10): 1151-1162.

Wenger, R. H., D. P. Stiehl, et al. (2005). "Integration of oxygen signaling at the consensus HRE." Science's STKE : signal transduction knowledge environment **2005**(306): re12.

Wharton, K. and R. Derynck (2009). "TGFbeta family signaling: novel insights in development and disease." Development **136**(22): 3691-3697.

White, K. E., G. Carn, et al. (2001). "Autosomal-dominant hypophosphatemic rickets (ADHR) mutations stabilize FGF-23." Kidney Int **60**(6): 2079-2086.

Wickner, R. B. and M. J. Leibowitz (1976). "Two chromosomal genes required for killing expression in killer strains of *Saccharomyces cerevisiae*." Genetics **82**(3): 429-442.

Wigglesworth, V. B. (1954). "GROWTH AND REGENERATION IN THE TRACHEAL SYSTEM OF AN INSECT, RHODNIUS-PROLIXUS (HEMIPTERA)." Quarterly Journal of Microscopical Science **95**(1): 115-&.

Wigglesworth, V. B. (1983). "The physiology of insect tracheoles." Advances in Insect Physiology **17**: 85-148.

Wilson, R., A. Battersby, et al. (2004). "A Functional Domain of Dof That Is Required for Fibroblast Growth Factor Signaling." Molecular and Cellular Biology **24**(6): 2263-2276.

Wilson, R., E. Vogelsang, et al. (2005). "FGF signalling and the mechanism of mesoderm spreading in *Drosophila* embryos." Development **132**(3): 491-501.

Yayon, A., M. Klagsbrun, et al. (1991). "Cell surface, heparin-like molecules are required for binding of basic fibroblast growth factor to its high affinity receptor." Cell **64**(4): 841-848.

Zhu, X., H. Komiya, et al. (1991). "Three-dimensional structures of acidic and basic fibroblast growth factors." Science **251**(4989): 90-93.

## Acknowledgements

The present work was carried out in the Research Group of Cellular Dynamics in the Department of Molecular Developmental Biology at the Max-Planck-Institute for Biophysical Chemistry in Göttingen under the supervision of Prof. Dr. Gerd Vorbrüggen.

First of all I want to thank Prof. Dr. Gerd Vorbrüggen for inviting me into his lab and taking me under his wings. I am not only grateful for his supervision, teaching, guidance and constant support, but also for his patience and encouragement.

I am thankful to Prof. Dr. Herbert Jäckle for giving me the opportunity to carry out my dissertation in his department.

I thank the rest of my committee members Prof. Dr. Ernst Wimmer and Prof. Dr. Reinhard Schuh for their time and critical discussion.

Thank you to Prof. Dr. Stefan Luschign and the members of his lab for cordially receiving me, while lending me their equipment and their knowledge.

I especially want to thank Tomma Eisbein. Her tireless support with the experimental work and friendly conversation were an enormous help.

Thank you to the former and current members of lab 5, Gerd, Andres, Alexey, Anna, Sebastian and Ninnett, for their support and advice and for creating a fruitful and pleasant working atmosphere.

Many thanks go to Phillip, Ralf and Andres not only for critical comments and technical help, but also for countless movie nights and many great evenings in the pub.

I want to express my gratitude to my family, Mama, Anna and Opa for their love and support. You have always believed in me and never doubted my decisions, even when I did. I could not have done it without you.

From the bottom of my heart: Thank you Anne. You kept me sane. Well, mostly.

# Curriculum Vitae

Name: Eva-Maria Rieß  
Date of Birth: 06.07.1986  
Place of Birth: Detmold

## Education

1992-1996 Werretalschule Remmighausen  
1996-2005 Abitur, Leopoldinum Detmold  
2005-2011 Diploma in biology, Georg-August Universität Göttingen  
(supervised by Prof. Dr. Sigrid Hoyer-Fender)  
Title: Transkriptionelle Regulation von Odf2 und sein  
Einfluss auf die Bildung des Centrosoms  
(Transcriptional regulation of Odf2 and its influence on the  
formation of the centrosome)  
2007-2008 Year abroad, University of Manchester  
2011-present PhD thesis in the Group of Molecular Cell Dynamics,  
Department of Molecular Developmental Biology,  
Max-Planck-Institute for biophysical Chemistry, Göttingen  
(supervised by Prof. Dr. Gerd Vorbrüggen)  
Title: Proteolytic Processing of *Drosophila* FGFs